



# **Lecture 3: Galaxy Evolution over the Last Half of Cosmic Time**

**Alexandria Winter School on Galaxy Formation**

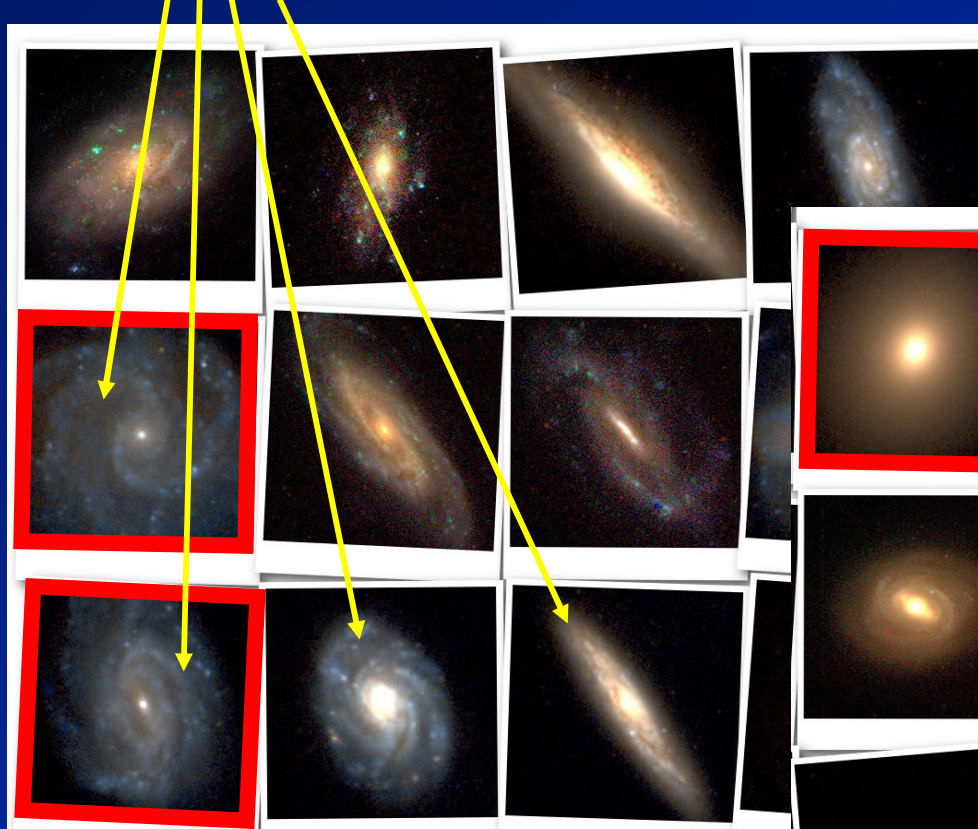
Sandra M. Faber

March 22, 2006

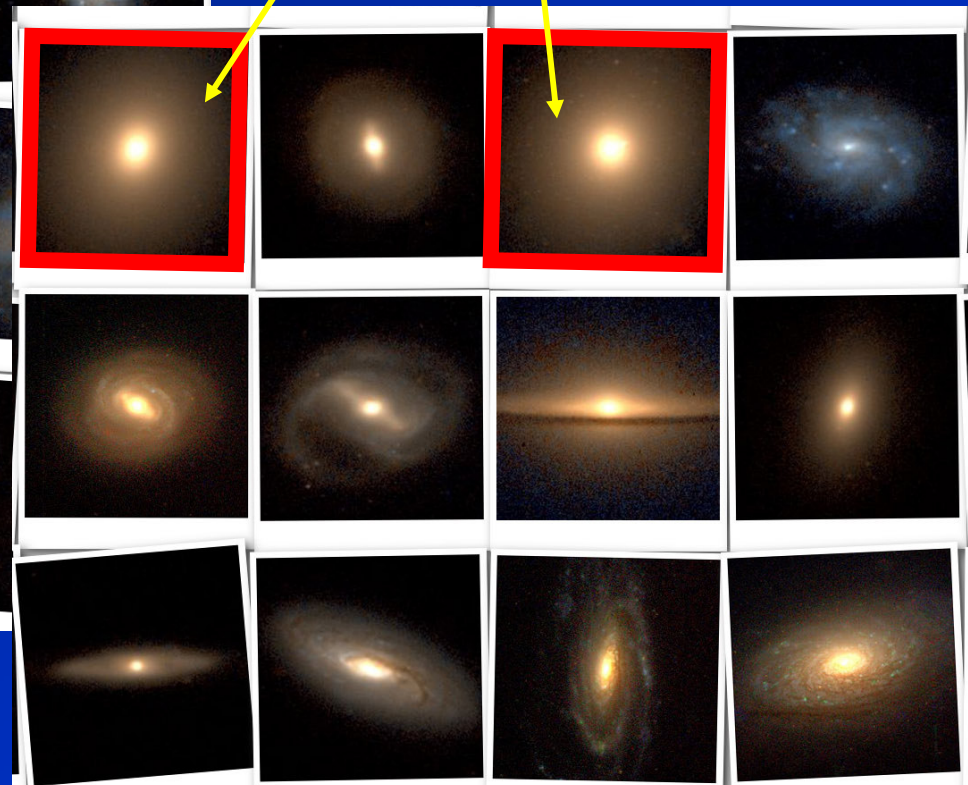


# A reminder about Hubble types: disky galaxies vs. spheroidal galaxies

Examples of disky/spiral galaxies

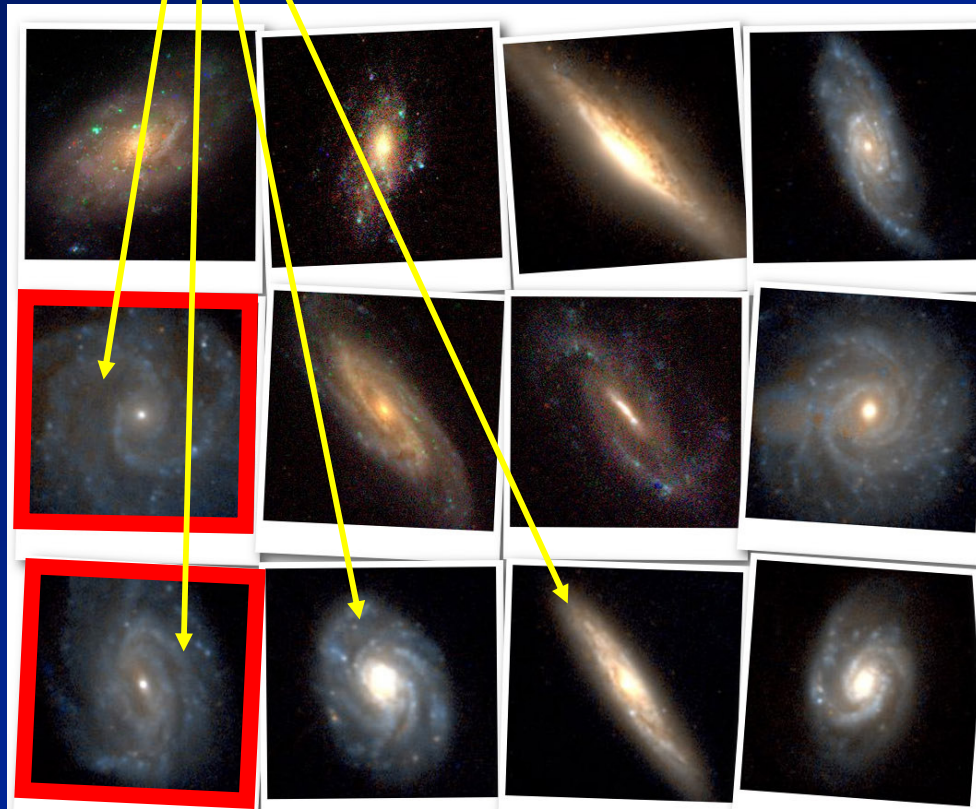


Examples of  
spheroidal/elliptical galaxies



# Properties of disk galaxies

Examples of disk/spiral galaxies



\* “**Cold**” means that orbiting objects have small **velocity dispersion** relative to one other.

- Flattened, rotating, “**cold**”\* systems with stars and gas in NEARLY CIRCULAR orbits.
- Supported by circular motion.
- Spiral arms are caused by spontaneous **gravitational instability** in cold disks.
- Have interstellar gas; **still making stars.**
- Intermediate to small stellar masses: few  $\times 10^{10} M_{\odot}$  down to  $10^{6-7} M_{\odot}$  “dwarfs.”

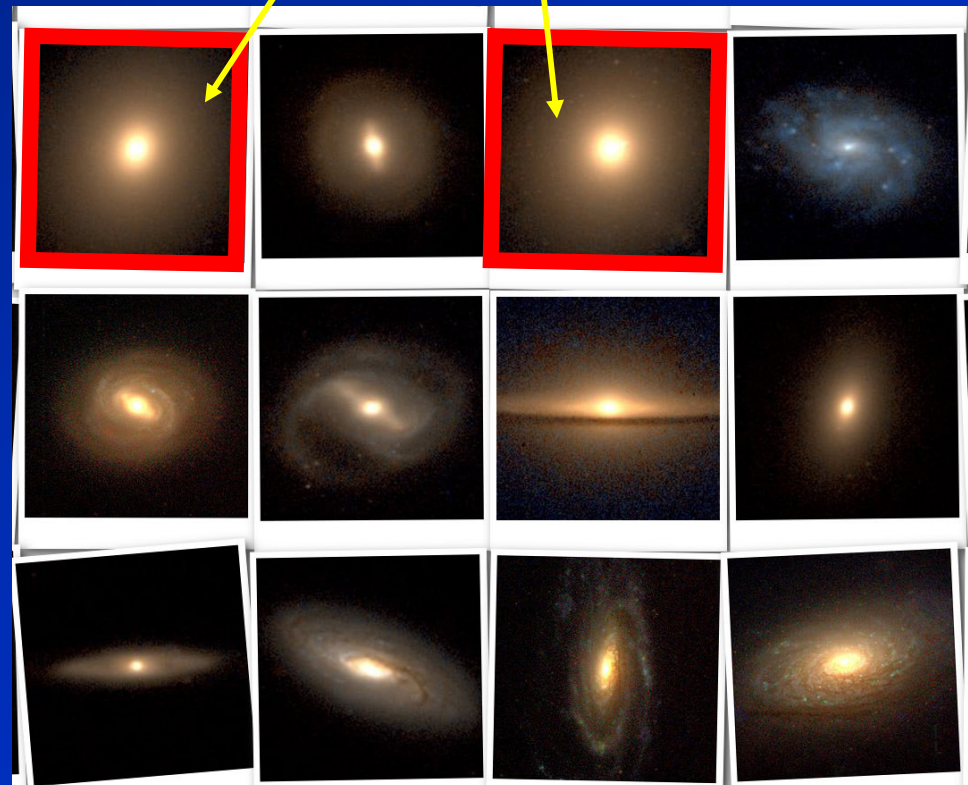


# Properties of spheroidal galaxies

- Roundish, slowly rotating, “hot”\* stellar systems with stars in RANDOMLY ORIENTED, ELLIPTICAL orbits.
- Supported by random motions (“pressure”).
- No spiral arms--too hot. Smooth structure with high central concentration.
- No gas, not forming stars.
- Intermediate to large stellar masses: few  $\times 10^{10} M_{\odot}$  up to to few  $\times 10^{12} M_{\odot}$ .

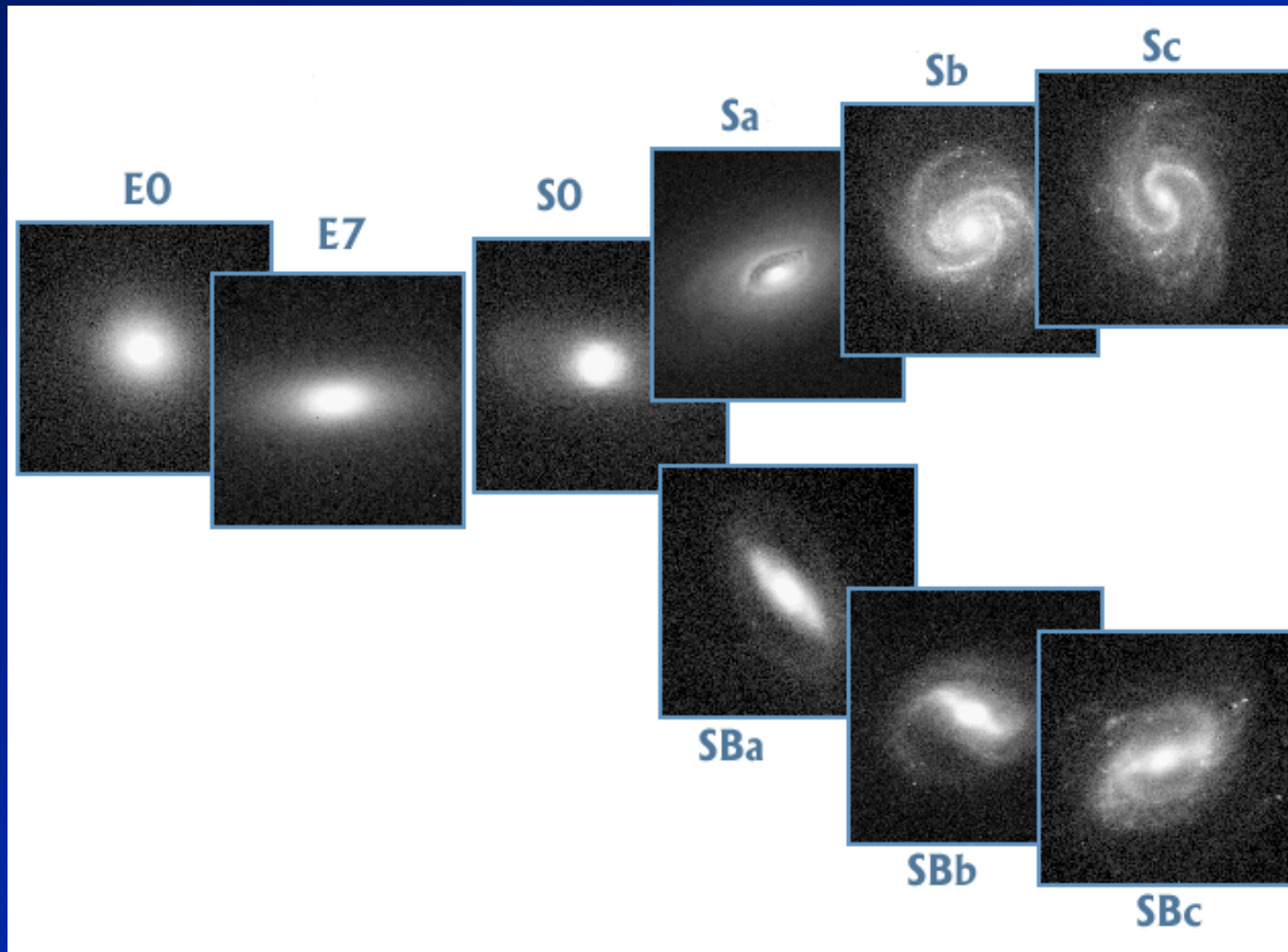
\* “Cold” means that orbiting objects have small *velocity dispersion* relative to one other.

Examples of spheroidal/elliptical galaxies





# The Hubble Sequence



# Trends along the Hubble Sequence

More spheroidal

Less rotation

Less circular orbits

Less gas

Less star formation

Less prominent spiral arms

Larger stellar mass  
mass

Bigger central black hole  
hole



More disk

More rotation

More circular orbits

More gas

More star formation

More prominent arms

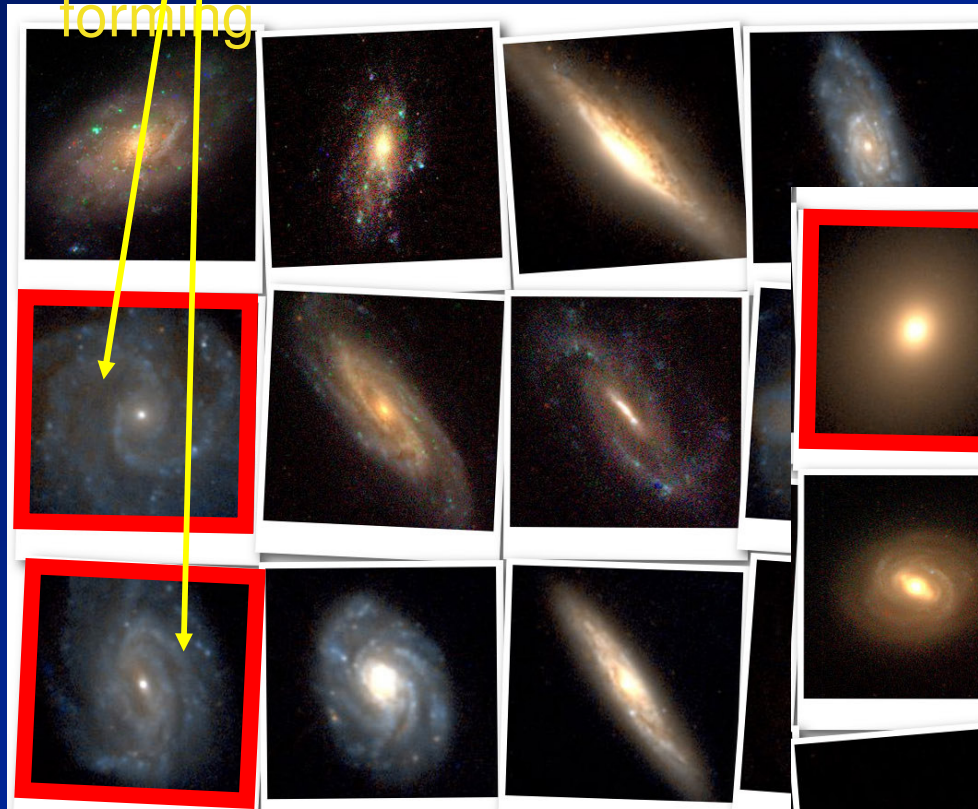
Smaller stellar

Small or no black



# Color indicates different amounts of recent or ongoing *star formation*

Disks are bluish--stars are forming



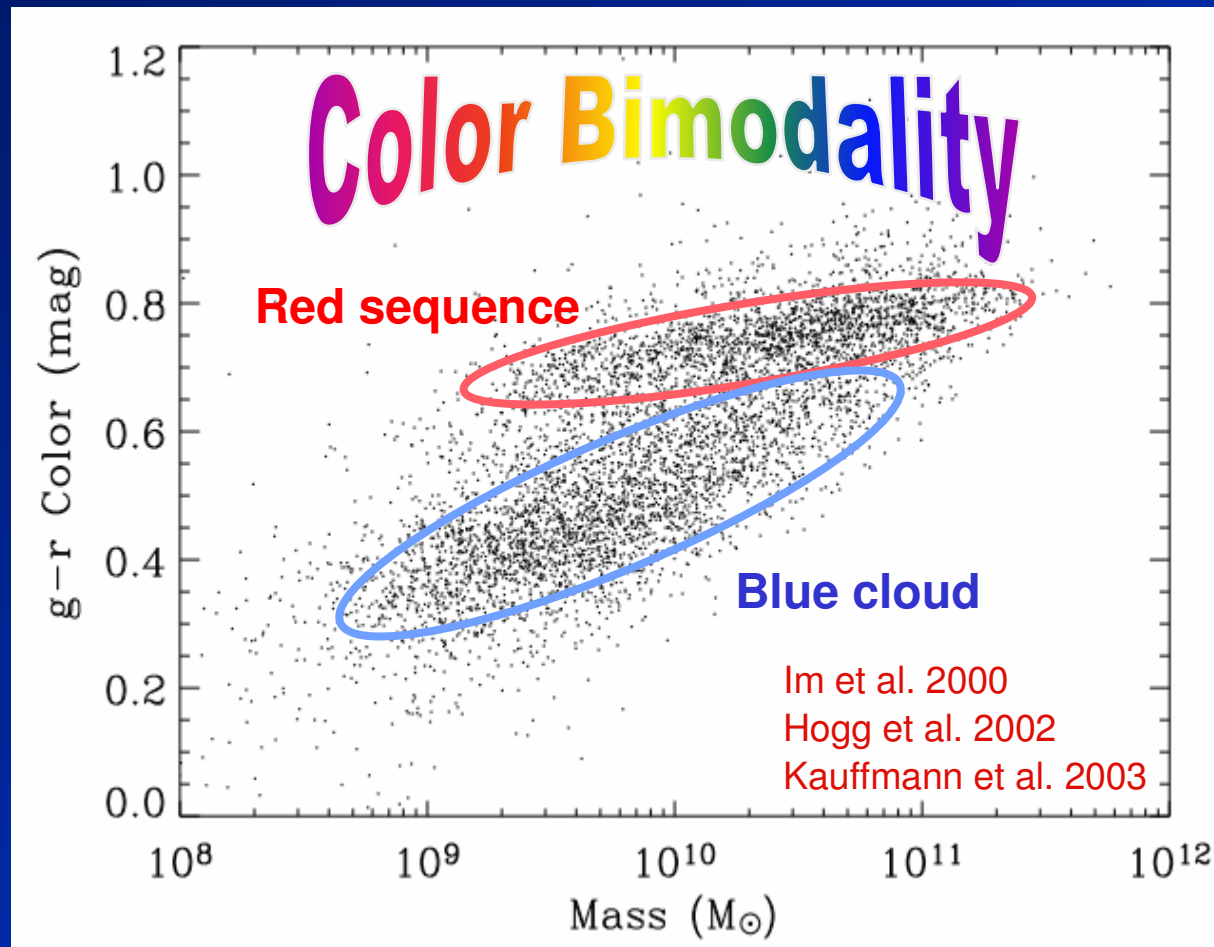
Young stars are blue  
Old stars are red

Spheroids are "red and dead"



# A major recent discovery: *color bimodality*

A color-magnitude diagram for nearby galaxies

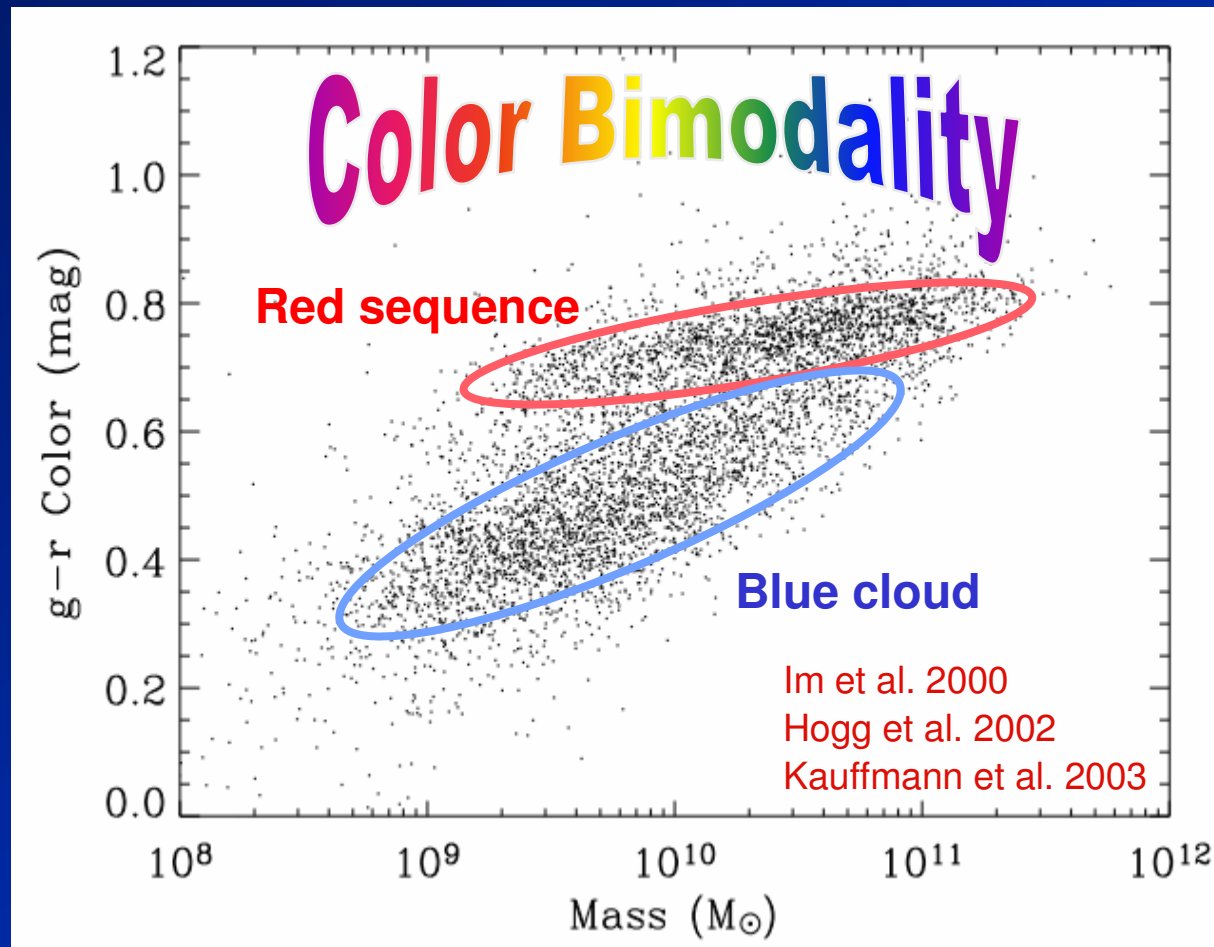


Color vs. stellar mass for Sloan Digital Sky Survey galaxies



# A major recent discovery: *color bimodality*

A color-magnitude diagram for nearby galaxies



Older stars

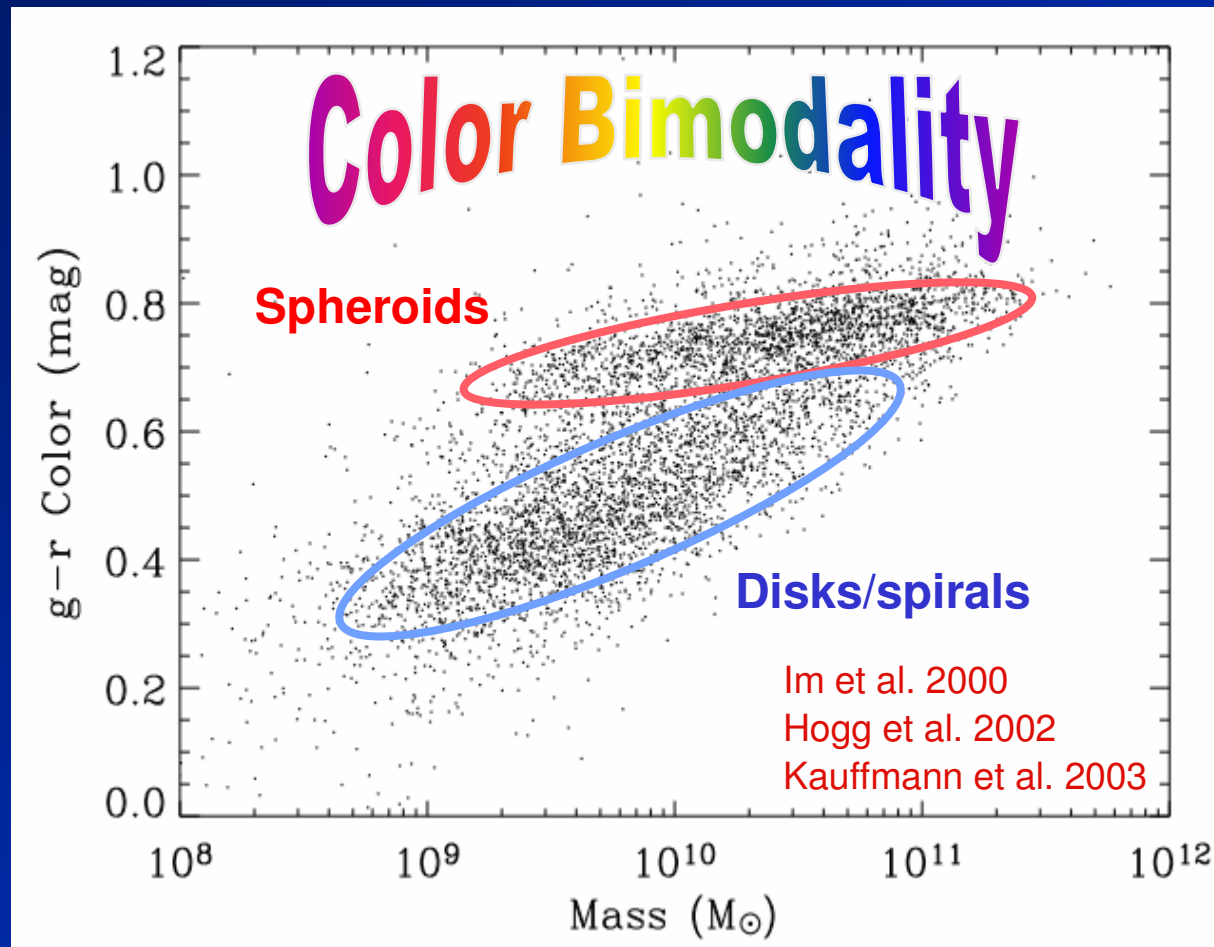


Younger stars

Color vs. stellar mass for Sloan Digital Sky Survey galaxies

# A major recent discovery: *color bimodality*

A color-magnitude diagram for nearby galaxies



Older stars



Younger stars

Color vs. stellar mass for Sloan Digital Sky Survey galaxies

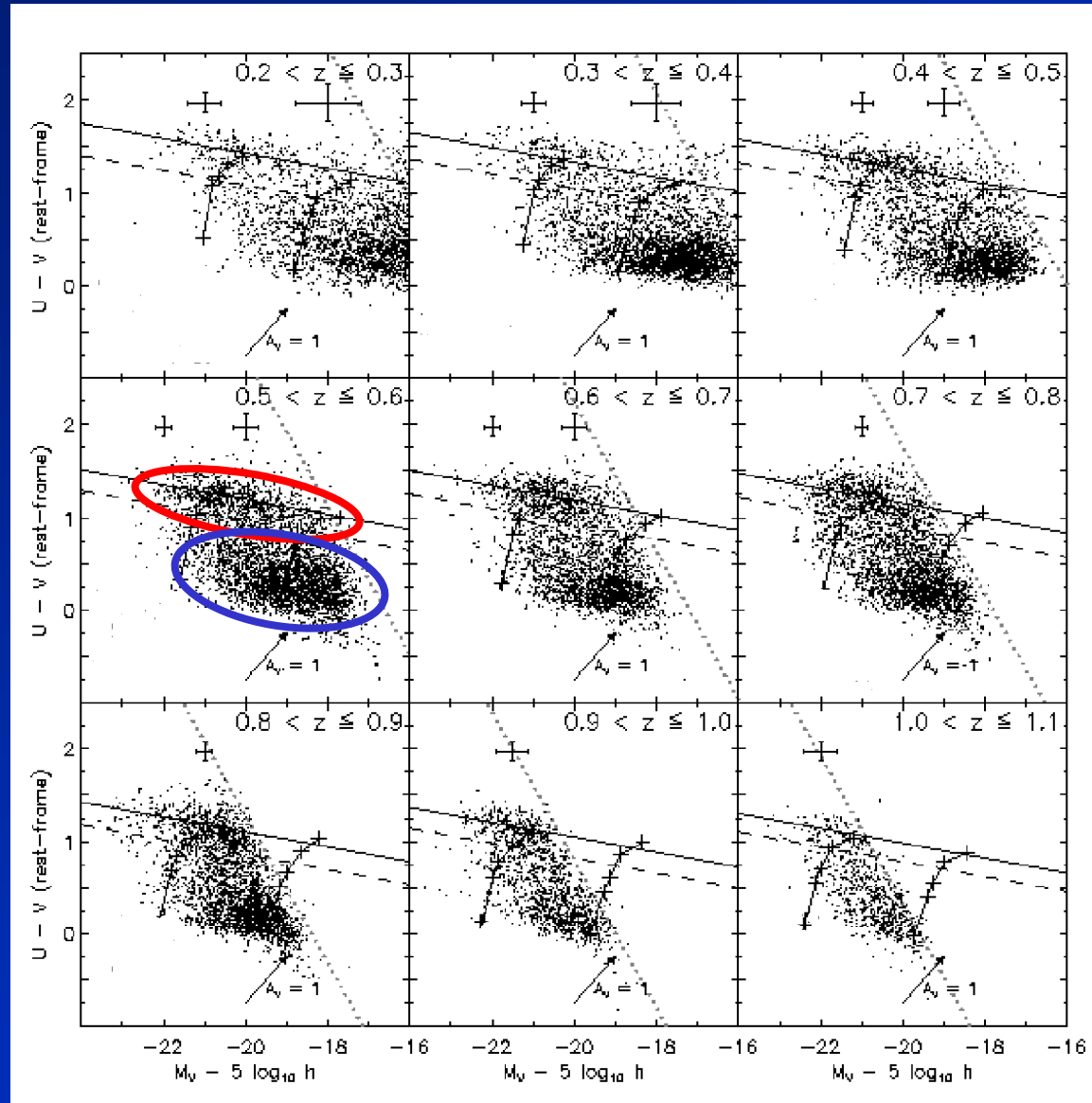


# Color bimodality continues out to at least $z \sim 1$

Combo-17 survey:  
25,000 galaxies

What causes color  
bimodality? At what  
epoch did it set in?

Bell et al. 2003



# Star formation in disk galaxies from $z \sim 1$ to the present



# ***Star-forming regions* as revealed by GALEX UV satellite**

UV shows young, hot stars

IR shows old, cool stars

**M101, a nearby Sc galaxy**



**Ultraviolet  
GALEX**



**Visible  
DSS**



**Near Infrared  
2MASS**

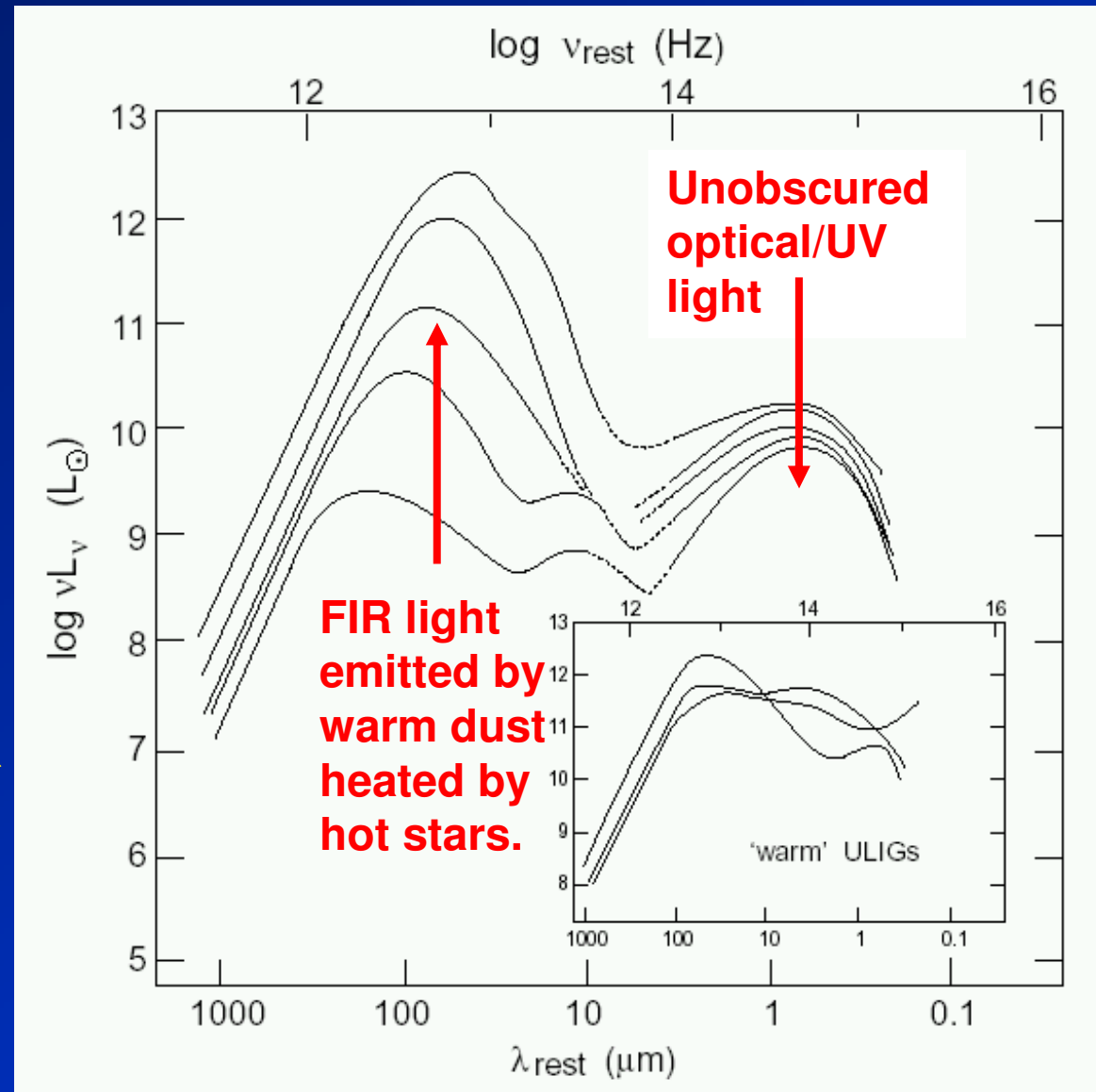
Star formation is triggered by motion of gas through the spiral pattern. Stars form when gas enters arm, gets shocked and compressed. Newly formed, young, hot, blue stars are visible at UV wavelengths; outline spiral structure like “beads on a string.”

## Much star formation is *obscured by dust*, is visible only in the far IR

Bolometric luminosities can vary by a factor of 1000, yet optical luminosities are constant to  $\times 3$ .

For normal spirals, the fraction or total energy emitted in the FIR is  $\sim 50\%$ . For rapidly star-forming galaxies, the FIR component is much larger.

Sanders & Mirabel, Ann Rev, 34, 749, 1996



# Ways to measure star formation

Kennicutt, Ann Rev, 36, 189, 1998

I. Ultraviolet continuum intensity (GALEX): direct but obscured by dust

$$\text{SFR}(M_{\odot} \text{ year}^{-1}) = 1.4 \times 10^{-28} L_{\nu}(\text{ergs s}^{-1} \text{ Hz}^{-1}).$$

II.  $\text{H}\alpha$  emission intensity: most widely used, also obscured by dust

$$\text{SFR}(M_{\odot} \text{ year}^{-1}) = 7.9 \times 10^{-42} L(\text{H}\alpha) (\text{ergs s}^{-1})$$

III. [O II] 3727 emission intensity: obscured by dust, intrinsic scatter

$$\text{SFR}(M_{\odot} \text{ year}^{-1}) = (1.4 \pm 0.4) \times 10^{-41} L[\text{OII}] (\text{ergs s}^{-1}),$$

IV. Far-IR continuum intensity: good for highly obscured regions

$$\text{SFR}(M_{\odot} \text{ year}^{-1}) = 4.5 \times 10^{-44} L_{\text{FIR}} (\text{ergs s}^{-1}) (\text{starbursts}),$$



# The “lookback effect”: an aid to studying galaxy formation

- The light of distant objects is redshifted owing to the expansion of the Universe. The light of farther objects is redshifted more. The ratio of the observed to emitted wavelength is given by:

$$\lambda_o/\lambda_e = (1 + z),$$

where the quantity **z** is termed the **redshift**.

- The **size of the Universe now** compared to its size when the light was emitted is also **(1+z)**.

- **Redshift is a measure of lookback time**, owing to the finite speed of light. Since the cosmological model is now tightly constrained, the relationship between redshift and epoch is well established (see Ned Wright’s website

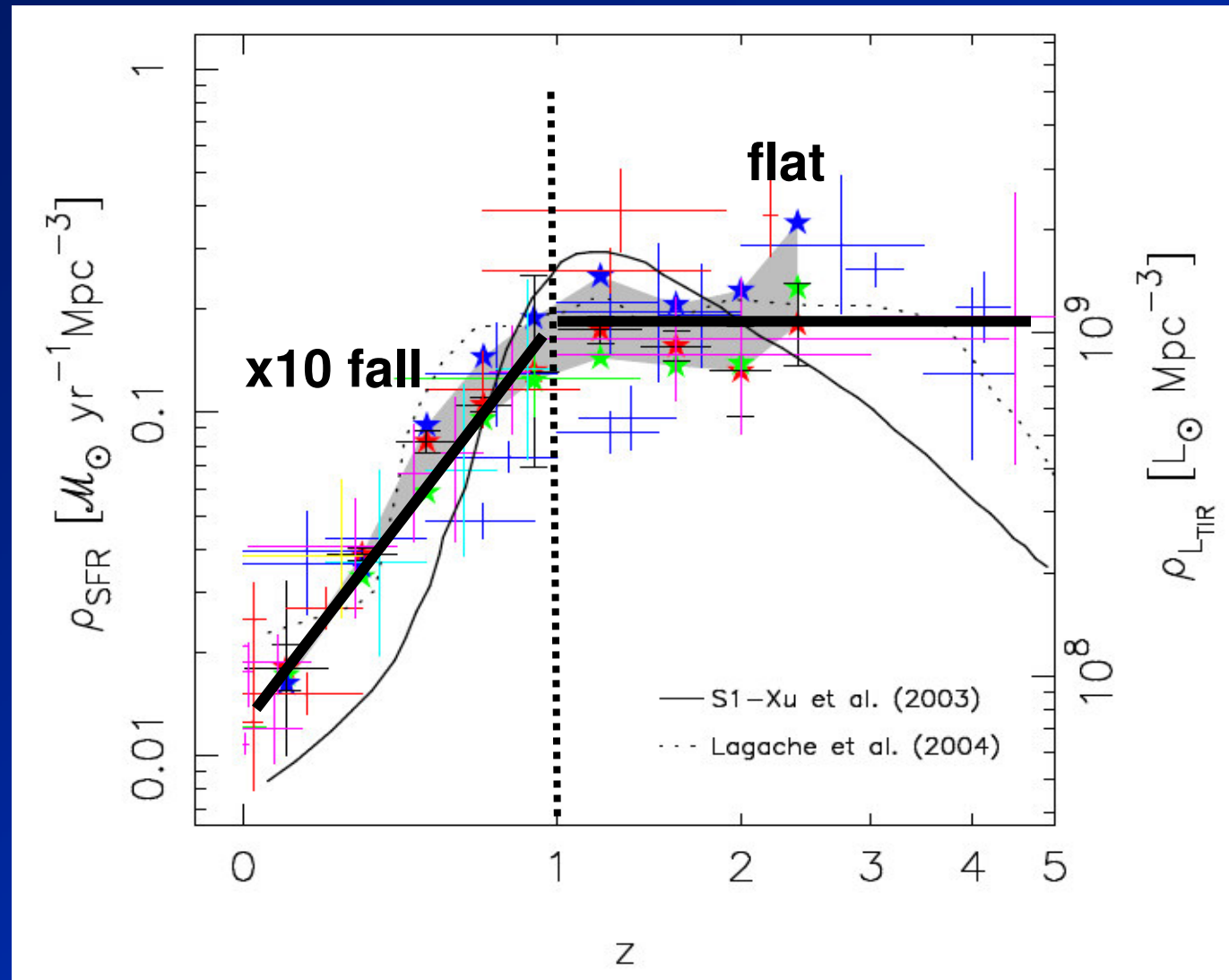
<http://www.astro.ucla.edu/~wright/CosmoCalc.html> for a handy cosmology calculator).

Here is a table of representative values with times in Gyr:

	z	time from Big Bang	lookback time	
My talk today	0.5	8.4	5.0	Age of Universe now = 13.5 Gyr
	1.0	5.7	7.7	
	2.0	3.2	10.2	
	3.0	2.1	11.4	
	5.0	1.2	12.3	
	10.0	0.5	13.0	

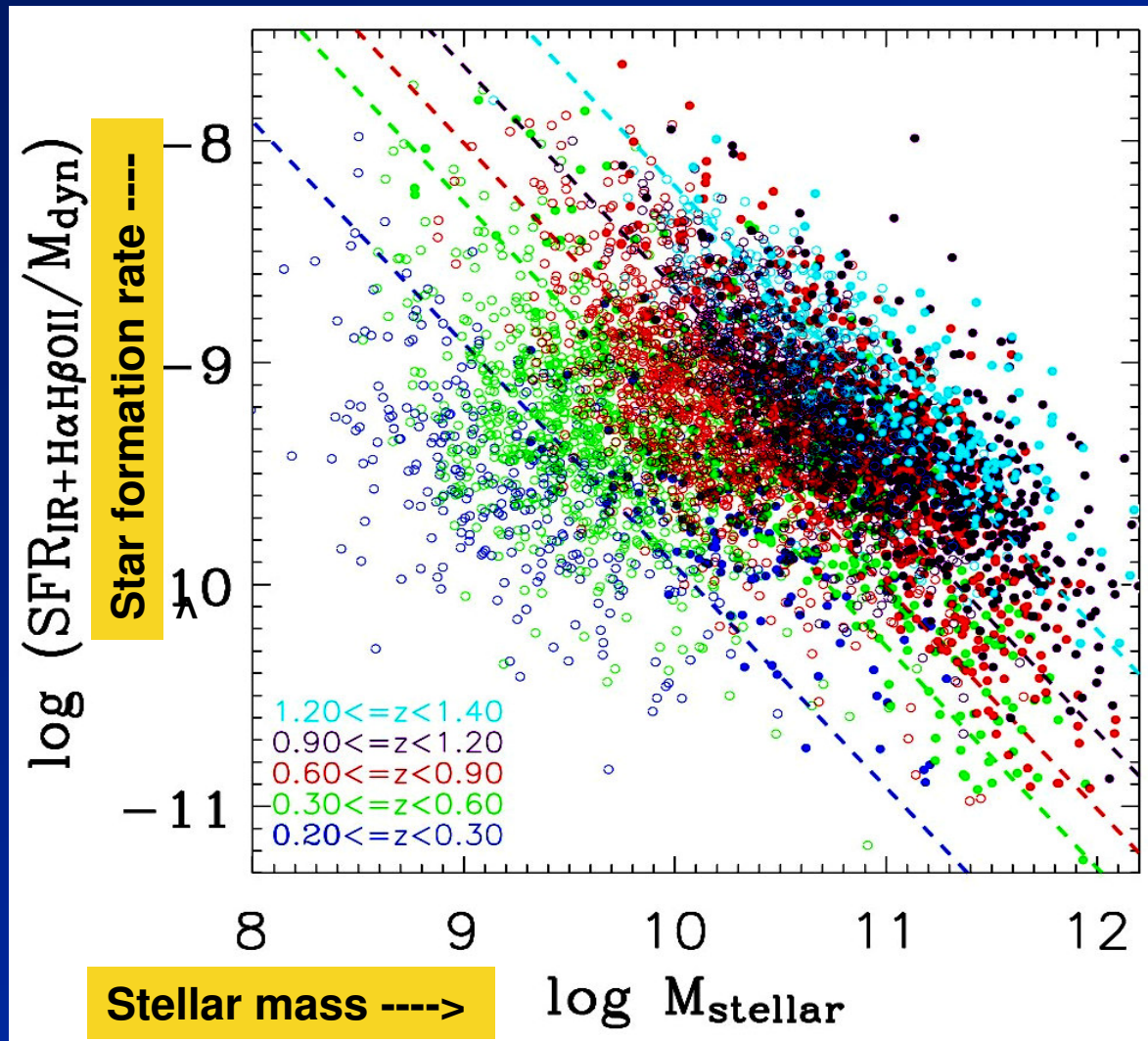
- Observing with large telescopes allows us to look far out in space, and therefore back in time. **We can make a “cosmic movie” of the formation of structure in the Universe by combining snapshots of galaxies and other data at different epochs.** When our theory of structure formation is correct, all snapshots will fit properly together. This is the ultimate test of

# The star-formation history of the Universe



Current version of the “*Madau diagram*” from Perez-Gonzalez et al. 2005

# The *star-formation histories of galaxies* broken down by stellar mass--recent Spitzer IR data



**Solid dots:** SFR from both MIPS + DEEP2 emission lines

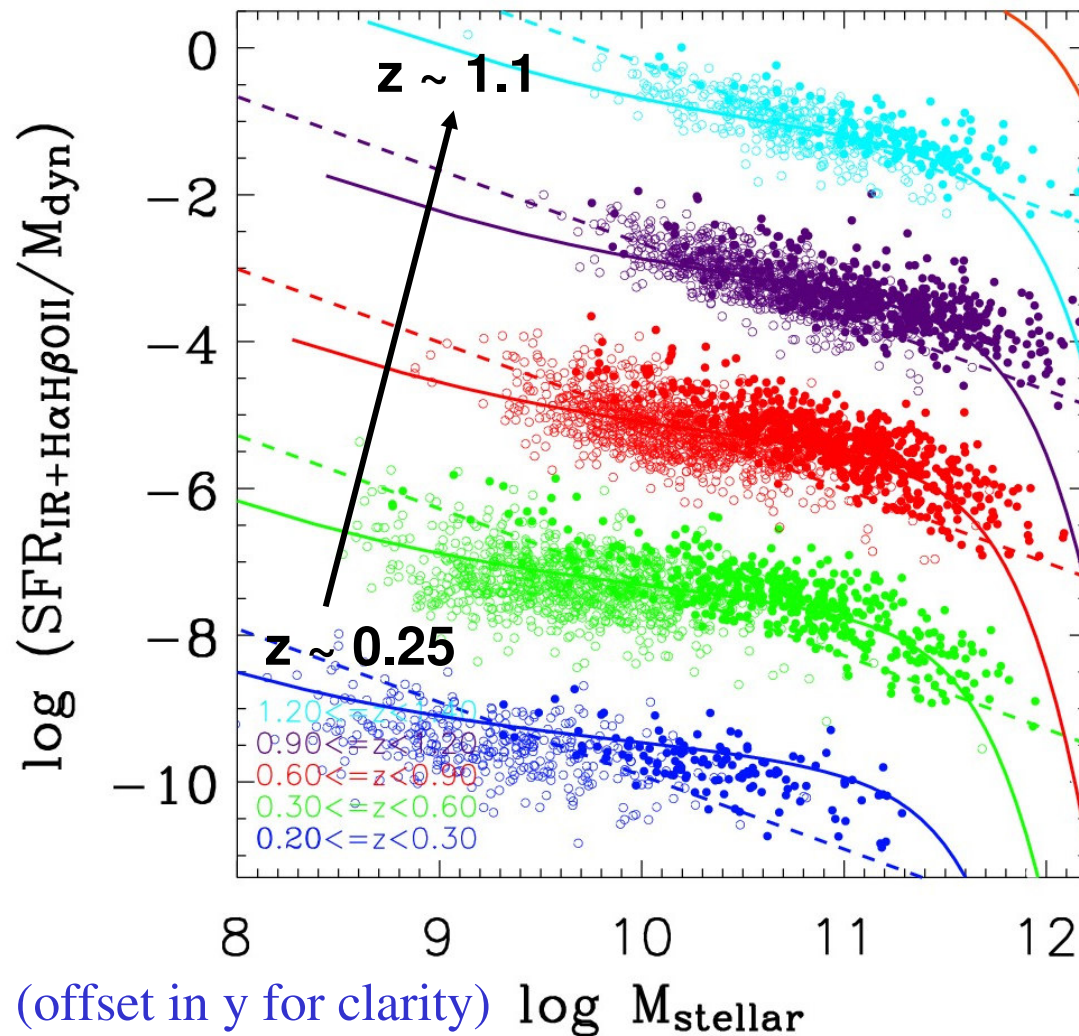
**Open circles:** SFR from DEEP2 emission lines (extinction-corrected)

**Dashed lines:** MIPS 24  $\mu$  80% completeness limit at center of redshift bin

Note the general rise at fixed stellar mass back in time. **The overall SFR in the Universe has fallen by x10** after  $z = 1$ .

Noeske et al. 2006

# A smoothly declining *exponential model* fits the star-forming histories of most galaxies



Noeske et al. 2006

The model has

$$\text{SFR} \sim e^{-t/\tau(M)}$$

starting at  $z_f$ , where

$$z_f = 4.5 \times (M_*/10^{12})^{0.33} - 1$$

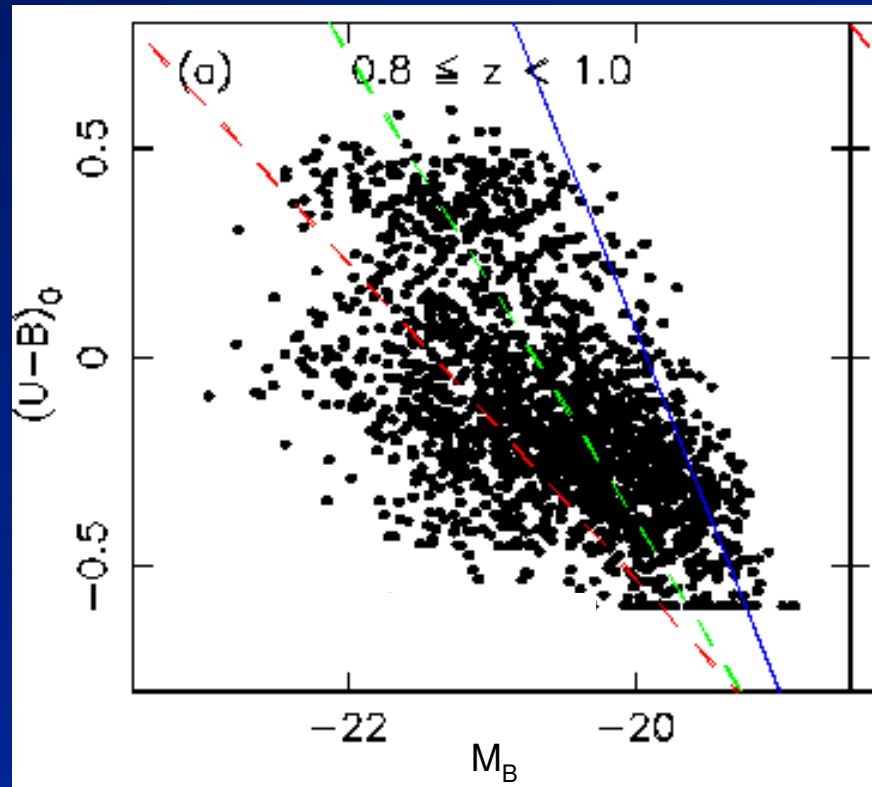
and

$$\tau(M) = 1 \text{ Gyr} \times (M_*/10^{11})^{-1}.$$

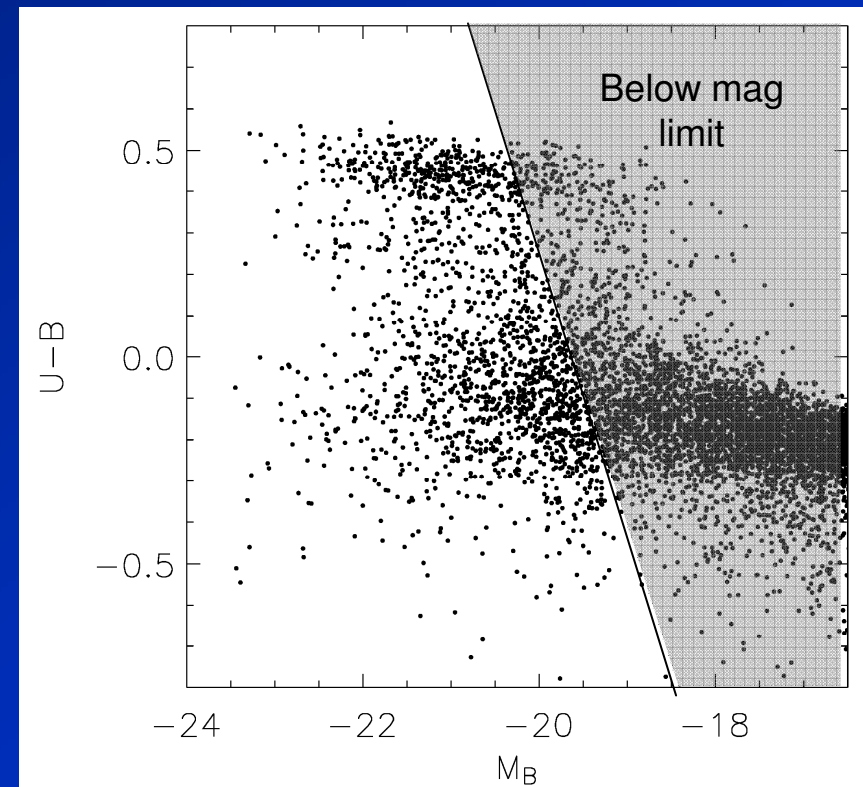
In the model, *larger galaxies start forming stars sooner and decline more rapidly (downsizing, Cowie et al. 1996)*. The stellar populations in larger galaxies are older. Most star formation seems to be in “quiescent” mode; the contribution by “starbursts” seems to be relatively small.



The model produces color-magnitude bimodality automatically by *shutting off SFR in massive galaxies at late times*. This is probably a clue to how it really happens



Actual CM diagram of distant galaxies from DEEP2 survey (Willmer et al. 2006)



Model CM diagram using SFR model, Noeske et al. 2006

# Dark matter halos

Navarro, Frenk & White, ApJ, 462, 563, 1996

## *NFW dark-matter halo density profile*

smooth curves represent fits to the simulation data using a model of the form proposed by Navarro et al. (1995c),

$$\frac{\rho(r)}{\rho_{\text{crit}}} = \frac{\delta_c}{(r/r_s)(1 + r/r_s)^2}, \quad (3)$$

where  $r_s = r_{200}/c$  is a characteristic radius and  $\rho_{\text{crit}} = 3H^2/8\pi G$  is the critical density ( $H$  is the current value of Hubble's constant);  $\delta_c$  and  $c$  are two dimensionless parameters. Note that  $r_{200}$  determines the mass of the halo,  $M_{200} = 200\rho_{\text{crit}}(4\pi/3)r_{200}^3$ , and that  $\delta_c$  and  $c$  are linked by the requirement that the mean density within  $r_{200}$  should be  $200 \times \rho_{\text{crit}}$ . That is,

$$\delta_c = \frac{200}{3} \frac{c^3}{[\ln(1 + c) - c/(1 + c)]}. \quad (4)$$

We will refer to  $\delta_c$  as the characteristic overdensity of the halo, to  $r_s$  as its scale radius, and to  $c$  as its concentration.

Navarro, Frenk & White, ApJ, 462, 563, 1996

*Radial density profiles of sample dark halos*

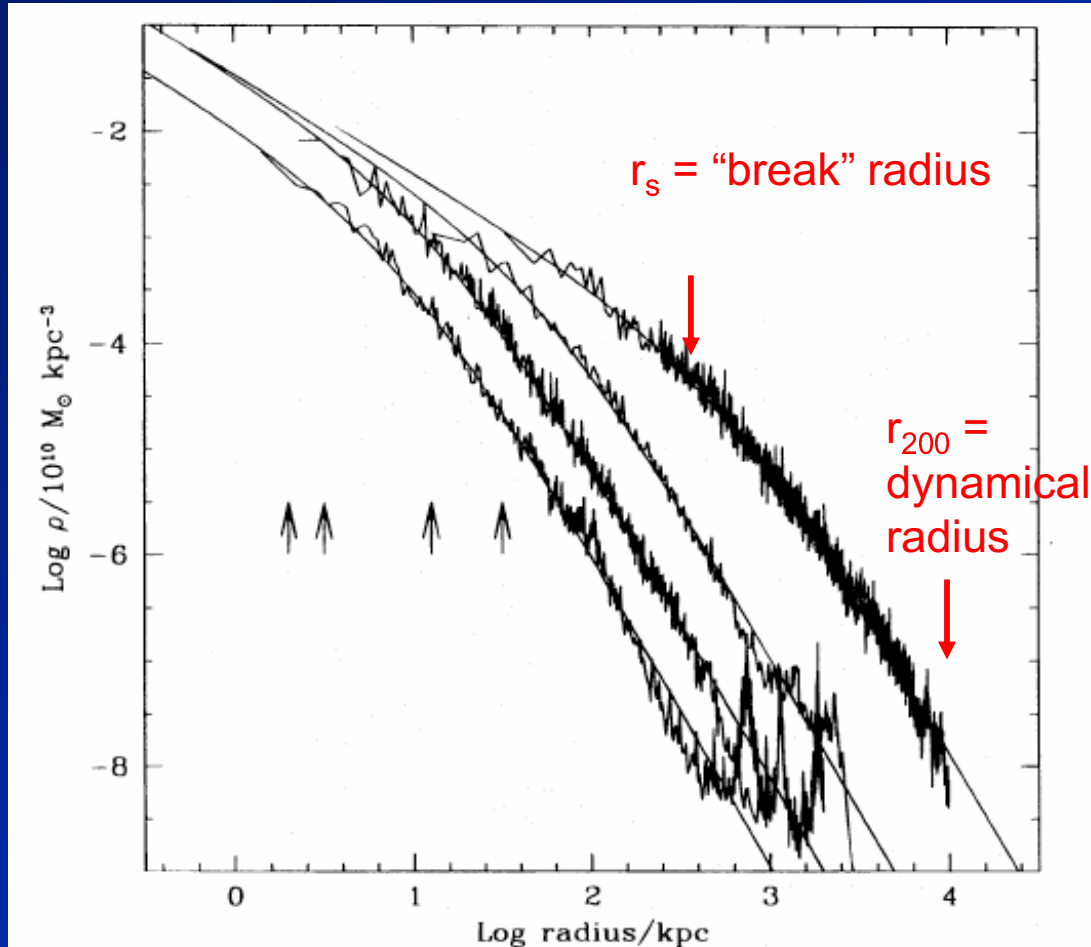


FIG. 3.—Density profiles of four halos spanning 4 orders of magnitude in mass. The arrows indicate the gravitational softening,  $h_g$ , of each simulation. Also shown are fits from eq. (3). The fits are good over two decades in radius, approximately from  $h_g$  out to the virial radius of each system.



Navarro, Frenk & White, ApJ, 462, 563, 1996

Circular velocity curves of dark halos. Note overall flatness.

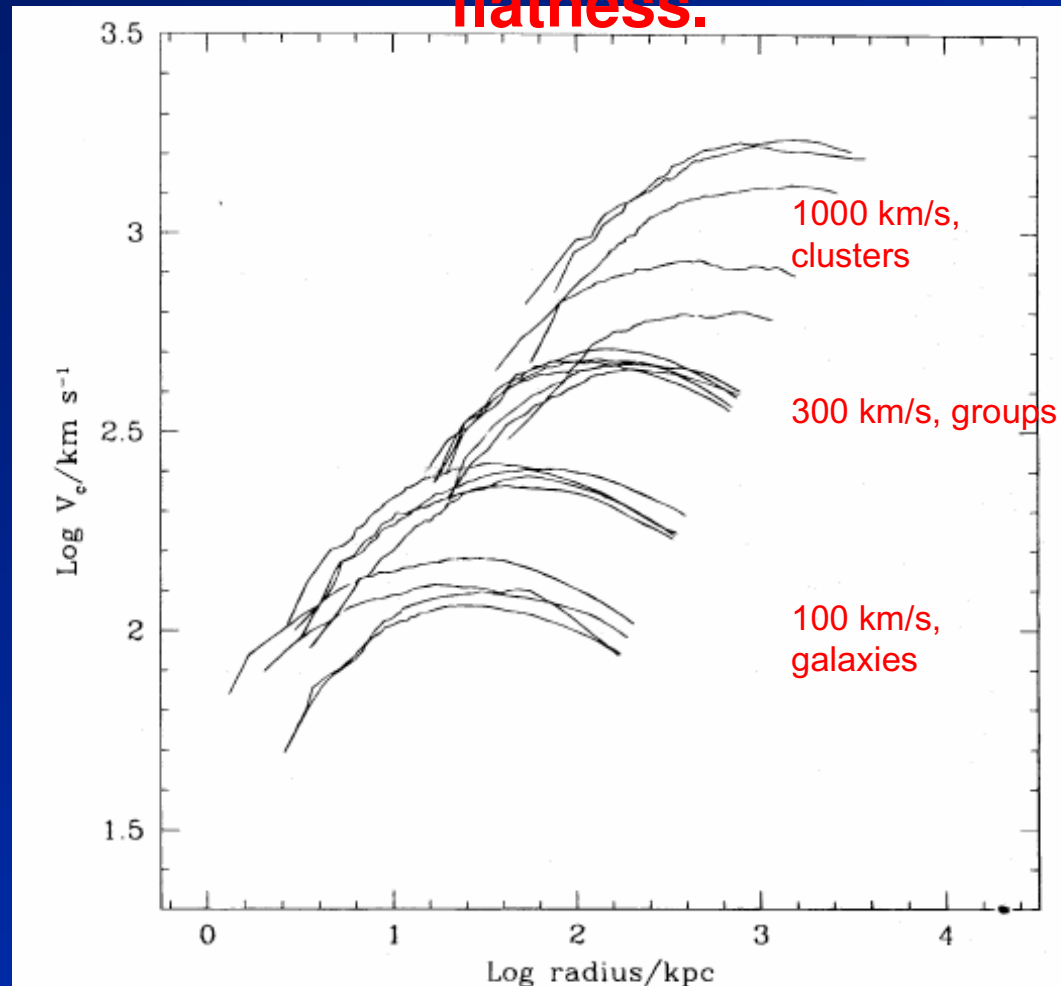
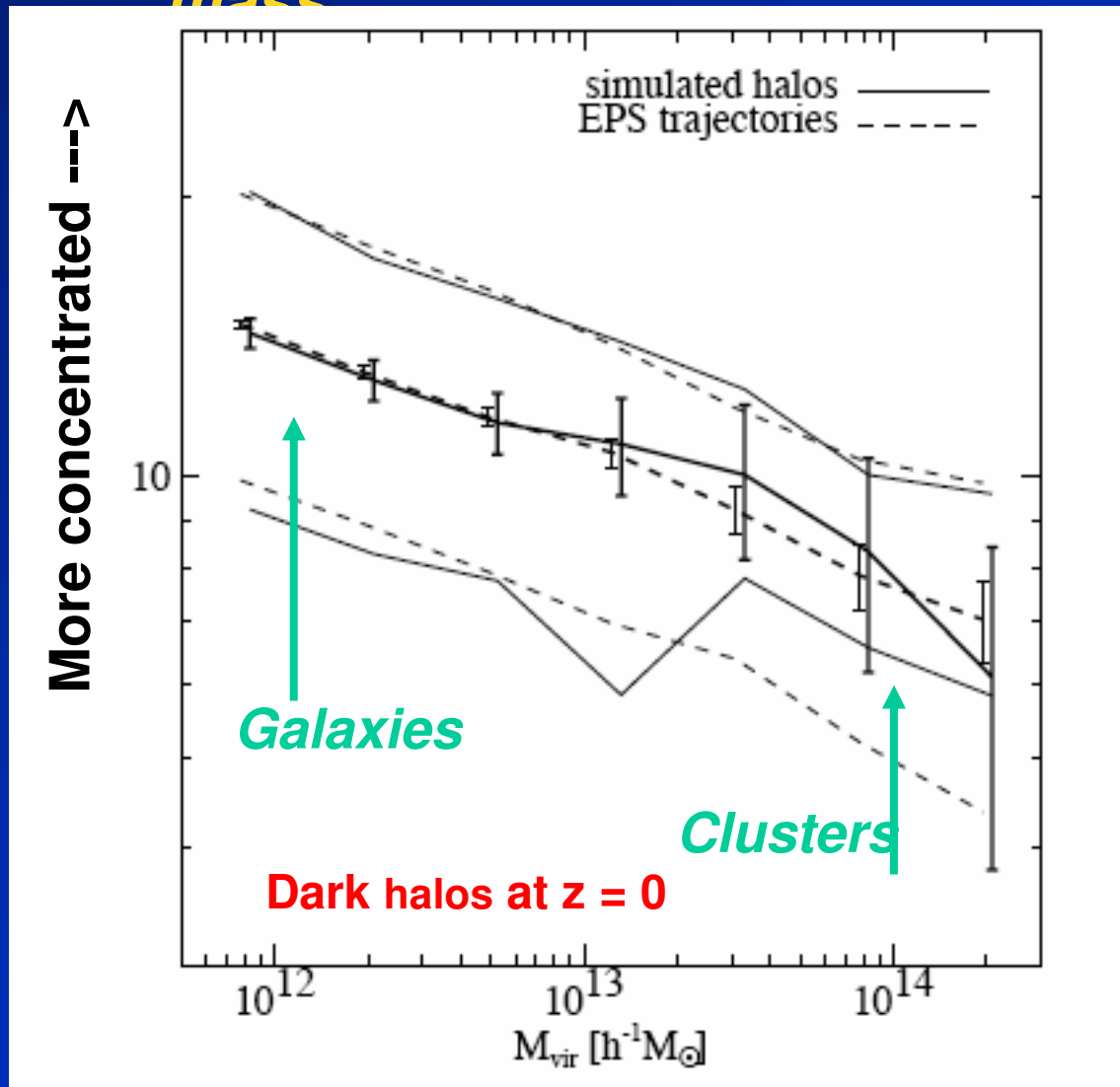


FIG. 5.—Circular velocity profiles of all 19 halos. The profiles are truncated at the virial radius,  $r_{200}$ . The gravitational softening is about  $10^{-2} \times r_{200}$ . Note that all profiles have the same shape.

Wechsler et al., ApJ, 658, 52, 2002

The profile shapes of dark halos *correlate closely with their mass*

Galaxy-sized halos  
are more  
concentrated than  
cluster-sized halos.

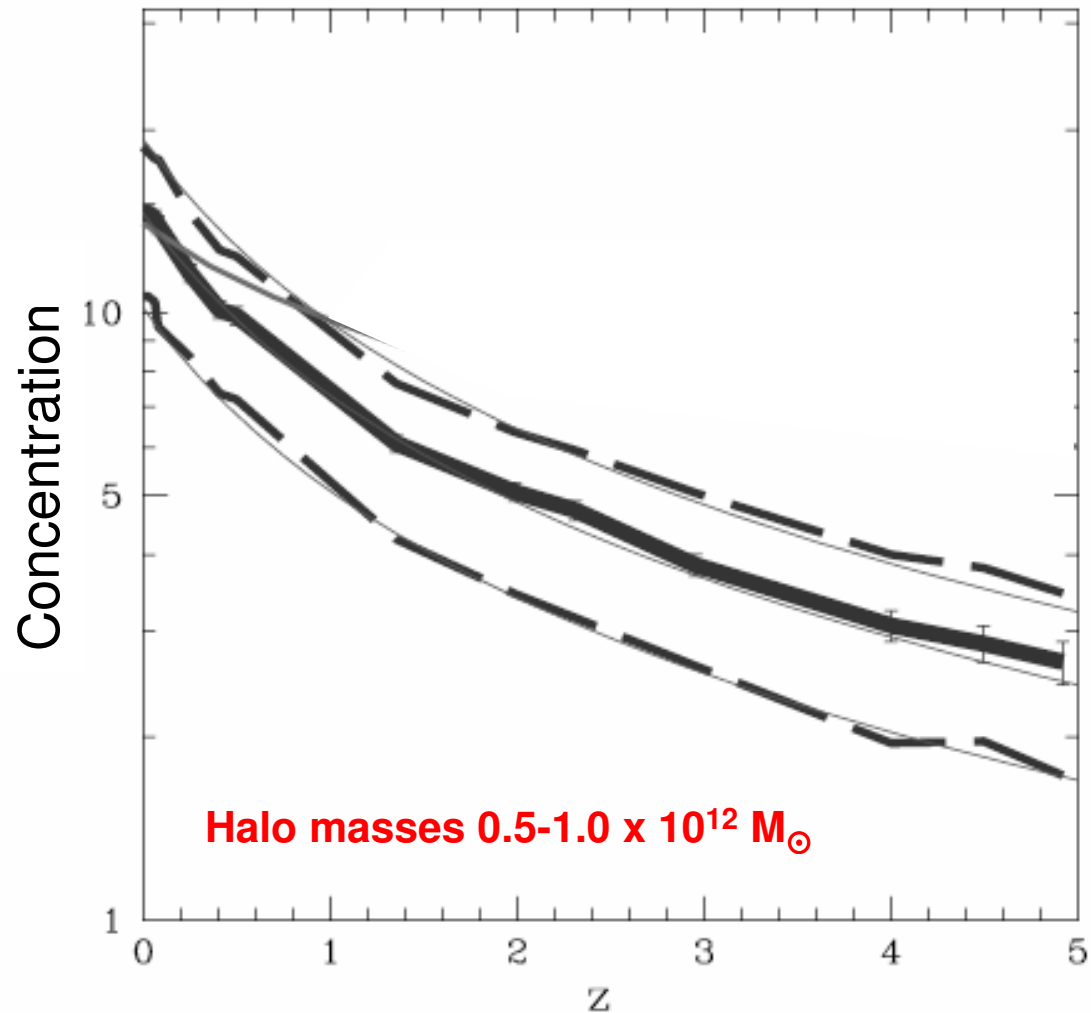


Bullock et al., MN, 321, 559, 2001

Dark halo concentrations also vary smoothly with redshift. High-redshift (early) halos are *less concentrated* than later

Concentration is an example of a *larger point*--the numbers, masses, sizes, and shapes of dark halos versus redshift are all *well understood*.

*We know how dark matter clusters.*



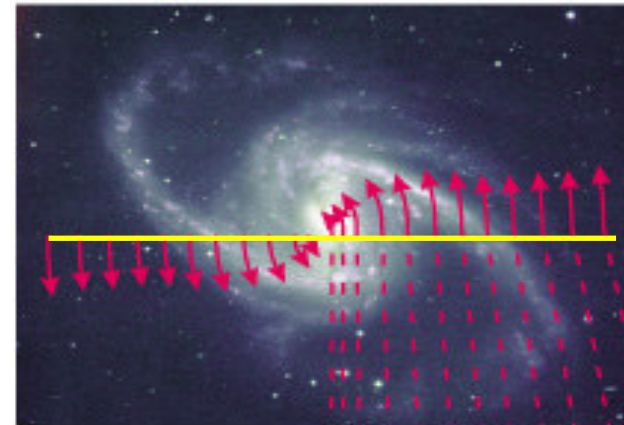
# **Disk galaxy rotation curves**



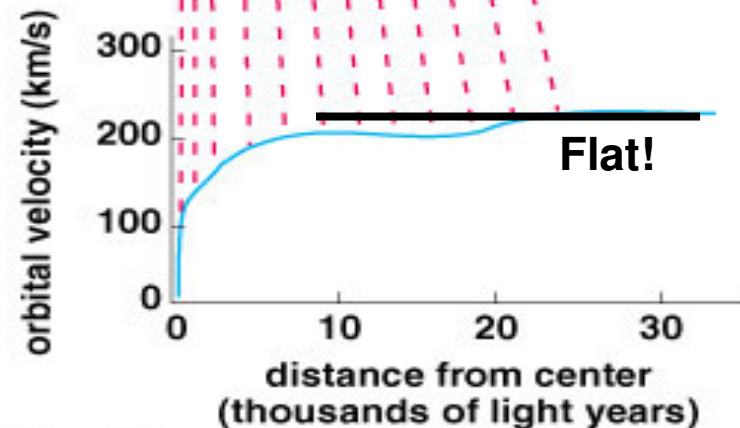
# The **rotation curve** shows the speed at which objects rotate around the center of a galaxy.

Interstellar gas clouds tend to be in nearly circular motion, and so the rotation speed of the gas is a good tracer of the **circular velocity profile** of the mass distribution.

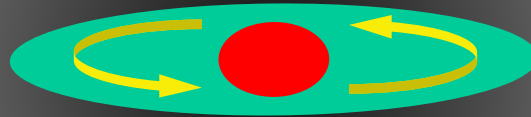
**Rotation curves** are measured by setting a spectrograph slit across the image of a galaxy. Emission lines appear in the spectrum from patches of gas that are ionized by the UV light of nearby hot, young stars. The **Doppler shift** of the emission frequency gives the average radial velocity of the galaxy, and the rotation speed is given by the difference in the shift between that point and the center.



Longer arrows represent larger orbital velocities.



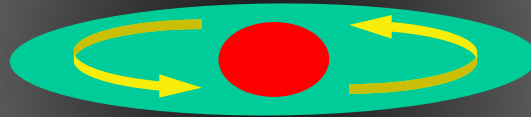
**The rotation curve is produced by a combination of matter in the disk, bulge, and dark halo**



**The enclosed mass is given by the circular speed  
and radius of the orbit.**

$$M(r) = v^2 r / G$$

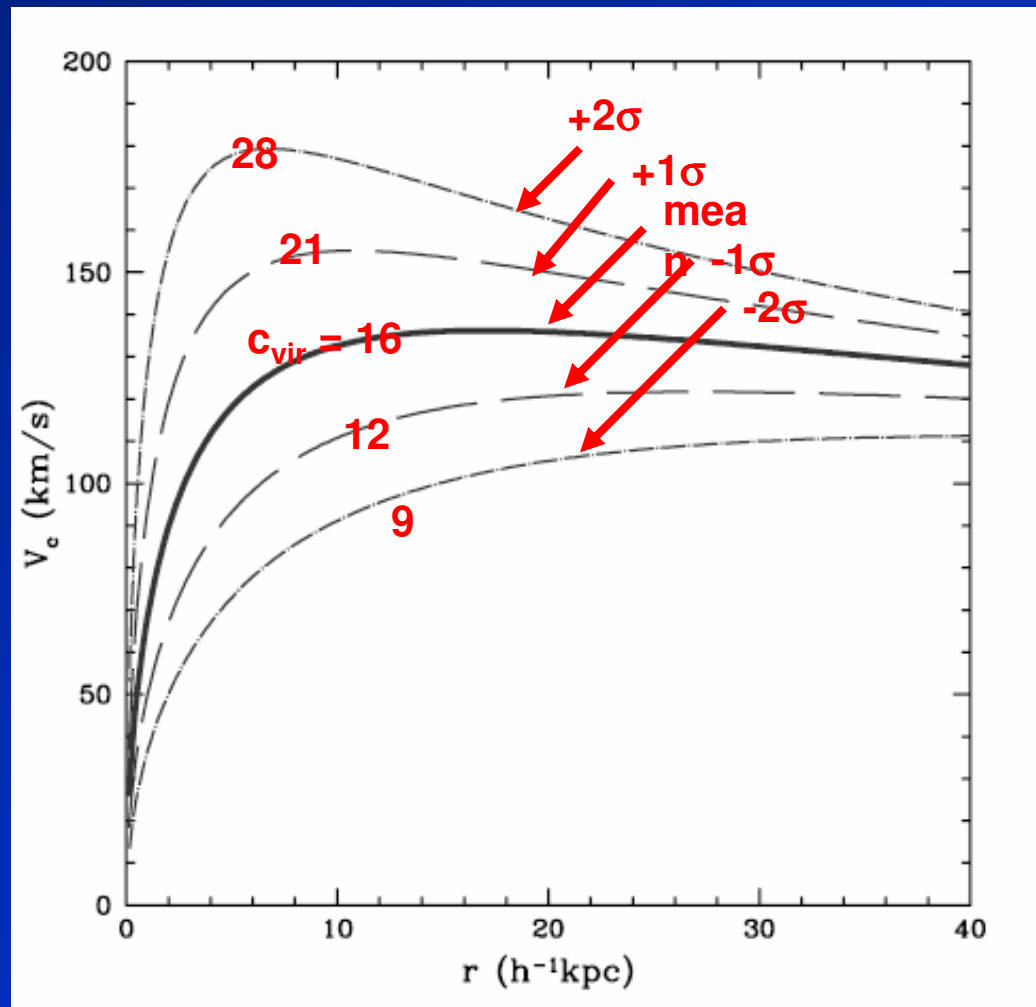
This is strictly valid only for a spherical mass distribution, but  
the correction for a flattened disk and spheroid is small,  
~10%.



Bullock et al., MN, 321, 559, 2001

Halo concentration affects the shape of the rotation curve. Here are a selection of rotation curves for halos of the same mass ( $3 \times 10^{11} M_{\odot}$ ) but different concentrations.

The circular velocity curves here reflect the dark matter halo only. Rotation curves of real galaxies are affected by baryonic infall and thus possibly **adiabatic contraction**. But the underlying distribution of dark matter by itself clearly has a big effect.





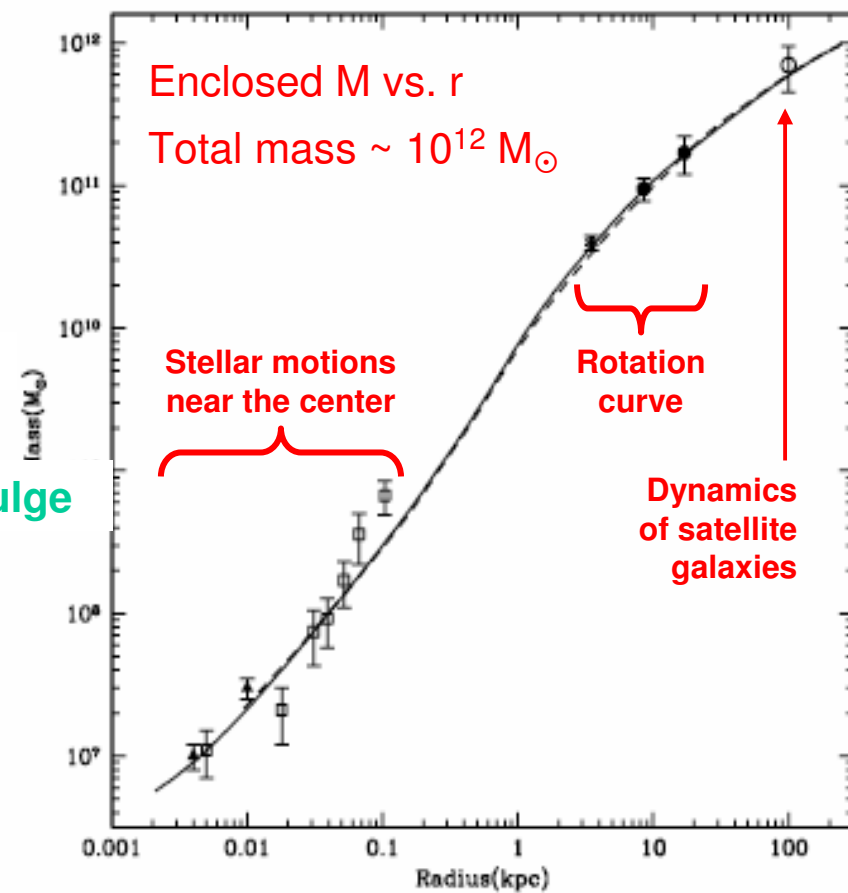
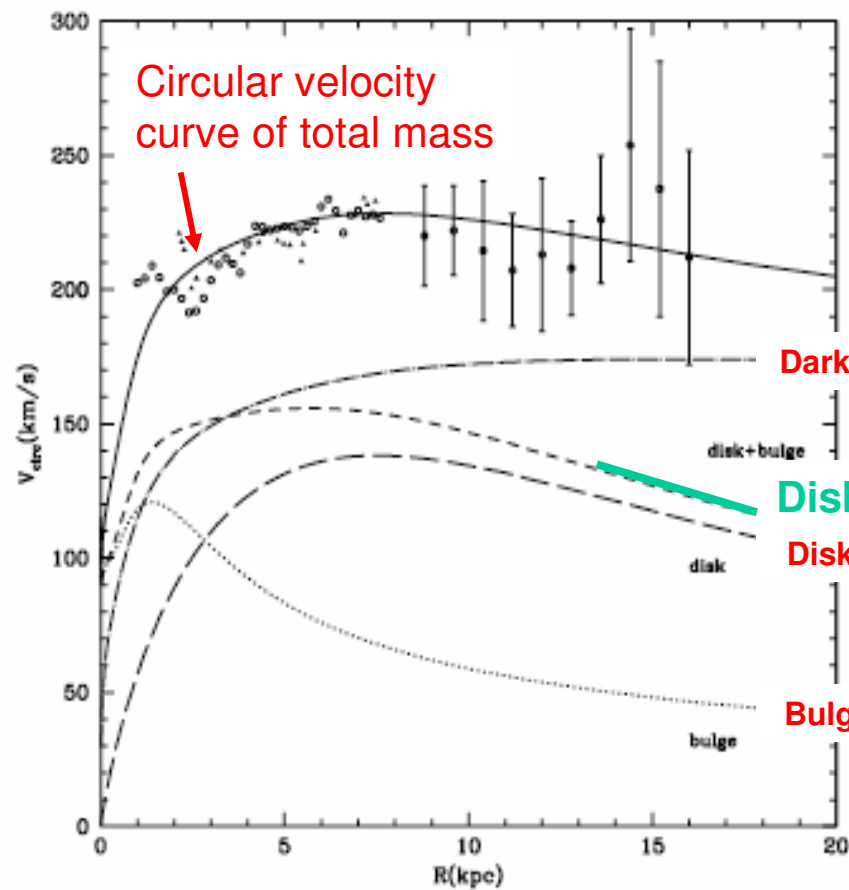
Klypin, Zhao & Somerville, ApJ, 573, 597, 2002

**Model Milky Way Galaxy:** decomposed circular velocity curves of dark matter halo, disk, and bulge, based on motions of various subpopulations

606

KLYPIN, ZHAO, & SOMERVILLE

Vol. 573



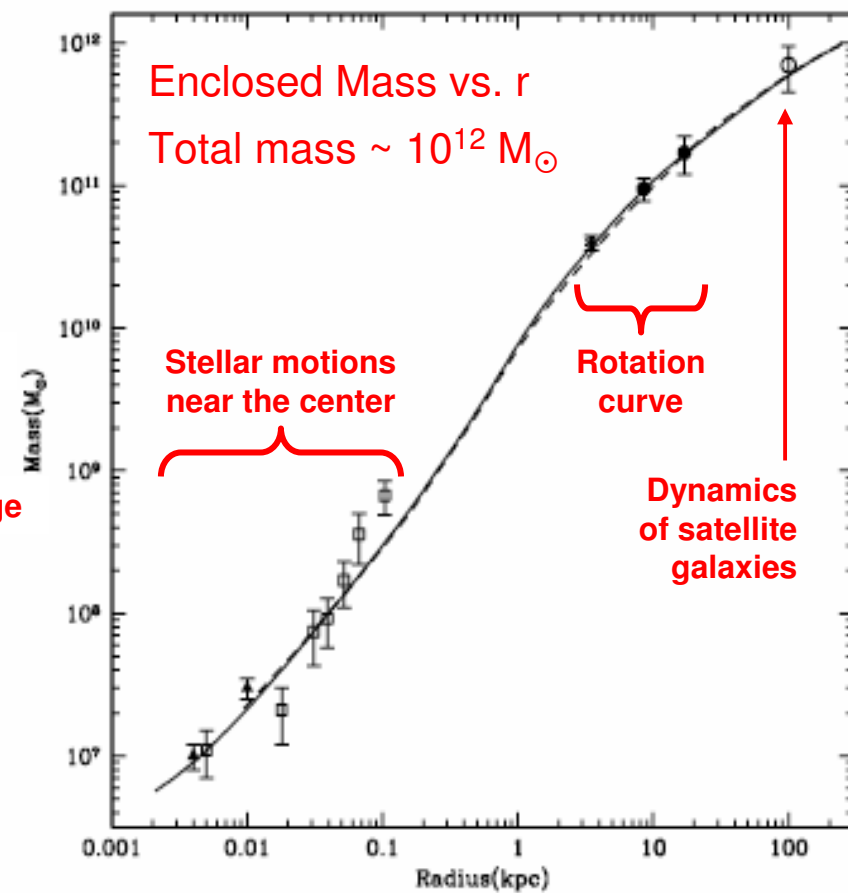
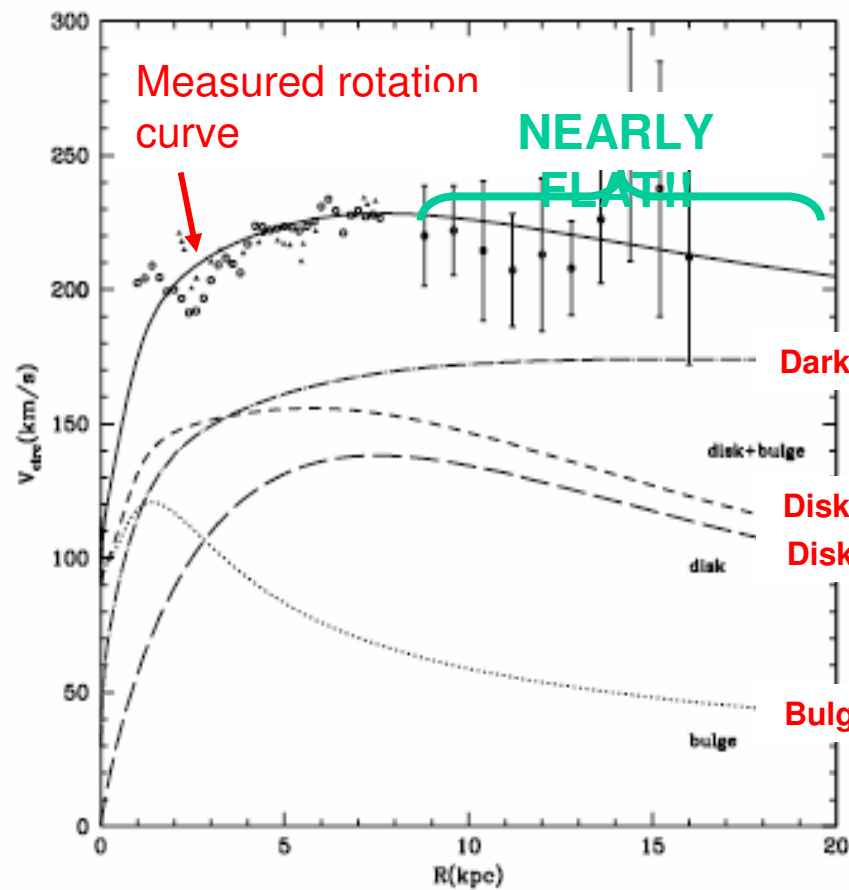
Note how **flat** the outer rotation curve of the Milky Way is. The predicted rotation curve from the disk and bulge is **falling**; the difference is made up by the dark matter. The Milky Way is typical--flat rotation curves are usually seen in the outer parts of disk galaxies.

**Flat rotation curves** in the outer parts of galaxies are one of the main pieces of evidence for dark halos.

606

KLYPIN, ZHAO, & SOMERVILLE

Vol. 573

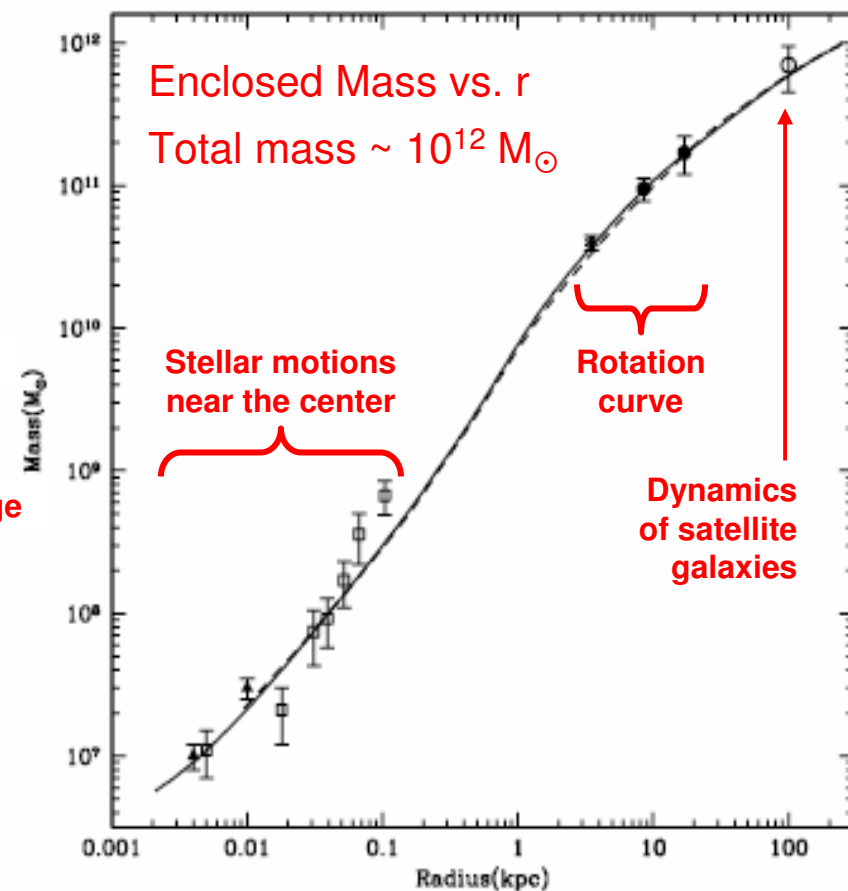
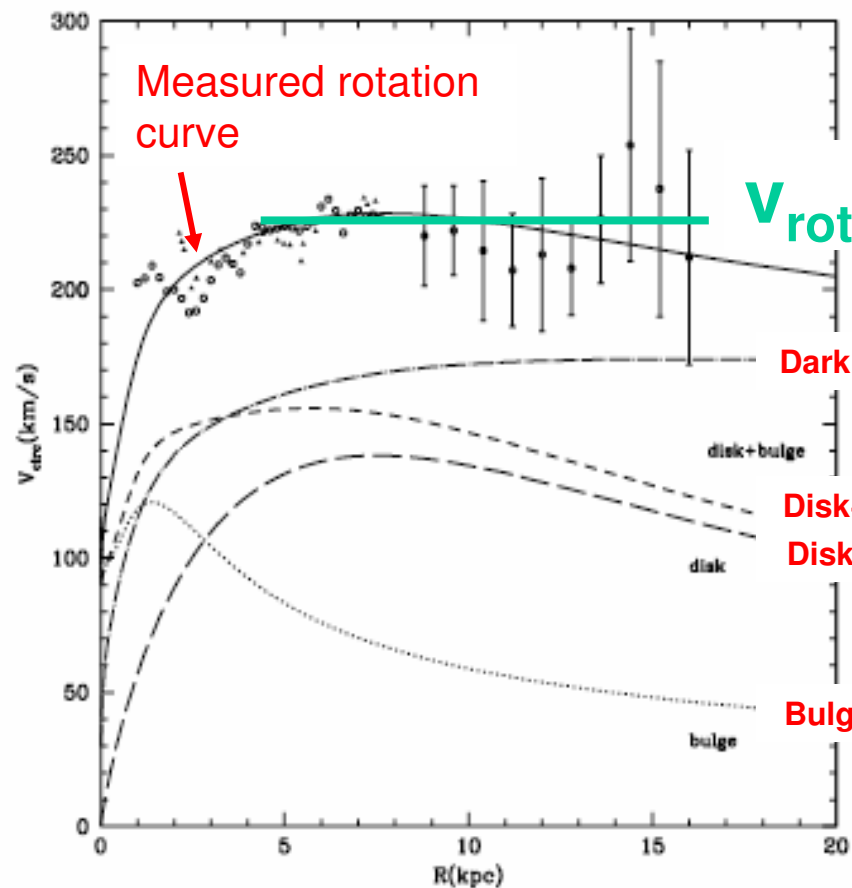


The rotation velocity on the flat part of the rotation curve is the *characteristic orbital speed*, denoted by  $V_{rot}$

606

KLYPIN, ZHAO, & SOMERVILLE

Vol. 573



# Disk galaxy brightness profiles

The classic disk light profile falls off *exponentially* with radius

$$\begin{aligned}\Sigma_d(r) &= \Sigma_e \exp \left[ -1.6783 \left( \frac{r}{r_e} - 1 \right) \right] = \exp(1.6783) \Sigma_e \exp \left( -\frac{1.6783}{r_e} r \right) \\ &= 5.3567 \Sigma_e \exp \left( -\frac{r}{r_e/1.6783} \right) = \Sigma_0 \exp \left( -\frac{r}{r_s} \right),\end{aligned}$$

$\Sigma_d$  = disk surface brightness profile

$r_e$  = effective radius (encloses half the light)

$r_s$  = radial exponential scale length of the light

$\Sigma_e$  = surface brightness at effective radius

$\Sigma_0$  = central surface brightness

The **scale length**  $r_s$  and **half-light radius**  $r_e$  are measures of disk size.

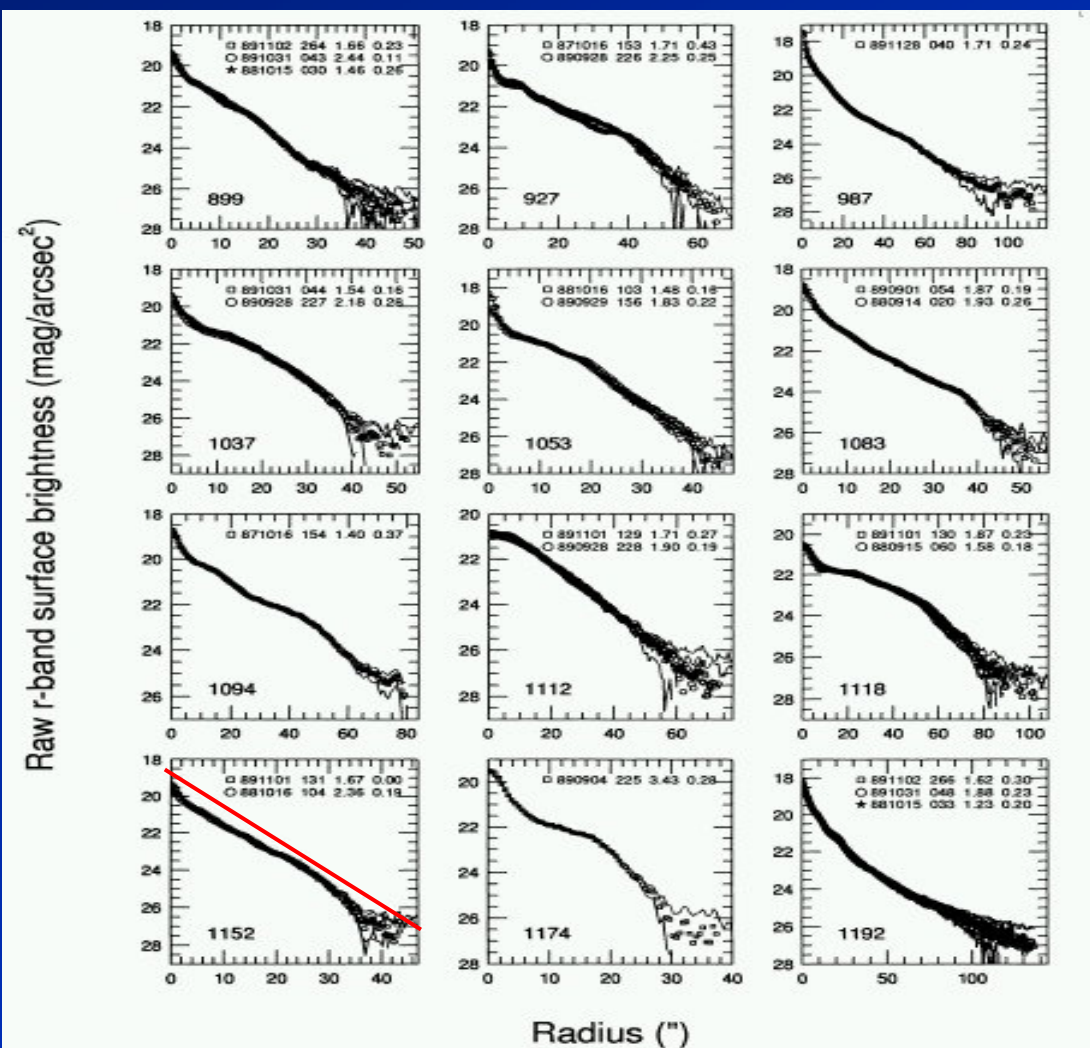


# Real disk surface brightness profiles are only approximately exponential.

Pure exponentials would be straight lines.

Typically there is excess brightness in the center and a drop-off at 4-5 scale lengths in the outer parts (not visible here).

But the exponential law is a useful approximation.



Courteau, ApJS, 103, 363, 1996

# Disk galaxy scaling laws

We have now accumulated some basic ***structural parameters*** for disk galaxies that compactly sum up their visible ***baryonic*** structure:

- \* Total luminosity or magnitude:  $M_B$  (luminosity in the blue band)
- \* Rotation velocity:  $v_{\text{rot}}$
- \* Disk radius:  $r_s$  or  $r_e$

When these quantities are plotted versus one another (in log-log coordinates) one finds power-law correlations called ***scaling laws***.

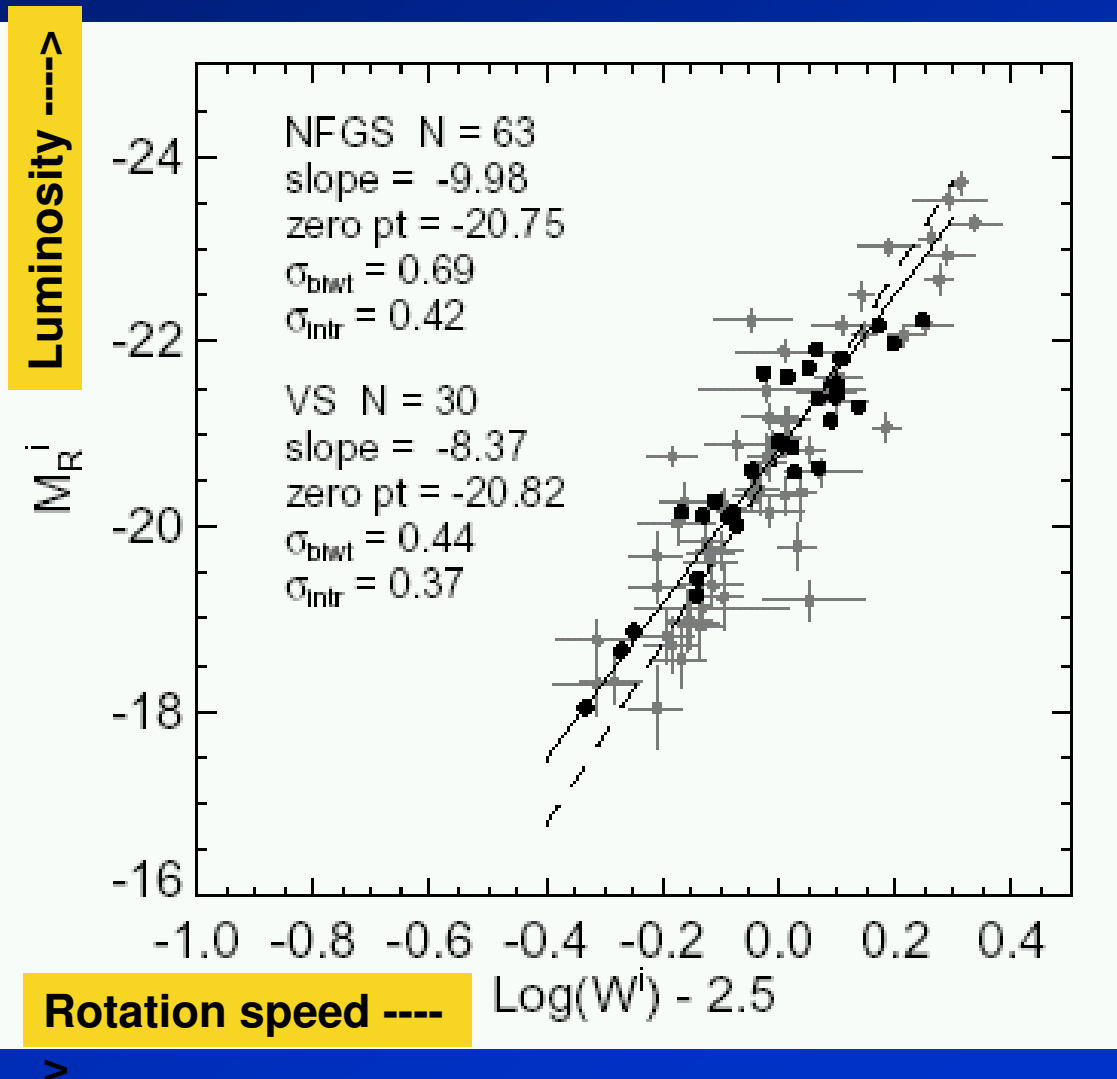
***Scaling laws are interesting because they preserve some memory of galaxy formation. Unlike stars, galaxies “remember” how they formed.***

# The *Tully-Fisher law* relates $v_{\text{rot}}$ and luminosity

The TF relation is the correlation between rotation speed and absolute magnitude for disk galaxies.

$W$  is **total linewidth**, which is close to but not exactly  $2v_{\text{rot}}$ .

The relation is approximately  $L \sim v^3$ .

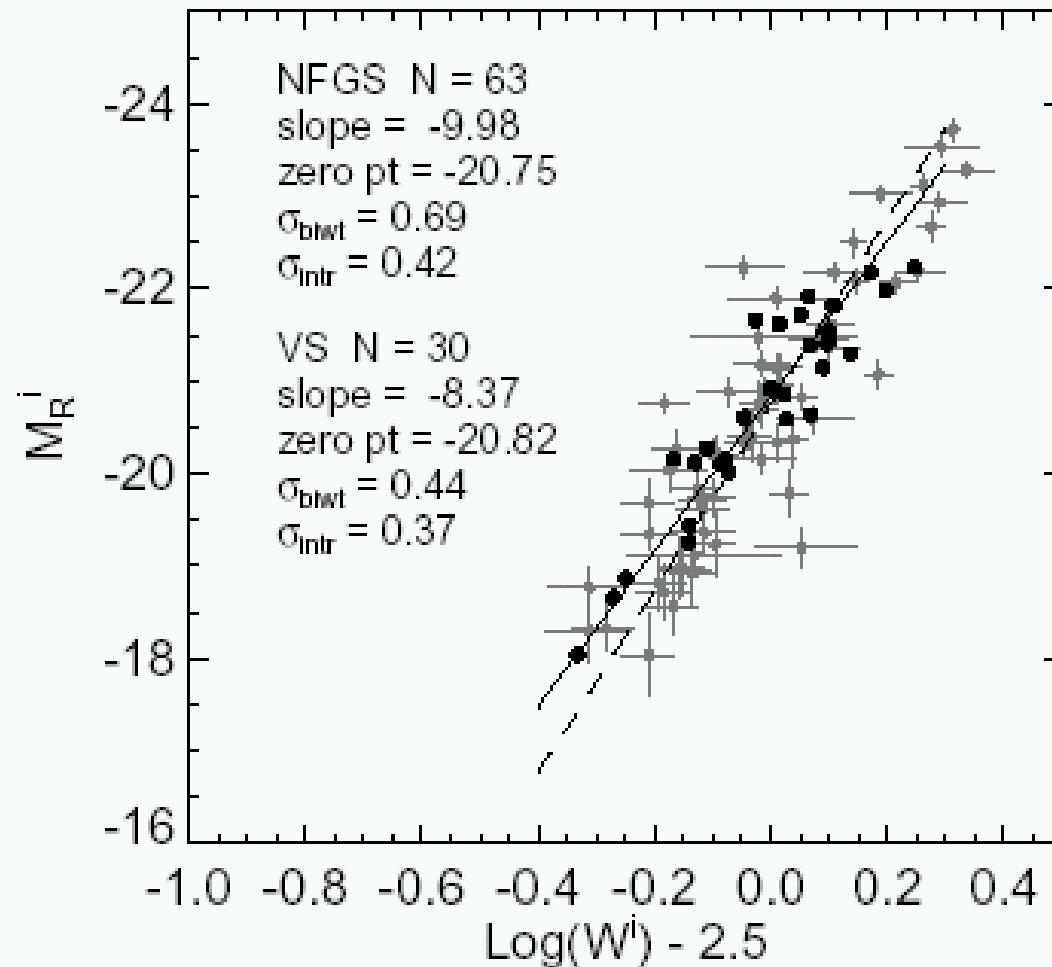


Kannappan et al., ApJ, 123, 2358, 2002

## The *Tully-Fisher law* relates $v_{\text{rot}}$ and luminosity

The scatter about the TF relation is only about 0.4 mag, and some of this is observational error. This means that ***mass-to-light ratio (M/L)*** scatters by only  $\sim \pm 30\%$  at a fixed point on the plane.

***The star-formation histories of structurally similar disk galaxies are remarkably similar.***

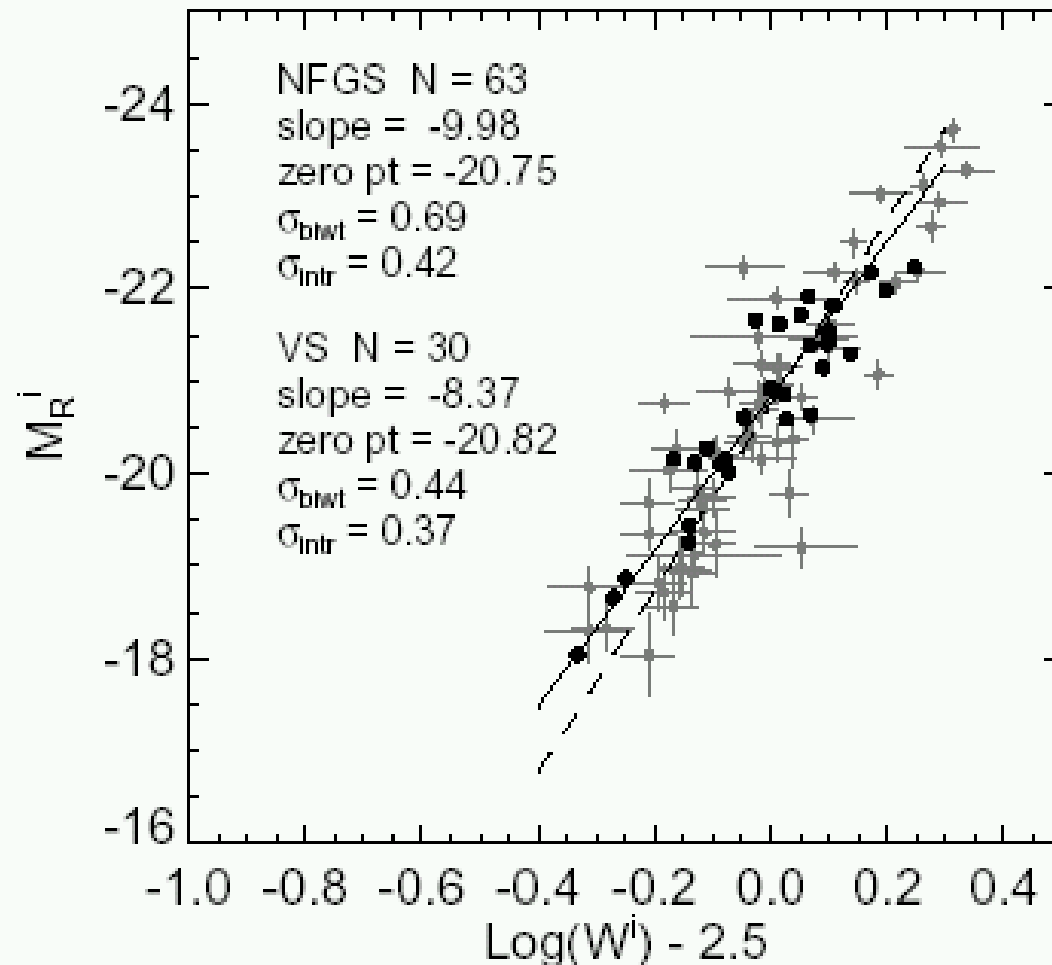


# The *Tully-Fisher law* relates $v_{\text{rot}}$ and luminosity

The TF relation is the **virial plane** of disk galaxies seen edge on. Galaxies in gravitational equilibrium obey

$$M \sim v^2 R / G.$$

This makes a plane in  **$M, v, R$ -space**. If  $L$  is well-behaved versus  $M$ , then we also have a plane in  **$L, v, R$ -space**. The TF relation for disks views this plane **edge-on**, making a tight relation.



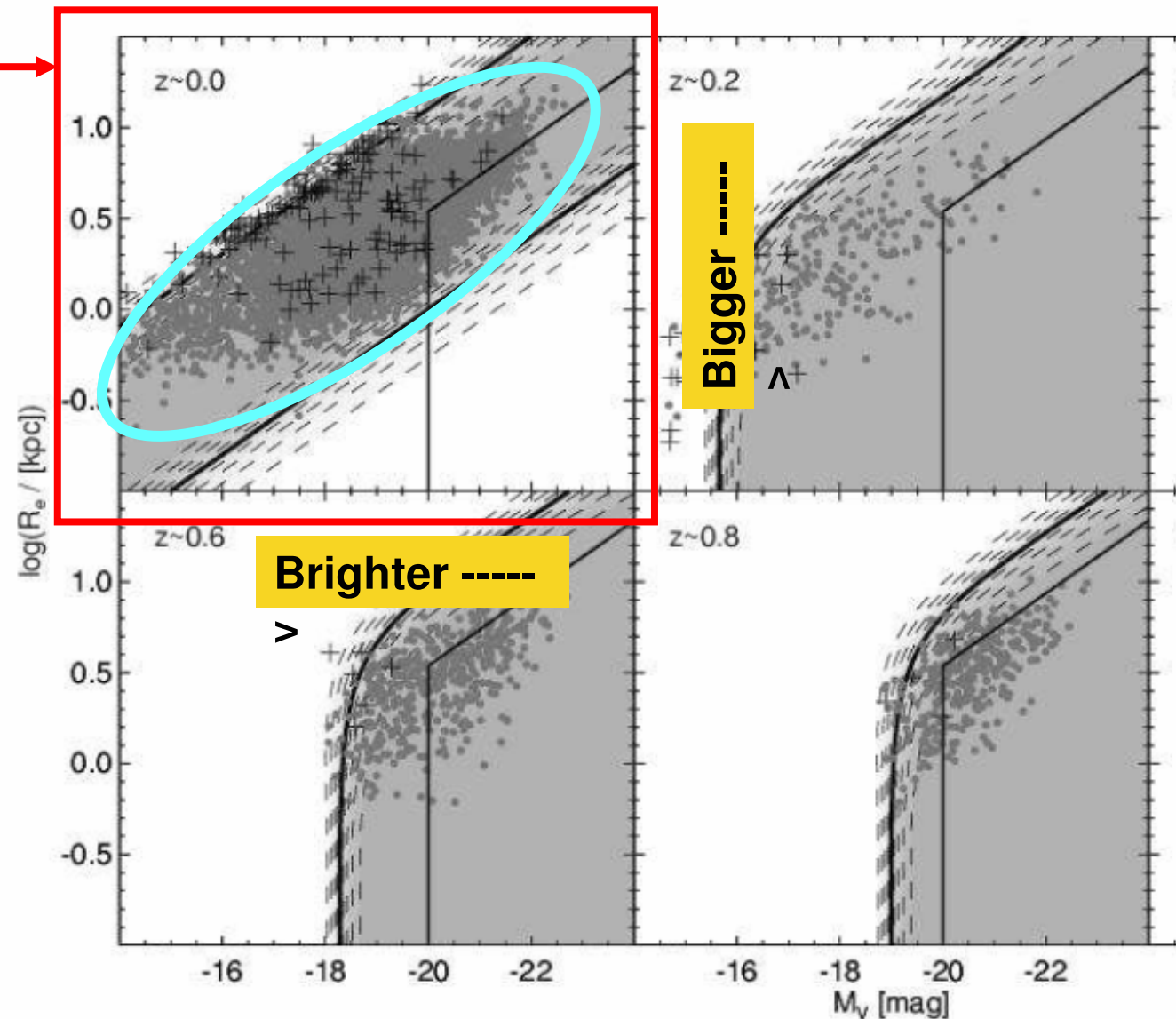
Kannappan et al., ApJ, 123, 2358, 2002



## Another scaling law is the *magnitude-radius relation*

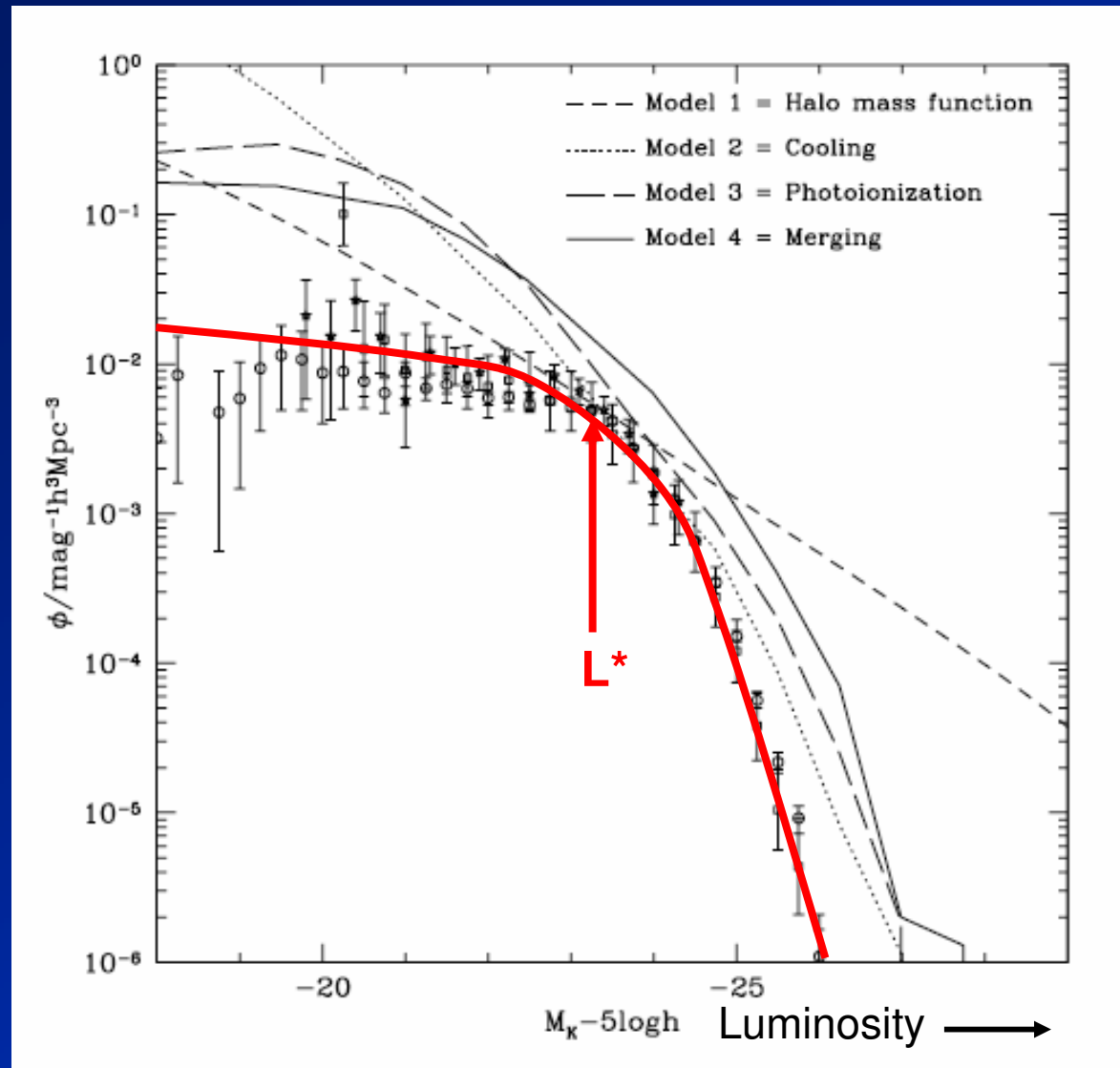
Galaxies at  
the present  
epoch

The gray points are from the Sloan Digital Sky Survey (SDSS). The black crosses are nearby galaxies from the GEMS survey.



Barden et al. 2005

The *luminosity function* describes the average number of galaxies per unit magnitude per unit volume.



The location of the “knee” is a characteristic luminosity called  $L^*$ .

The structural parameters  $M_B$ ,  $v_{rot}$ , *and radius*  $R$  describe *individual* galaxies.

The quantity  $L^*$  describes the *population of galaxies*.

Benson et al. 2003

# The scaling laws and luminosity function are *major clues* to how galaxies formed.

The structural parameters that describe visible galaxies are *produced jointly* by the **dark matter halos** plus the behavior of the **baryons**. The major factors affecting the appearance of disk galaxies at any epoch are:

- \* The masses and density distributions of the **underlying DM halos**.
- \* The **timing and amount of baryonic infall** onto galaxies.
- \* **How much angular momentum the baryons received** as the matter clustered and how much they retained or gained as they fell in---angular momentum determines the radii where the baryons settle, and thus disk radii.
- \* How fast the baryons turned into stars, i.e., the **star-formation history**.
- \* How much gas was driven out by **feedback**.

**Measuring the scaling laws and the luminosity function back in time provides a compact, quantitative record of galaxy**

# The Virial Plane

Consider a self-gravitating object in dynamical equilibrium:

It obeys the equation:

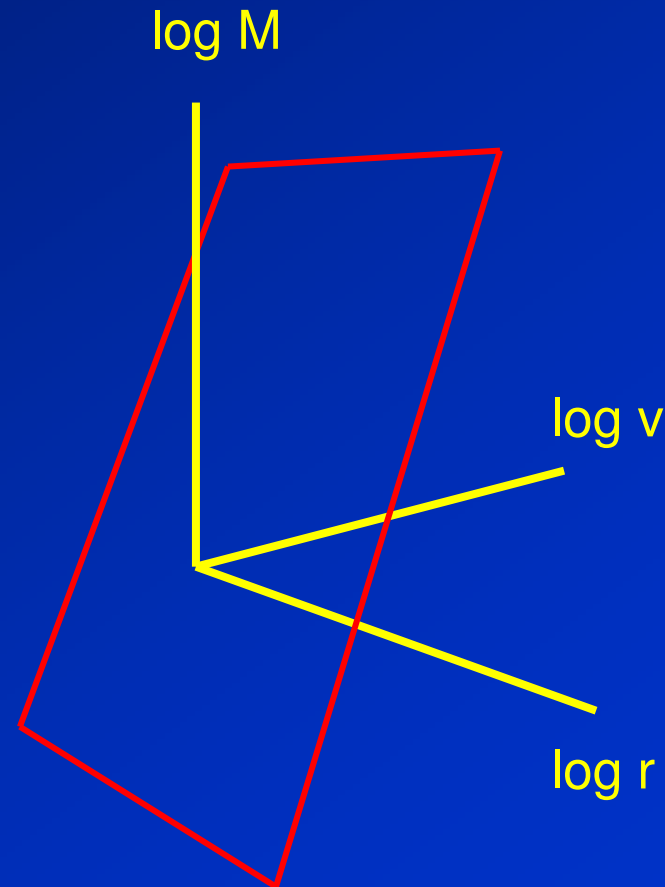
$$M = v^2 r / G$$

where:

$M$  = total mass

$r$  = characteristic radius, e.g.  
 $r_e$

$v$  = characteristic internal velocity



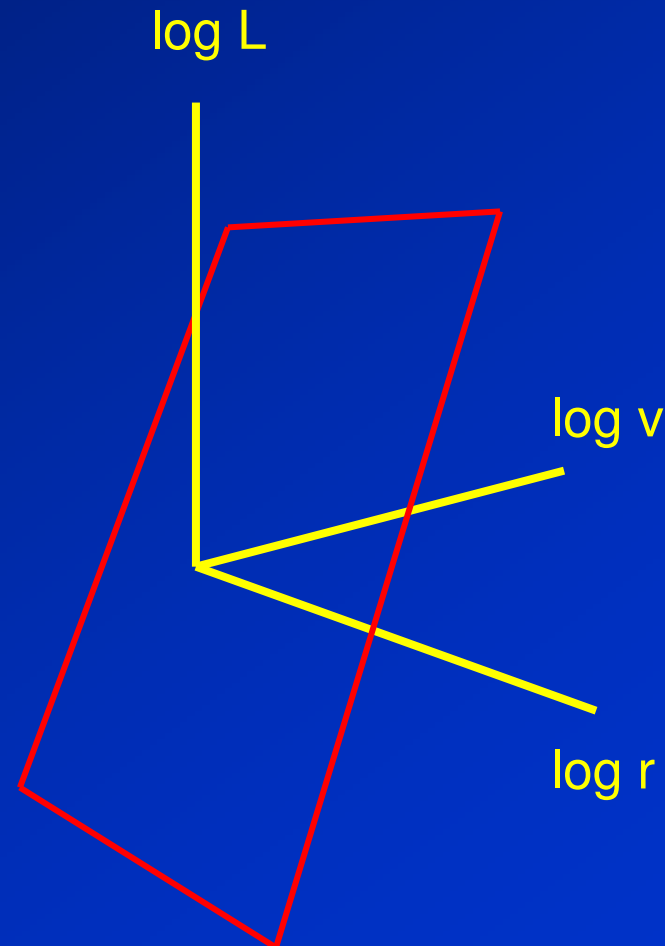
Such objects populate a plane in log-log space called the “Virial Plane”

# Transform from Mass to Luminosity

Endow these objects with luminosity and **CONSTANT** mass-to-light ratio  $M/L$ :

Plot the location of these objects in a similar space but with  $L$  substituted for  $M$

The objects will populate the **SAME PLANE** but shifted down or up by the amount  $-\log M/L$





# Allow Variable Mass/Light Ratio

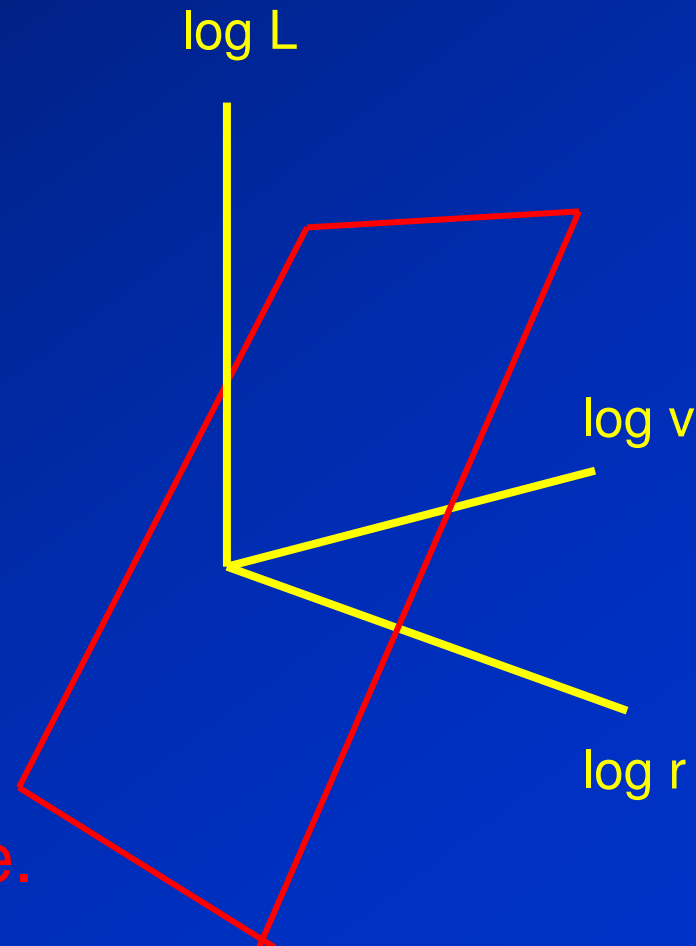
Now let  $M/L$  vary... but only as a power of  $r$  and  $v$ :

$$M/L = \text{const } v^\alpha r^\beta$$

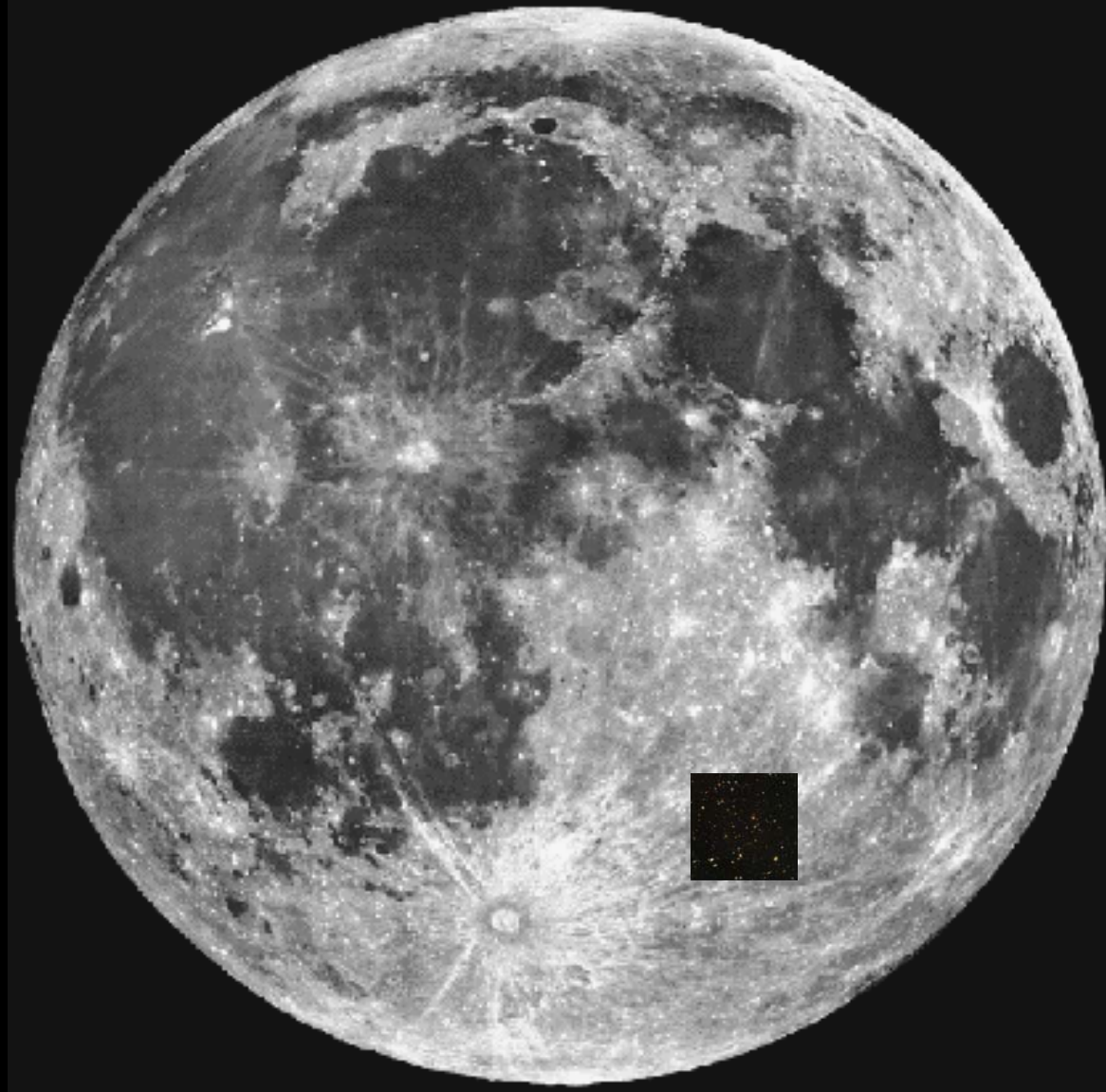
The plane remains a plane but tilts from the virial plane by an amount set by  $\alpha$  and  $\beta$

This new plane is called the “Fundamental Plane”

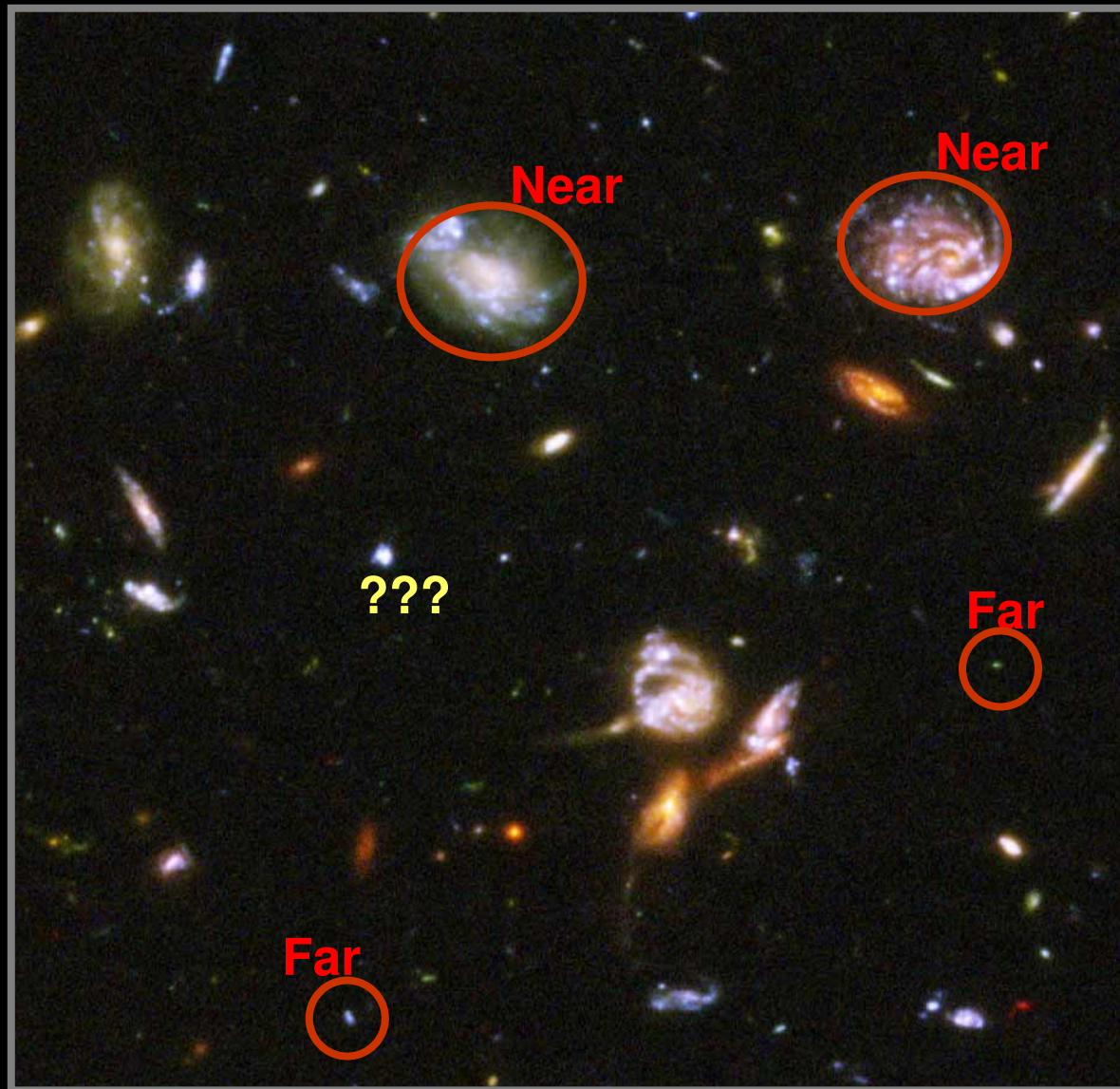
The space has no good name.  
Usually just called  
“Fundamental Manifold” space.



# The Hubble Ultradeep Field to scale

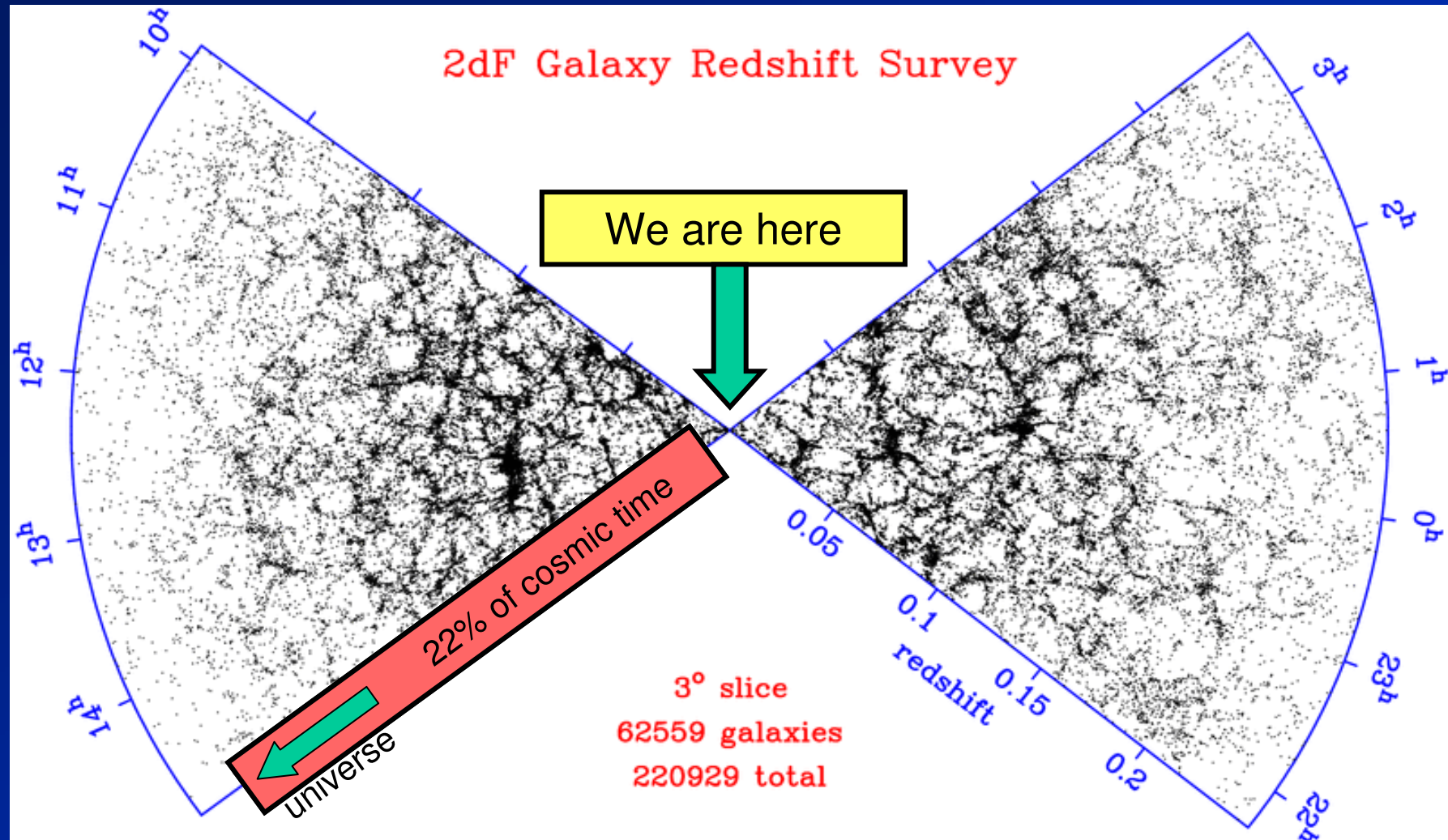


# Ultradeep field detail

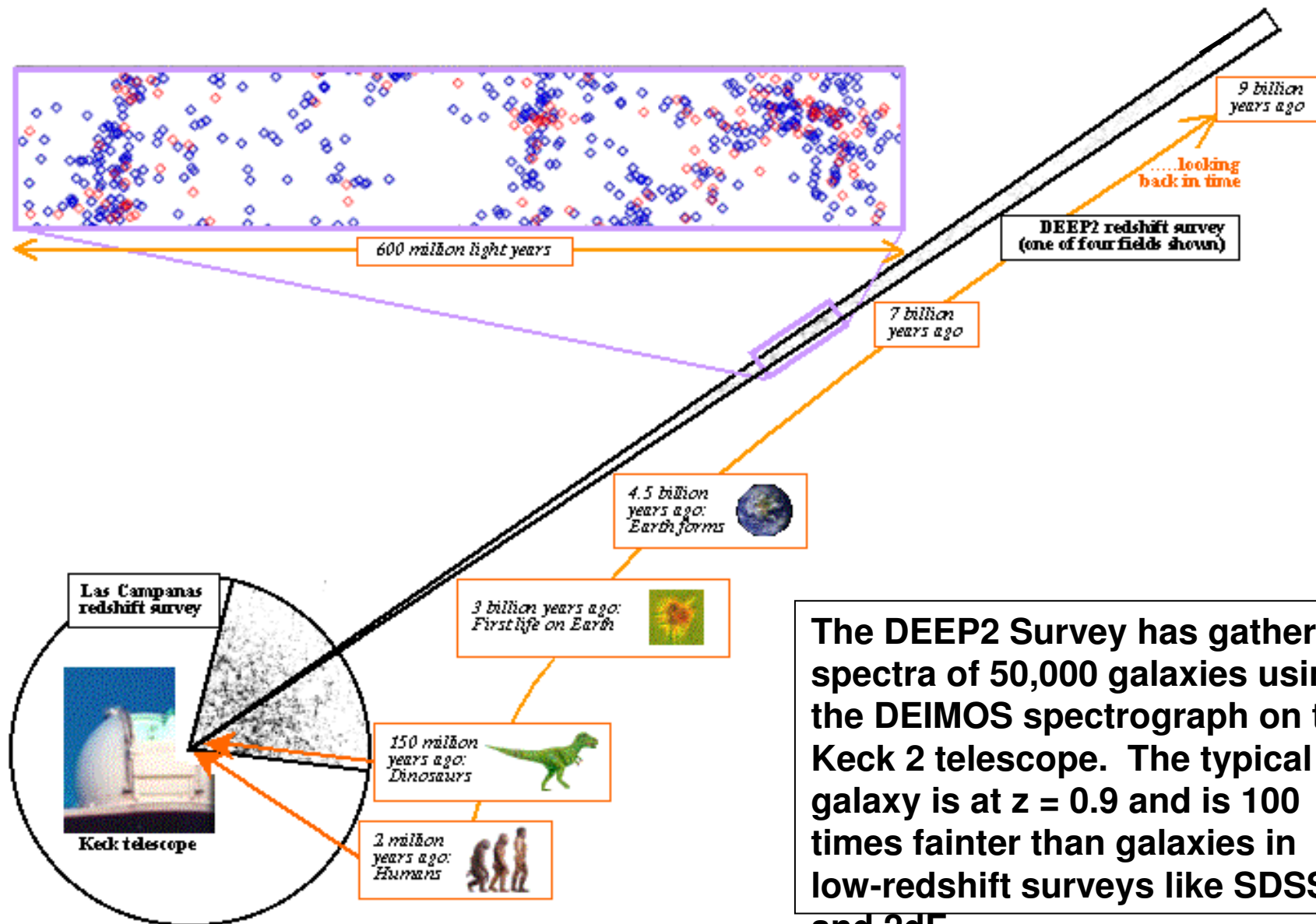




# Looking out in space is looking back in time

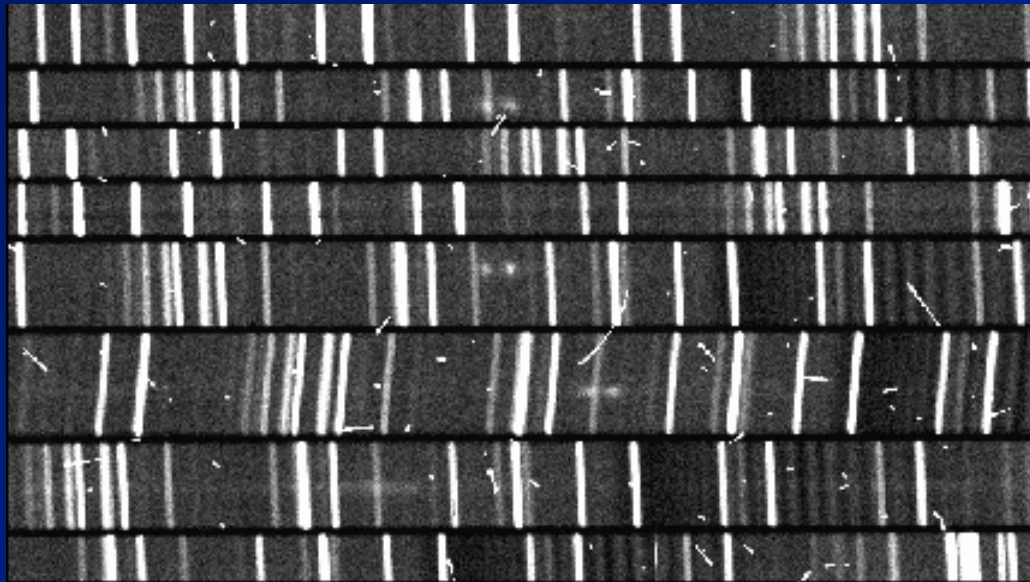


# ***DEEP2 looks 2/3 of the way back to the Big Bang***



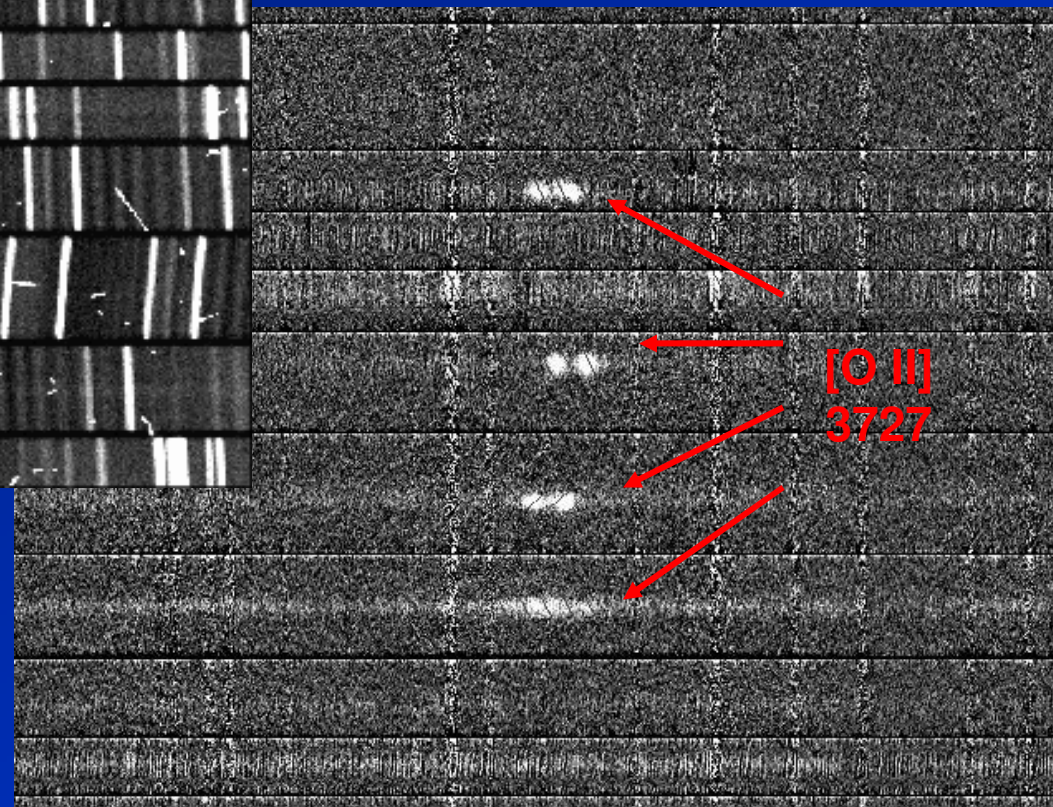


**Multi-object spectrographs** take spectra of up to several hundred galaxies per exposure, several thousand galaxies per night



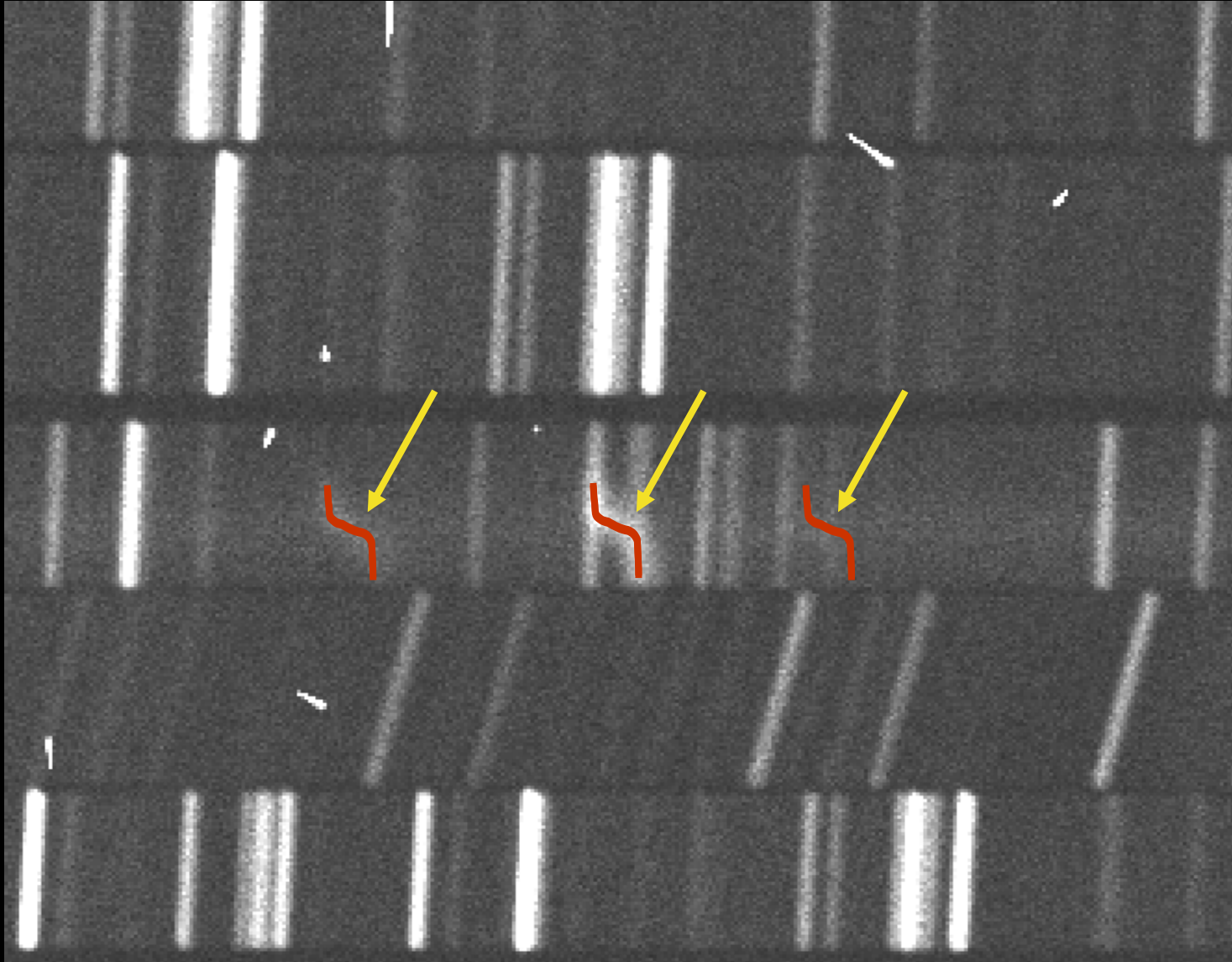
Each stripe is the spectrum of one galaxy. The vertical bright lines are OH atmospheric lines and must be removed along with cosmic rays.

DEIMOS spectra from Keck 2



A few percent of one DEEP2 mask, rectified, flat-fielded, CR cleaned, wavelength-rectified, and sky subtracted. Note the resolved **[OII] doublets**. Shown is a **small group of galaxies** with velocity dispersion  $\sigma \sim 250$  km/s at  $z \approx 1$ .

# A rotating galaxy 7 billion years ago





# Many data can be measured for each galaxy

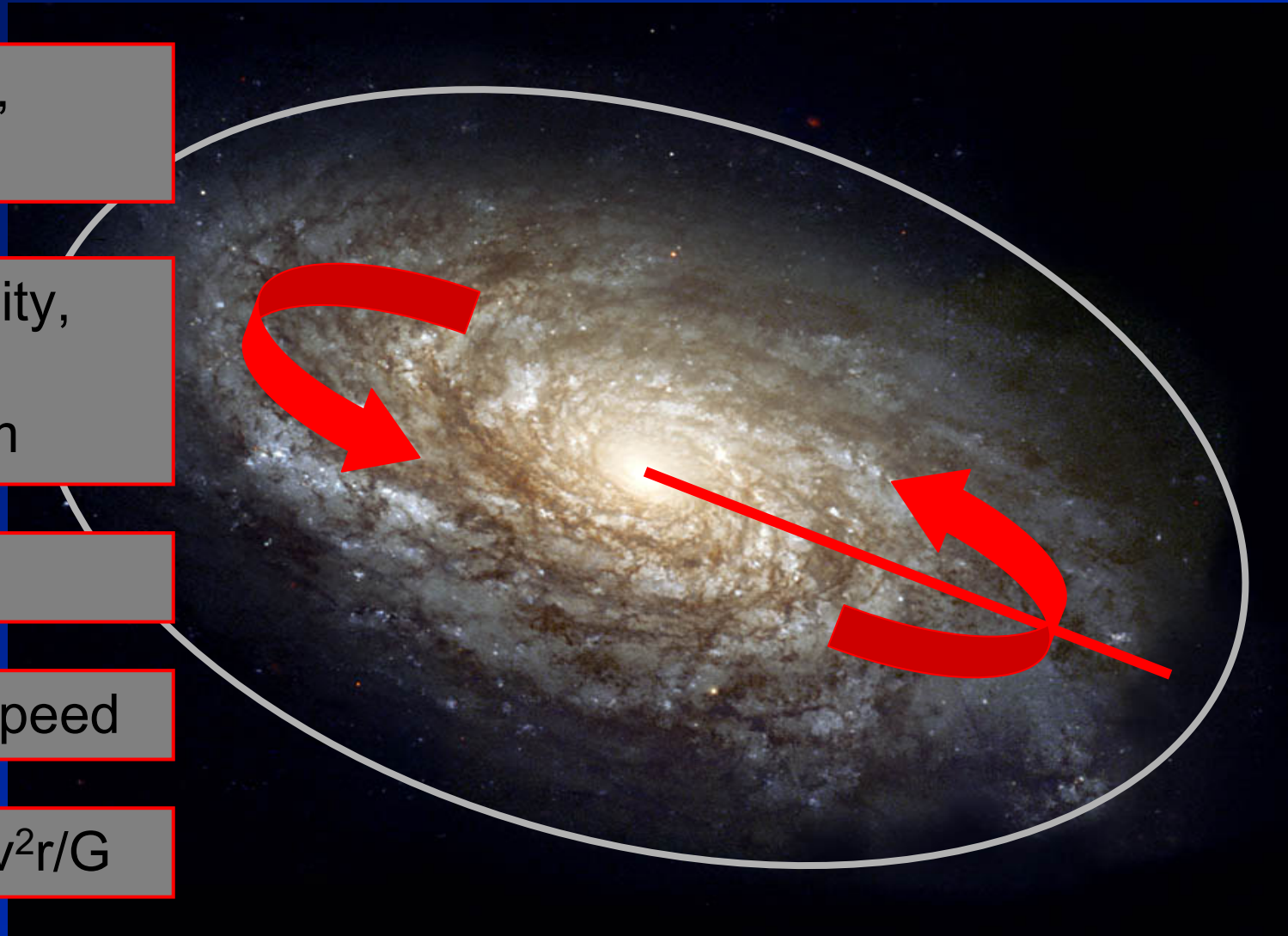
Redshift,  
distance

Luminosity,  
color,  
spectrum

Radius

Orbital speed

Mass  $\sim v^2 r / G$





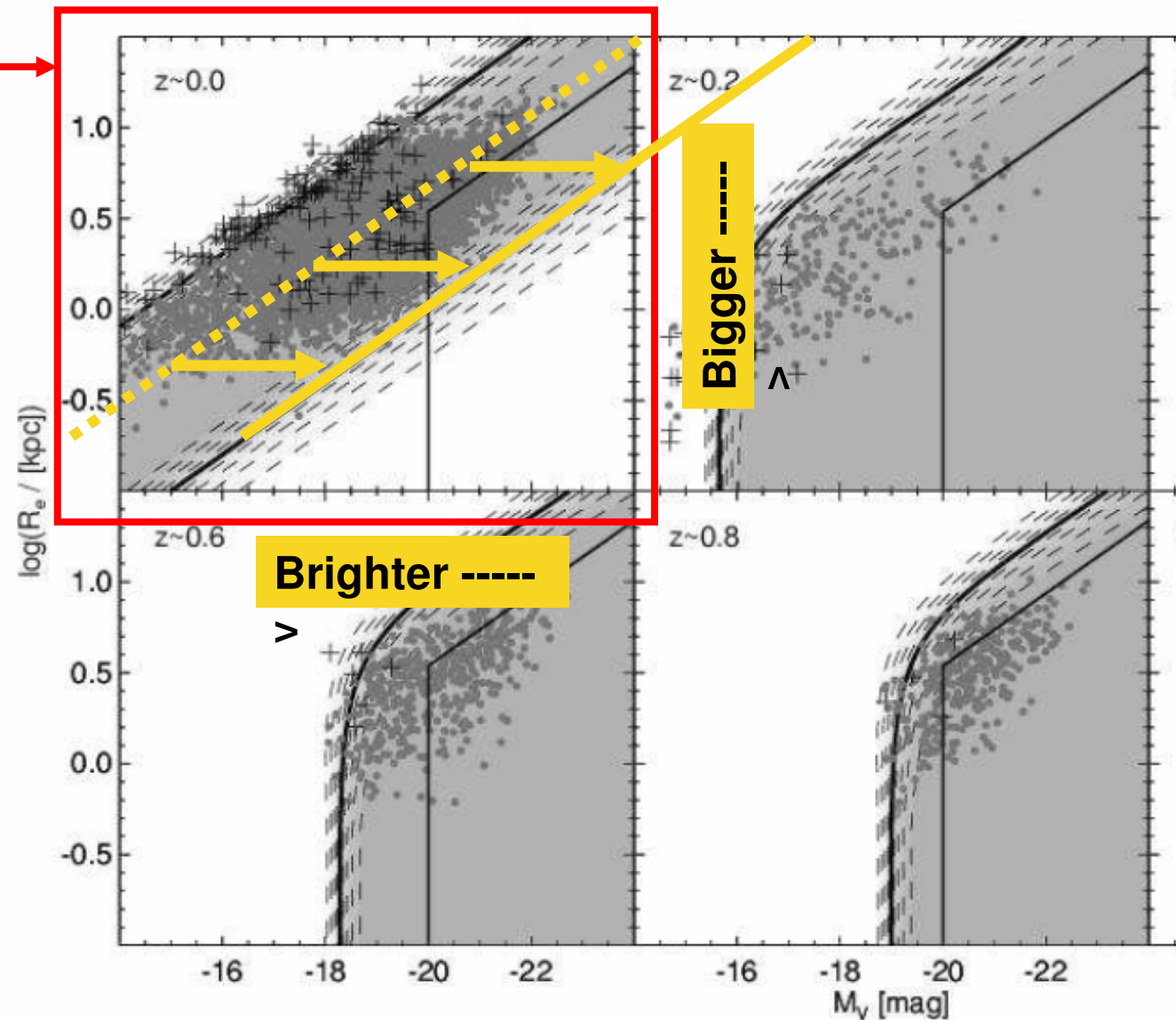
# Evolution of disk scaling laws since $z \sim 1$



## Recall the *magnitude-radius relation*...

Galaxies at  
the present  
epoch

The gray points are from the Sloan Digital Sky Survey (SDSS). The black crosses are nearby galaxies from the GEMS survey.

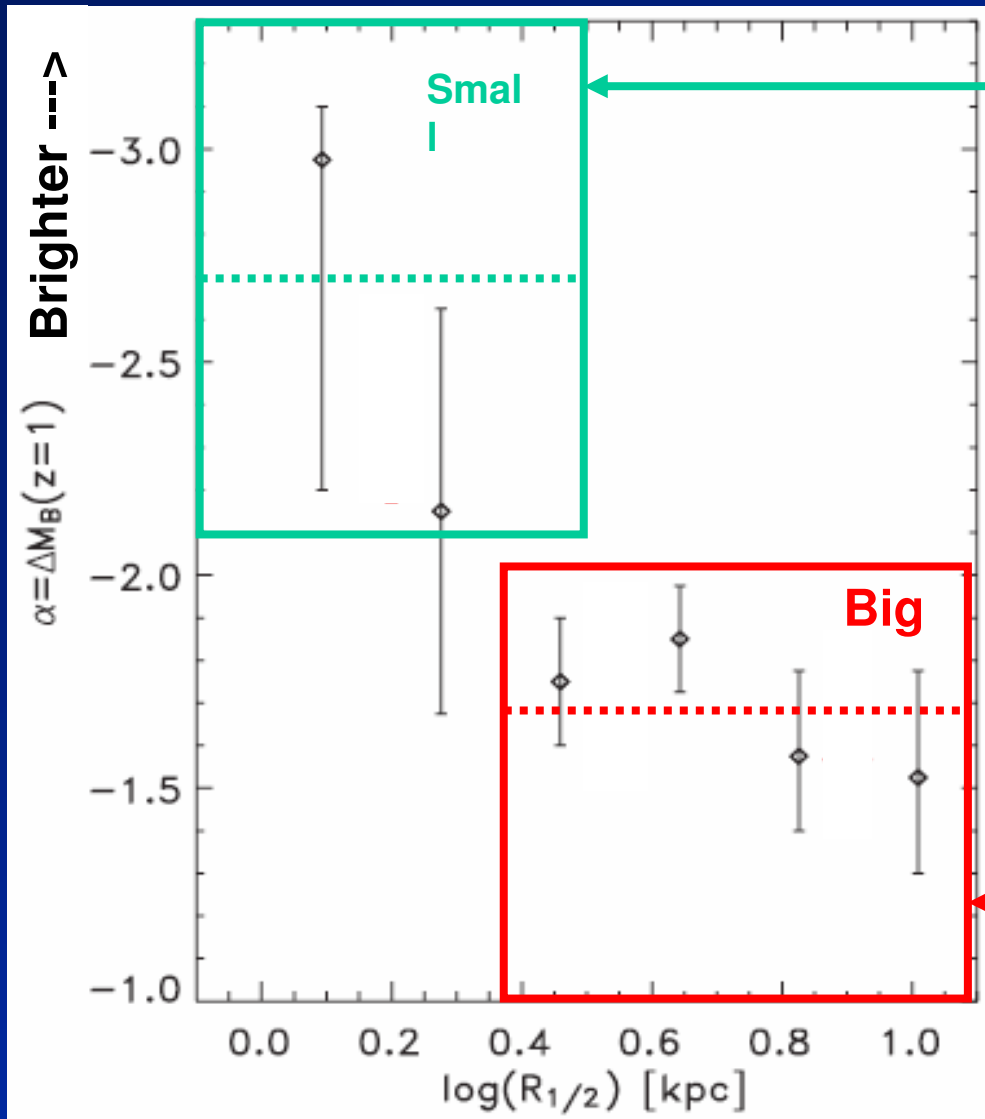


Barden et al. 2005



# Evolution in disk-galaxy mag-radius relation

( $\Delta M_B$  at fixed galaxy size from  $z = 0$  back to  $z = 1$ )



**Small galaxies** are  **$\sim 2.7$  mag brighter** at  $z \sim 1$ . This is impossible...probably due to a trace population of small “bursting” galaxies that later fade and disappear.

**Big galaxies** are  **$\sim 1.7 \pm 0.2$  mag brighter** at fixed size at  $z \sim 1$ .

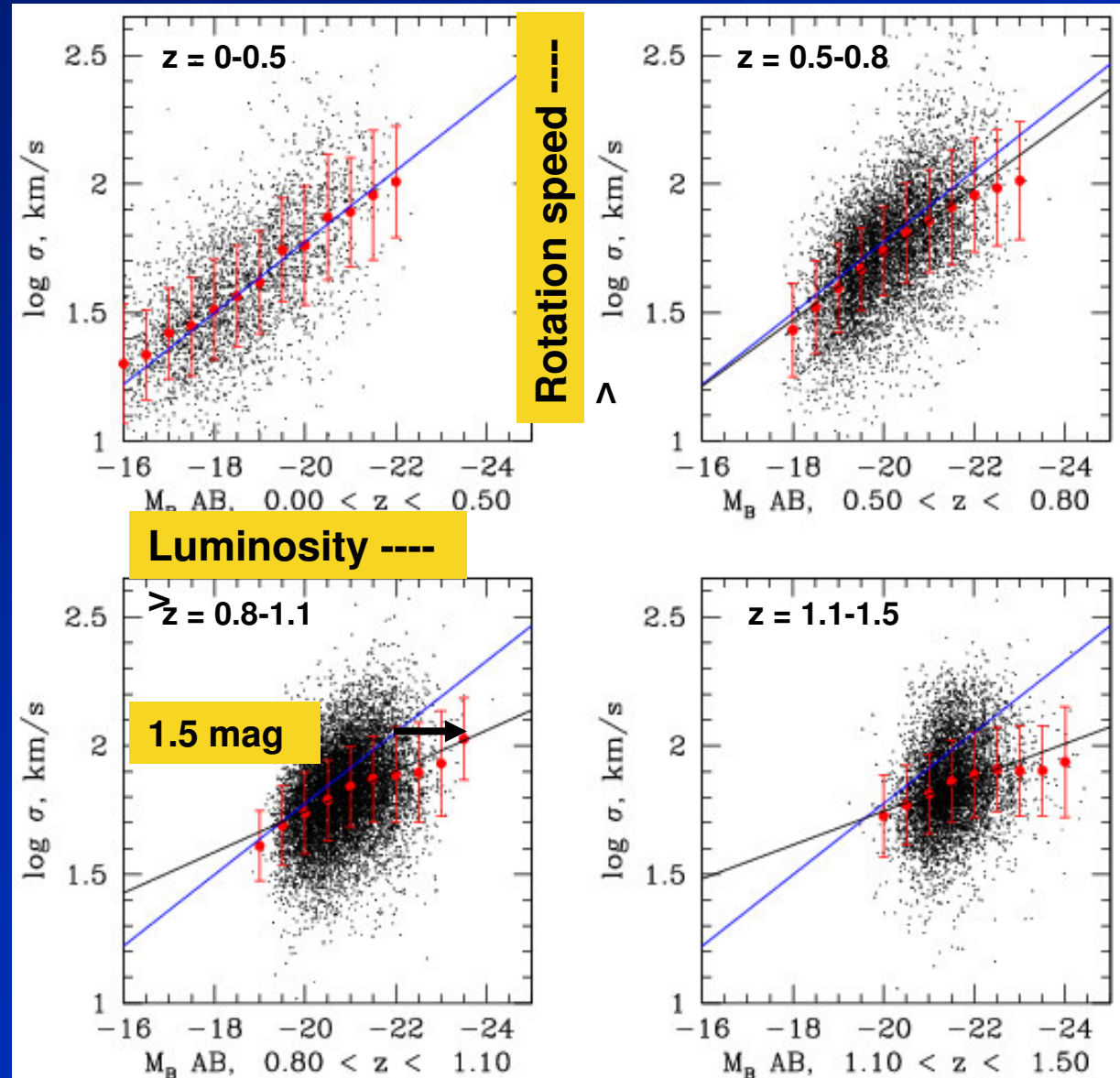
DEEP2, Melbourne et al.  
2006; also GEMS, Barden et  
al. 2005

# Evolution in disk-galaxy Tully-Fisher relation ( $\Delta M_B$ at fixed line-width from $z = 0$ back to $z = 1$ )

DEEP2, 26,000 galaxies

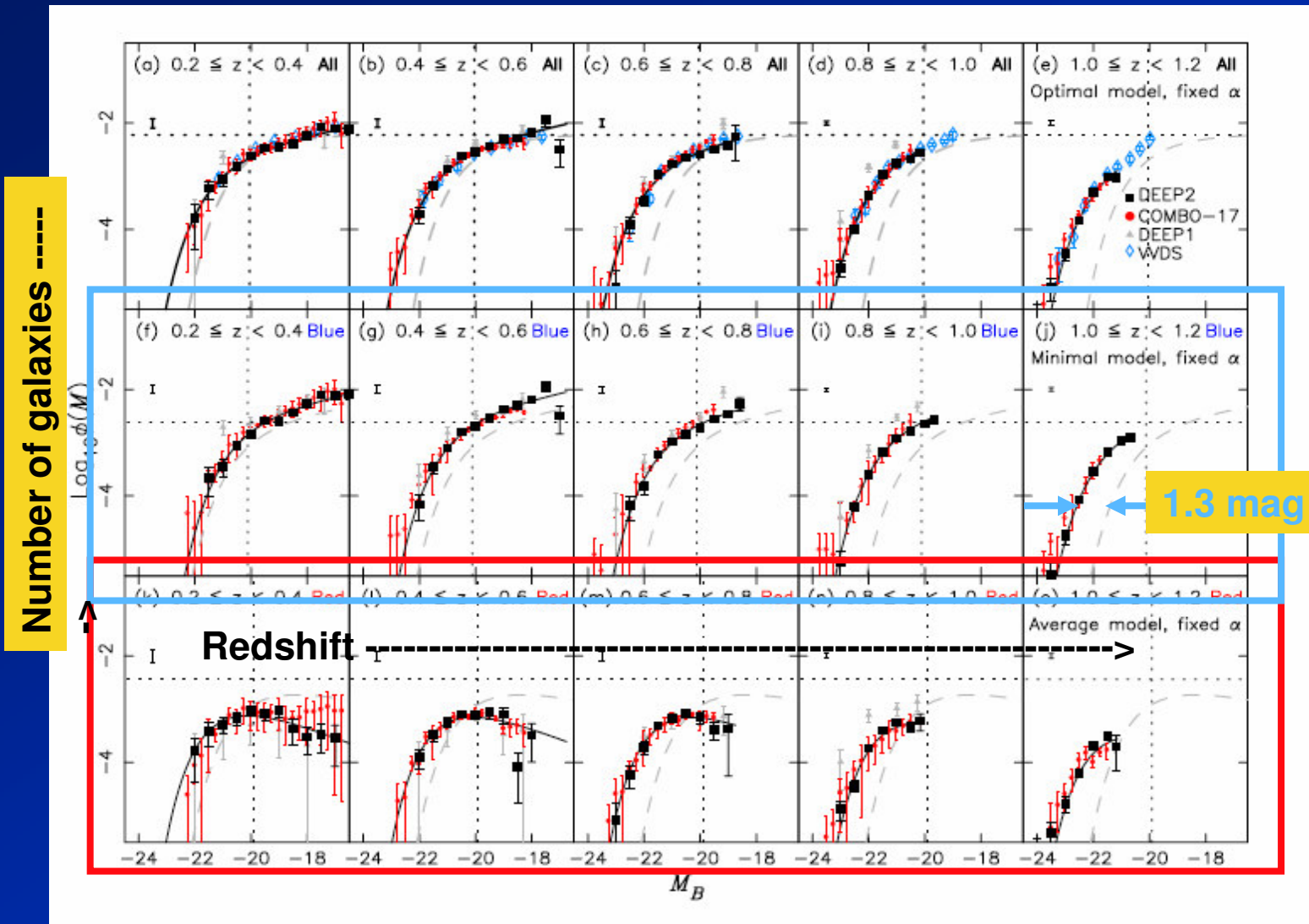
**Large galaxies** are  
 $\sim 1.5 \pm 0.3$  mag brighter at  
fixed rotation speed at  $z = 1$   
compared to now.

Again, smaller galaxies  
seem to differ. This time  
they **fade less**.



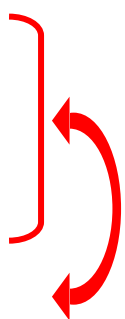
Weiner et al., 2006

# DEEP2 and COMBO-17 *luminosity functions* divided by color back in time



Willmer et al. 2005, Faber et al. 2005

# Collected data on the evolution of *bright/large* disk galaxies from $z = 1$ to $z = 0$

- Fade in luminosity at fixed radius:  $\Delta M_B \sim 1.7 \pm 0.2 \text{ mag}$
  - Fade in luminosity at fixed rotation speed:  $\Delta M_B \sim 1.5 \pm 0.3 \text{ mag}$
  - Fade in  $L^*$  of whole population:  $\Delta M_B \sim 1.3 \pm 0.2 \text{ mag}$
  - Predicted aging stellar-pop fade:  $\Delta M_B \sim 1.5 \pm 0.3 \text{ mag}$
- 
- Same!**

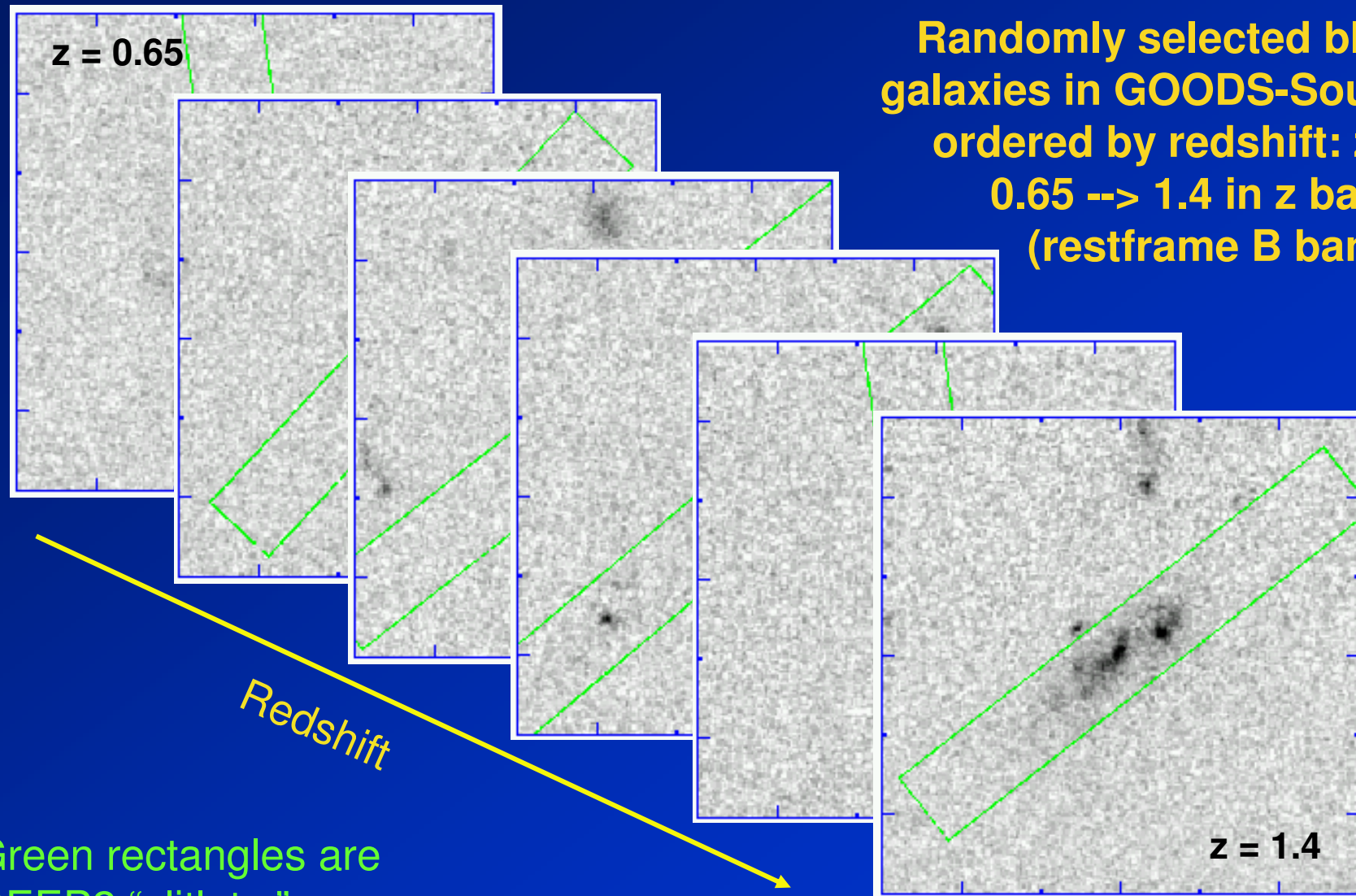
**➡ This implies little change in average stellar mass!**

- Also...no detectable change in number density (to  $\pm 30\%$ )

***These data are consistent with a basically fixed population of large, bright disks that were largely in place by  $z = 1$ , after which they don't merge, change number, or change mass by very much--their stars merely fade.***



**But...disk-galaxy morphologies evolve strongly back in time. *Distant disks look disorganized, as if just settling.***



# **Spheroidal galaxies : Brightness profiles and dark matter**



The classic spheroid law is the *de Vaucouleurs law*

$$\begin{aligned} I(R) &= I(0) \exp(-kR^{0.25}) \\ &= I_e \exp \left\{ -7.67 \left[ \left( \frac{R}{R_e} \right)^{0.25} - 1 \right] \right\}, \end{aligned}$$

$I$  = spheroid surface brightness profile

$R_e$  = effective radius (encloses half the light)

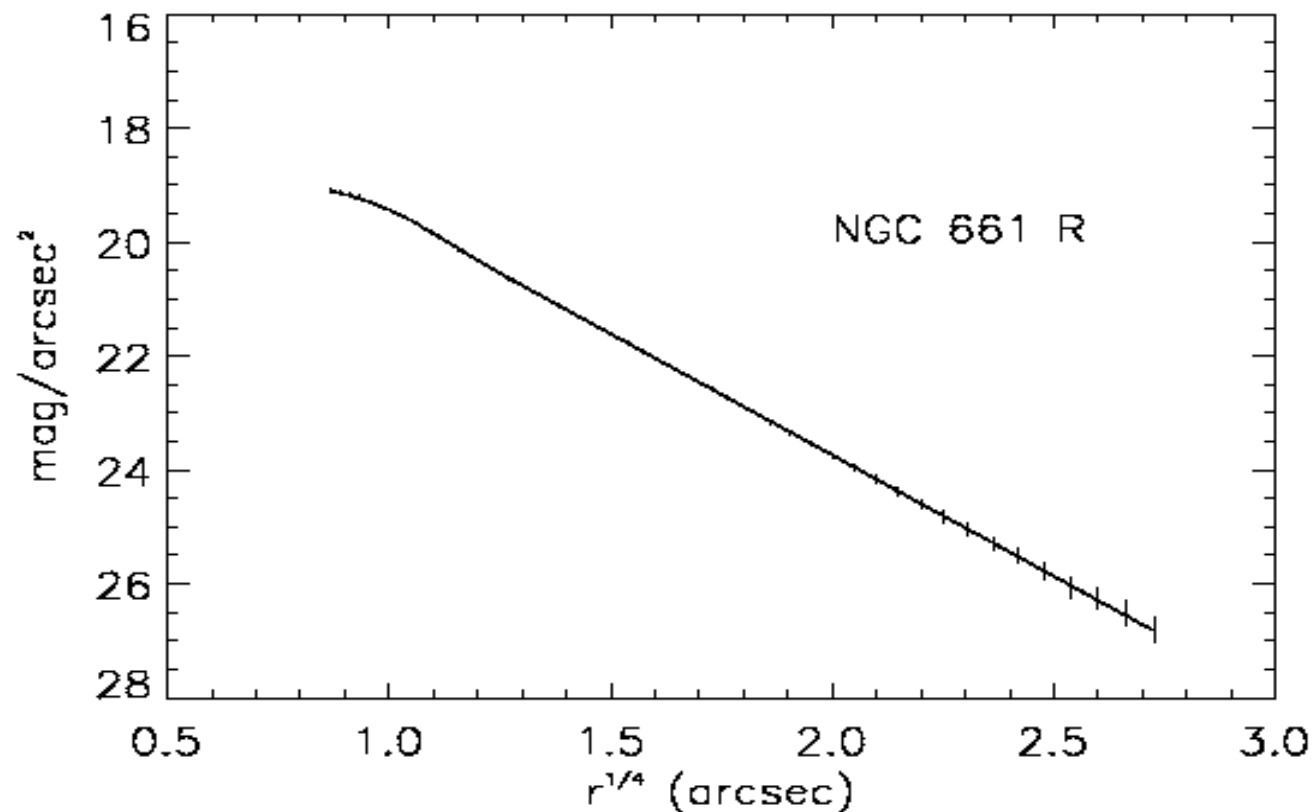
$I_e$  = surface brightness at effective radius

$I(0)$  = central surface brightness

The exponent of  $R$  here is 0.25, not 1 as in the disk exponential law. The de Vaucouleurs law is sometimes called the “r-to-the-1/4 law.”

## A typical spheroid plotted vs. $r^{1/4}$

The line is straight except for slight rounding at the center. The *innermost light profiles* of spheroids are complicated, not fit by the de Vaucouleurs law, are different from large to small spheroids, and are *probably affected by black hole formation and black-hole mergers*.



the 1990s, the incidence of *S. flexneri* has increased in the United Kingdom [10]. In the United States, *S. flexneri* has been reported as the most common serotype in the 1990s [11].

There is a paucity of data on the epidemiology of *S. flexneri* in the United Kingdom. In the 1980s, *S. flexneri* was the most commonly isolated serotype from patients with acute bacterial dysentery in the United Kingdom [12]. In the 1990s, *S. flexneri* was the most commonly isolated serotype from patients with acute bacterial dysentery in the United Kingdom [13].

The purpose of this study was to determine the prevalence of *S. flexneri* in the United Kingdom. The study was designed to determine the prevalence of *S. flexneri* in the United Kingdom. The study was designed to determine the prevalence of *S. flexneri* in the United Kingdom.

The study was designed to determine the prevalence of *S. flexneri* in the United Kingdom. The study was designed to determine the prevalence of *S. flexneri* in the United Kingdom. The study was designed to determine the prevalence of *S. flexneri* in the United Kingdom.

The study was designed to determine the prevalence of *S. flexneri* in the United Kingdom. The study was designed to determine the prevalence of *S. flexneri* in the United Kingdom. The study was designed to determine the prevalence of *S. flexneri* in the United Kingdom.

The study was designed to determine the prevalence of *S. flexneri* in the United Kingdom. The study was designed to determine the prevalence of *S. flexneri* in the United Kingdom. The study was designed to determine the prevalence of *S. flexneri* in the United Kingdom.

The study was designed to determine the prevalence of *S. flexneri* in the United Kingdom. The study was designed to determine the prevalence of *S. flexneri* in the United Kingdom. The study was designed to determine the prevalence of *S. flexneri* in the United Kingdom.

The study was designed to determine the prevalence of *S. flexneri* in the United Kingdom. The study was designed to determine the prevalence of *S. flexneri* in the United Kingdom. The study was designed to determine the prevalence of *S. flexneri* in the United Kingdom.

The study was designed to determine the prevalence of *S. flexneri* in the United Kingdom. The study was designed to determine the prevalence of *S. flexneri* in the United Kingdom. The study was designed to determine the prevalence of *S. flexneri* in the United Kingdom.

the 1990s, the incidence of *S. flexneri* has increased in the United Kingdom [10]. In the United States, *S. flexneri* has been reported as the most common serotype in children with acute bacterial dysentery [11].

There is a paucity of data on the epidemiology of *S. flexneri* in the United Kingdom. In the 1970s, *S. flexneri* was the most commonly isolated serotype from patients with acute bacterial dysentery in the United Kingdom [12]. In the 1980s, *S. flexneri* was the most commonly isolated serotype from patients with acute bacterial dysentery in the United Kingdom [13].

In the 1990s, *S. flexneri* was the most commonly isolated serotype from patients with acute bacterial dysentery in the United Kingdom [14]. In the 2000s, *S. flexneri* was the most commonly isolated serotype from patients with acute bacterial dysentery in the United Kingdom [15].

In the 2010s, *S. flexneri* was the most commonly isolated serotype from patients with acute bacterial dysentery in the United Kingdom [16]. In the 2020s, *S. flexneri* was the most commonly isolated serotype from patients with acute bacterial dysentery in the United Kingdom [17].

In the 2030s, *S. flexneri* was the most commonly isolated serotype from patients with acute bacterial dysentery in the United Kingdom [18]. In the 2040s, *S. flexneri* was the most commonly isolated serotype from patients with acute bacterial dysentery in the United Kingdom [19].

In the 2050s, *S. flexneri* was the most commonly isolated serotype from patients with acute bacterial dysentery in the United Kingdom [20]. In the 2060s, *S. flexneri* was the most commonly isolated serotype from patients with acute bacterial dysentery in the United Kingdom [21].

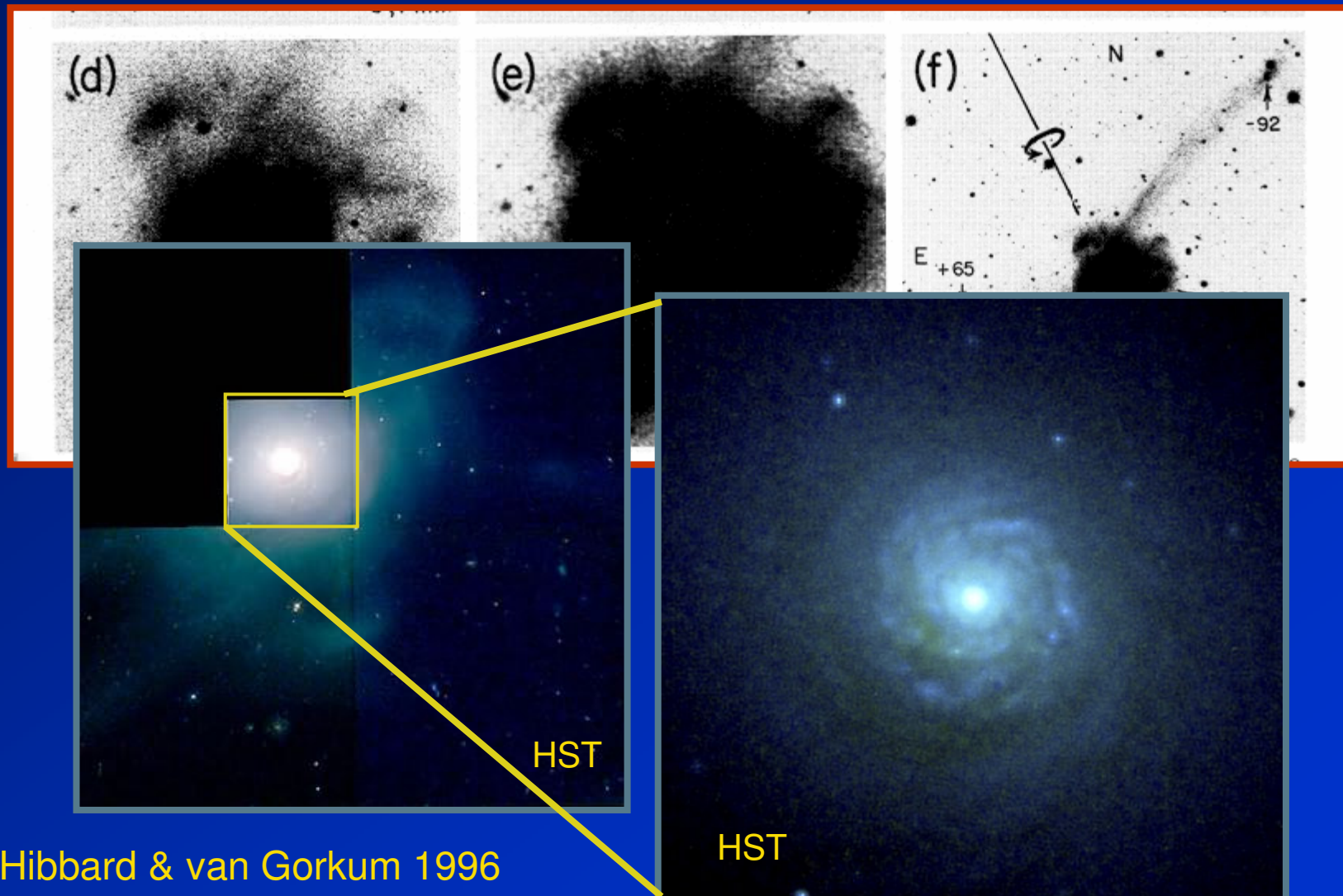
In the 2070s, *S. flexneri* was the most commonly isolated serotype from patients with acute bacterial dysentery in the United Kingdom [22]. In the 2080s, *S. flexneri* was the most commonly isolated serotype from patients with acute bacterial dysentery in the United Kingdom [23].

In the 2090s, *S. flexneri* was the most commonly isolated serotype from patients with acute bacterial dysentery in the United Kingdom [24]. In the 2100s, *S. flexneri* was the most commonly isolated serotype from patients with acute bacterial dysentery in the United Kingdom [25].

# **Spheroids: merger evidence**

# 1982: Schweizer -- Merger evidence

## NGC 7252 -- “Atoms for Peace” galaxy

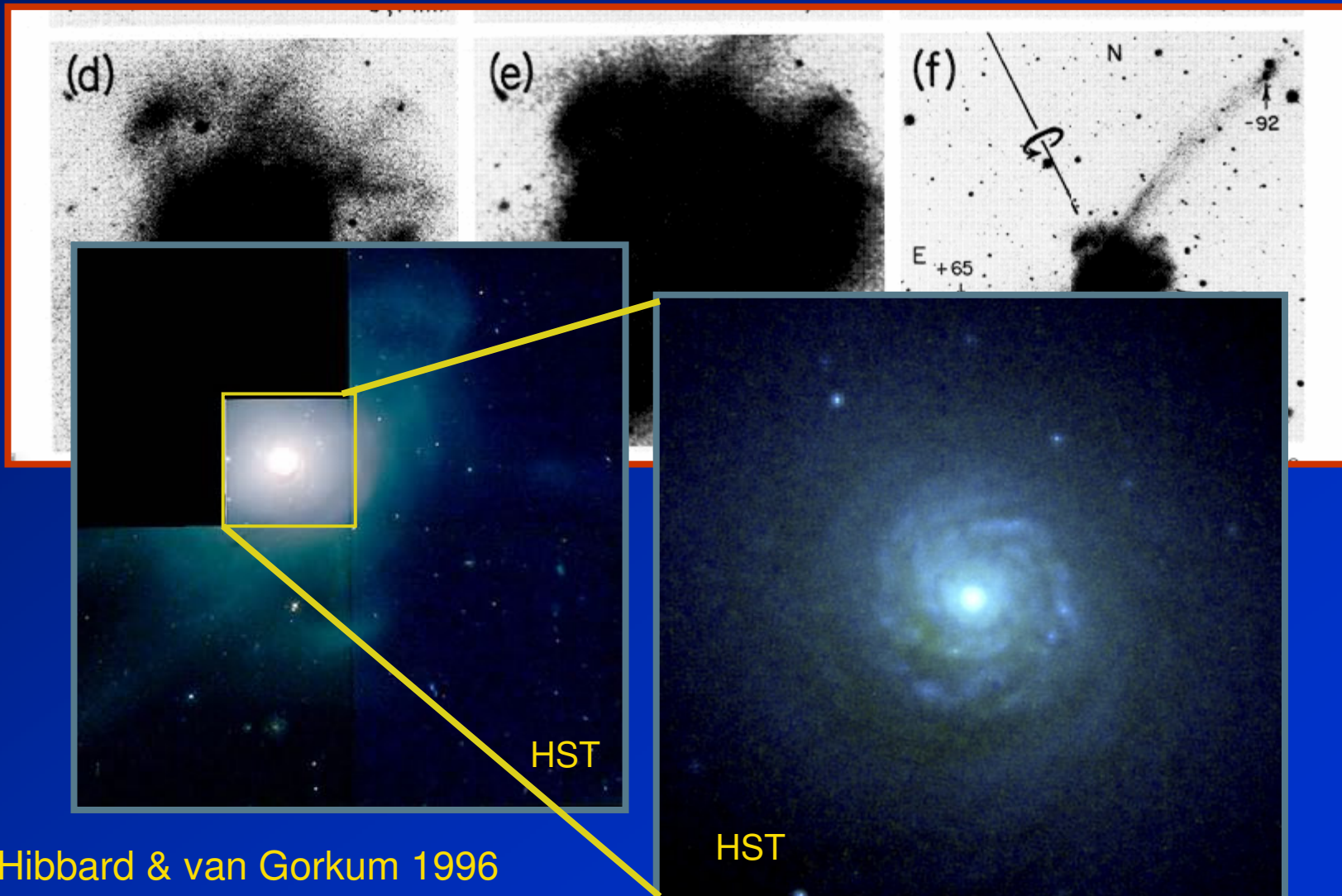


Also Hibbard & van Gorkum 1996



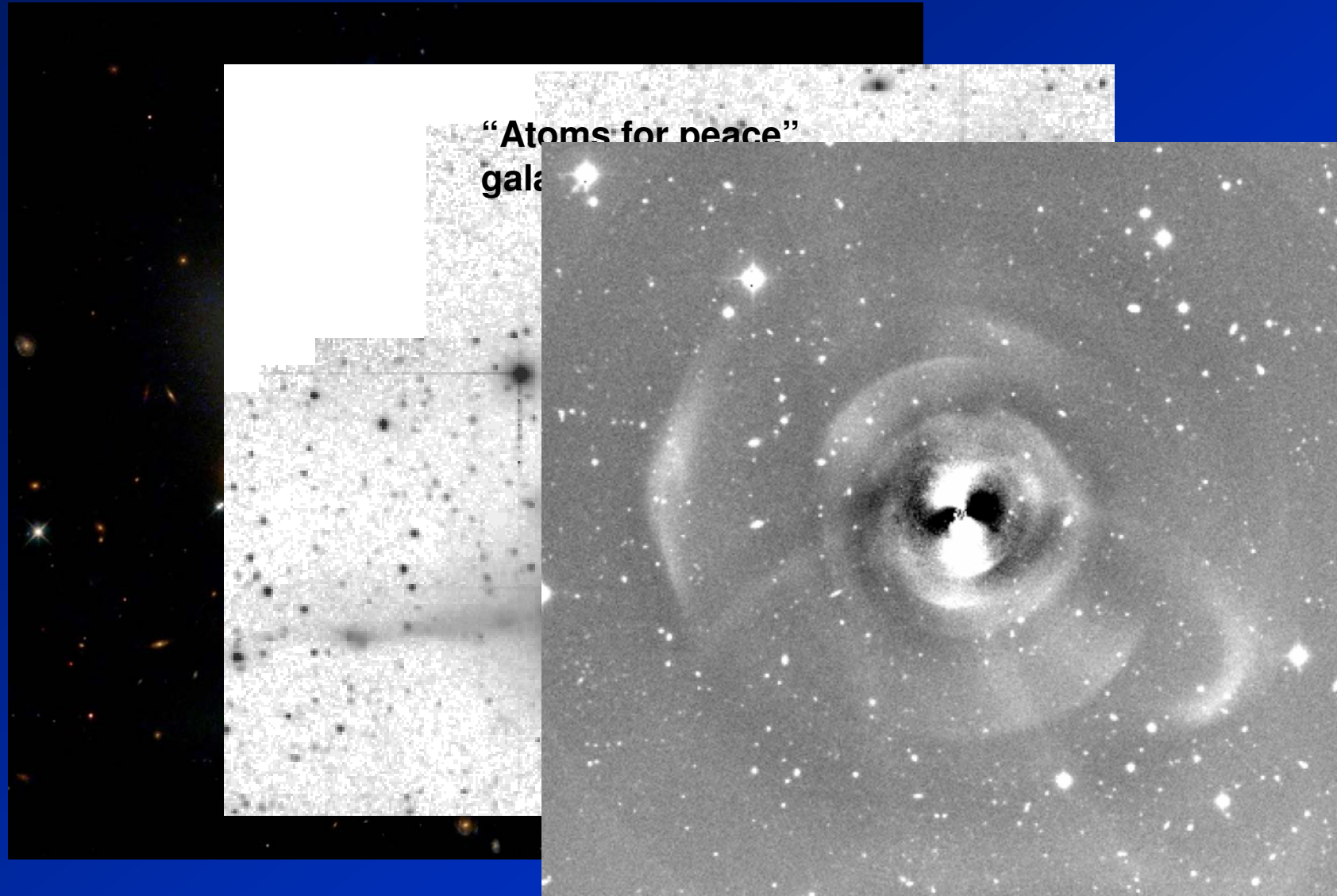
# 1982: Schweizer -- Merger evidence

*Mean light profile is de Vaucouleurs law even though lumpy with tidal tails; wait and these will smooth out*



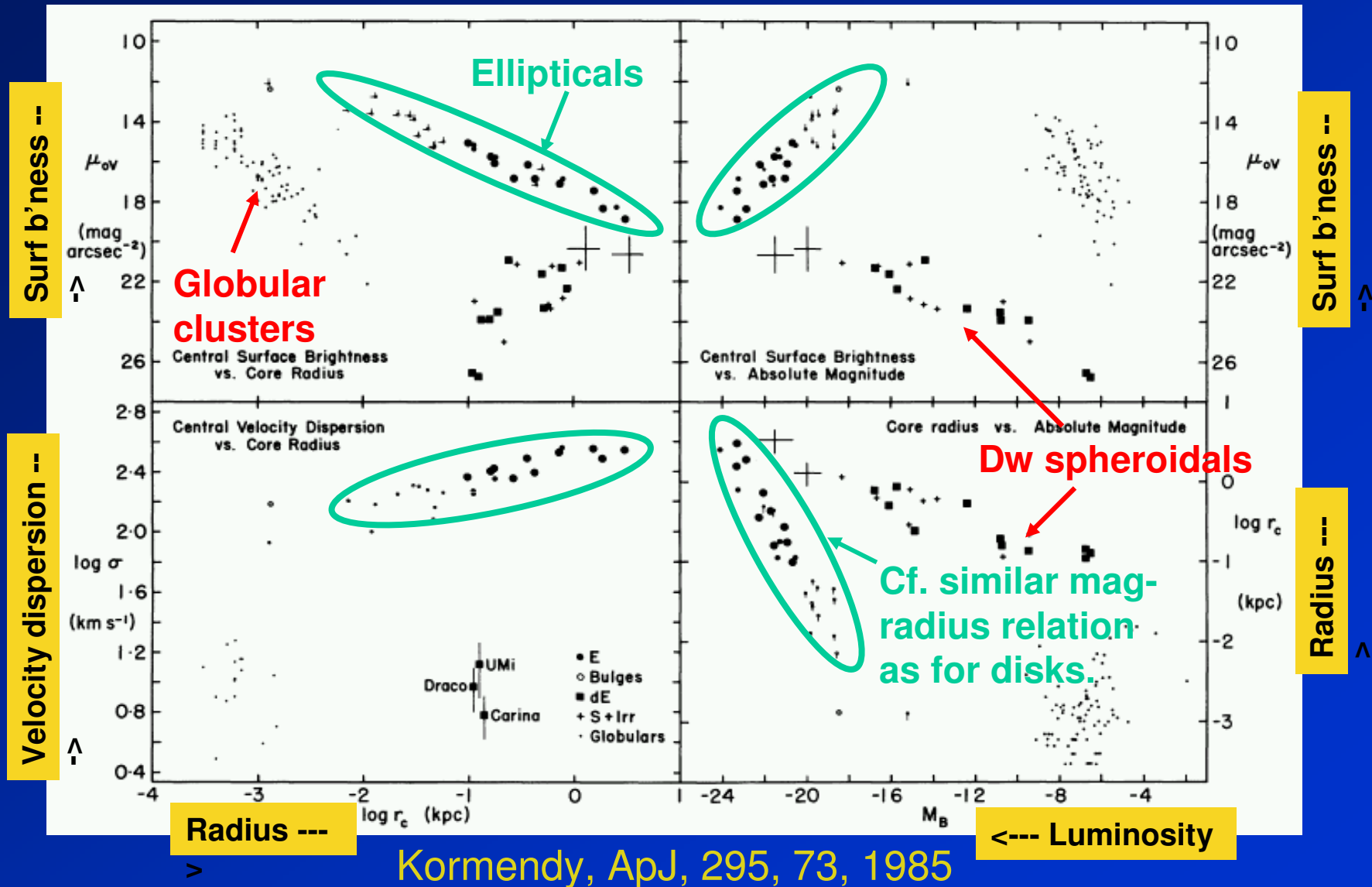
Also Hibbard & van Gorkum 1996

Merging galaxies and *merger remnants* are fairly common now that we know what to look for



# Spheroid scaling laws

The **scaling laws** for large spheroidal systems resemble those for disks. (Globular clusters and dwarf galaxies obey different laws, showing that they formed differently.)

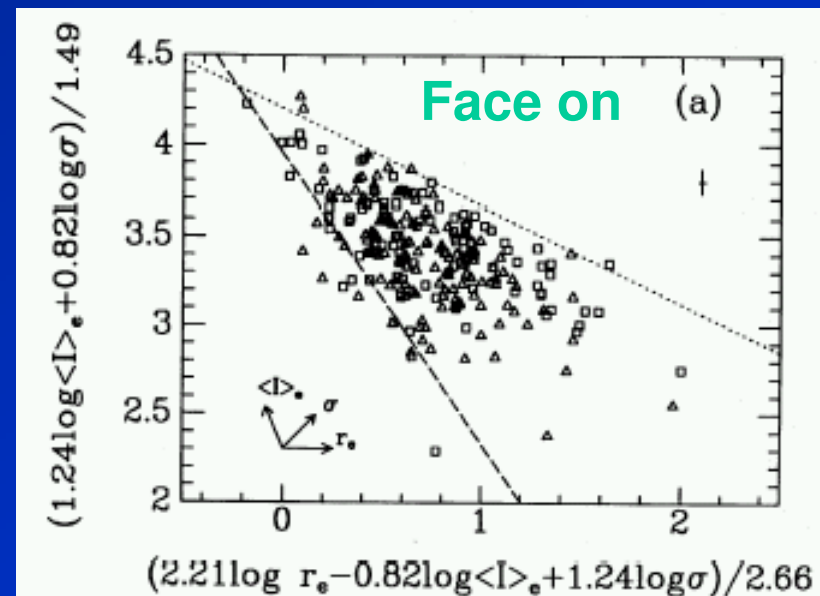
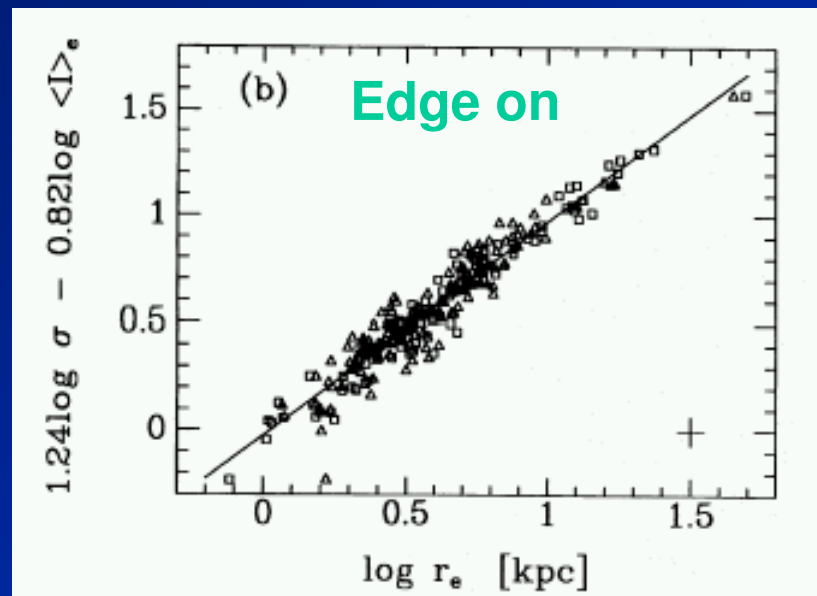


# The analog of the TF relation for spheroids is the *Fundamental Plane*

The Fundamental Plane correlates  $R_e$ , **surface brightness**, and  $\sigma$  for spheroidal galaxies. Since surface brightness  $\Sigma \sim L/(R_e)^2$ , this is the **same  $L, v, R$ -space** as for the TF relation.

The thinness of the FP means that the mass-to-light ratios of the stars in spheroidal galaxies are a well-behaved function of their structural parameters. **Structurally similar spheroidal galaxies have similar star-forming histories.** This is what we also found for disks.

The FP for spheroidals and the TF plane for disks are two parts of the **same Virial Plane** for all galaxies. The two parts are slightly tilted w/r one another and join at a “hinge” where the stellar populations change. This is the same spot that divides the blue cloud from the red sequence.



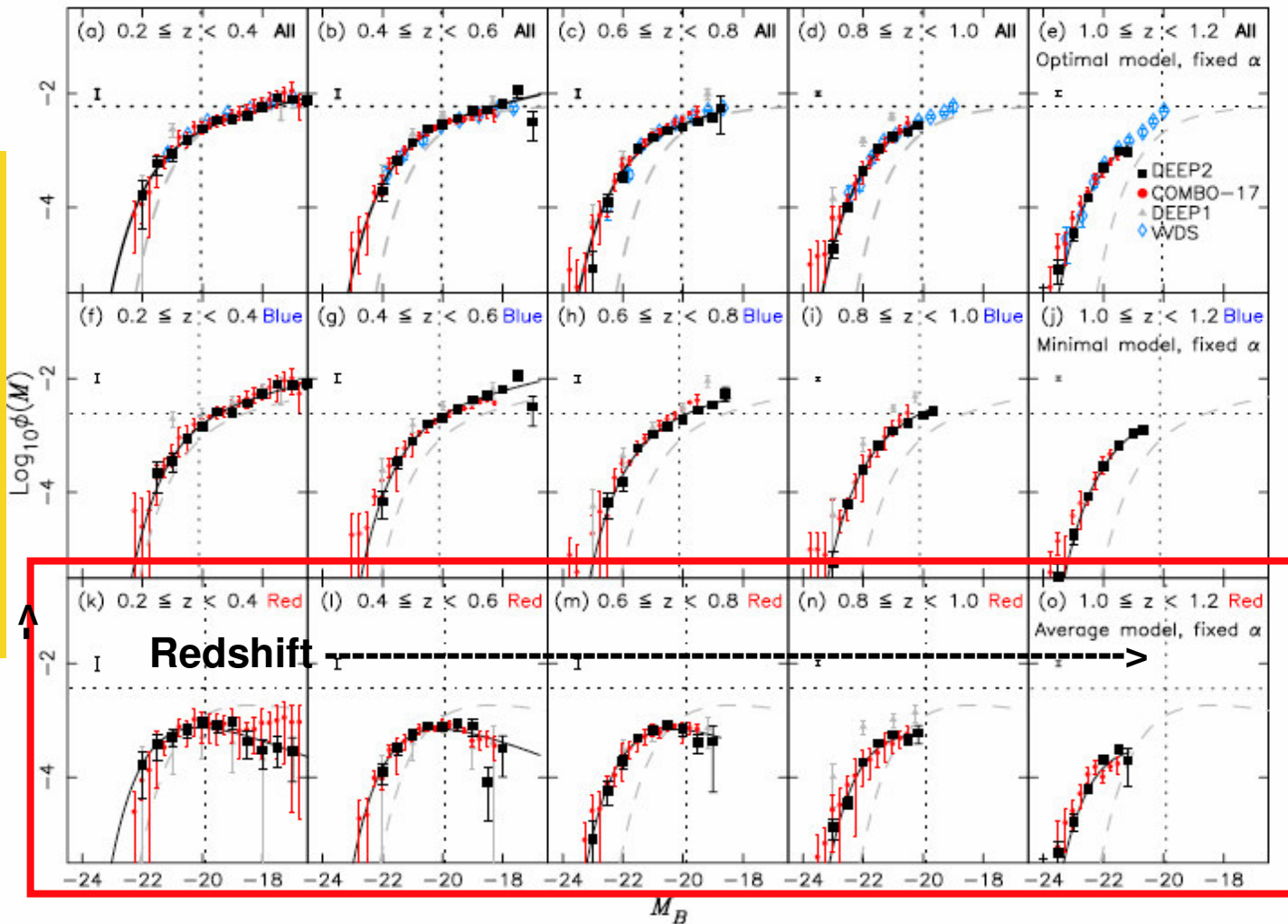
The Fundamental Plane for nearby cluster spheroidals, Jorgensen et al., 1996.

# Spheroid number density evolution



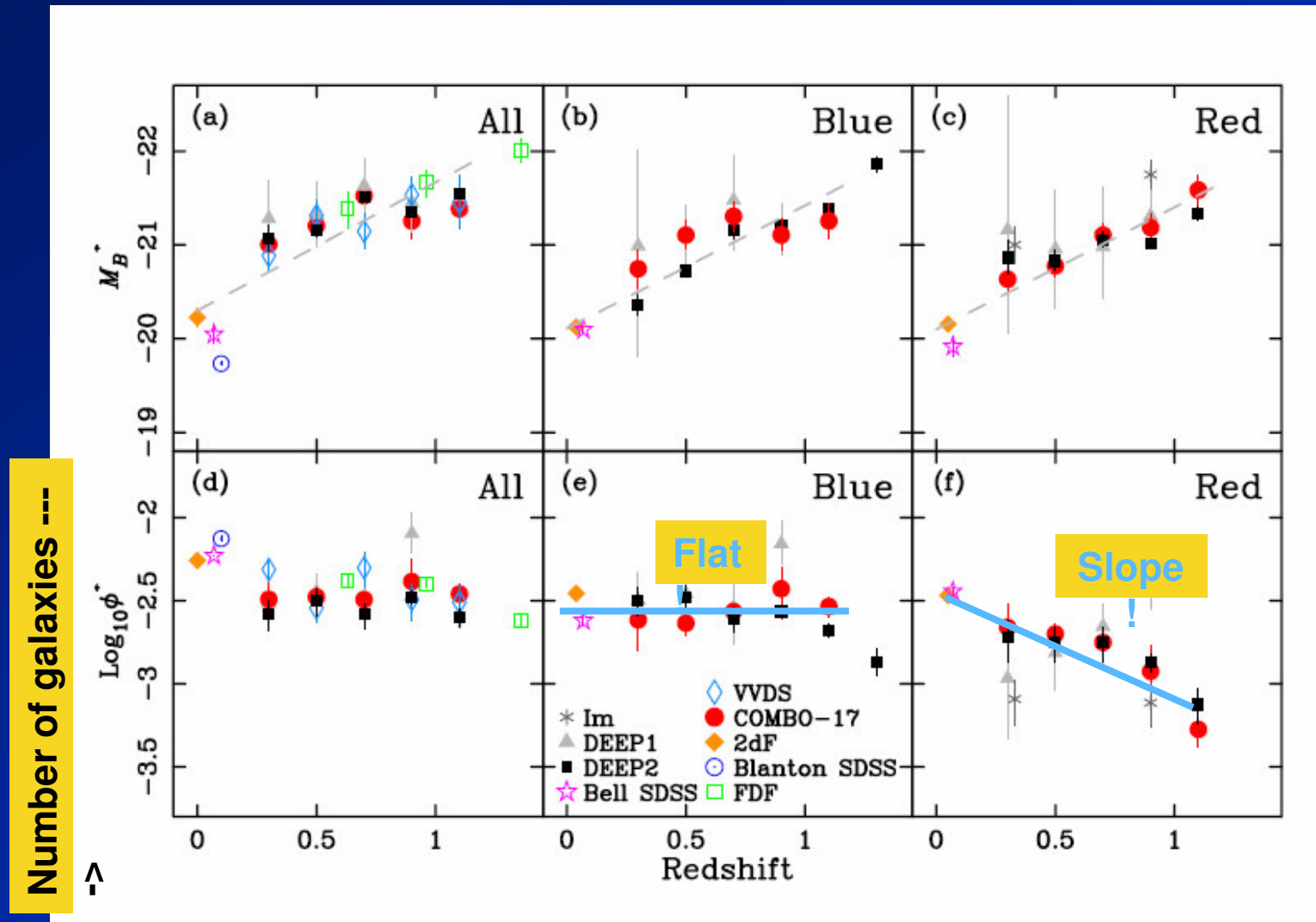
# DEEP2 and COMBO-17 *luminosity functions* divided by color back in time

Number of galaxies -----



Willmer et al. 2005, Faber et al. 2005

# DEEP2 and COMBO-17: Most red galaxies *appeared after $z = 1$*



Willmer et al. 2005, Faber et al. 2005

# ***Two requirements are needed for making a red spheroid out of blue disks***

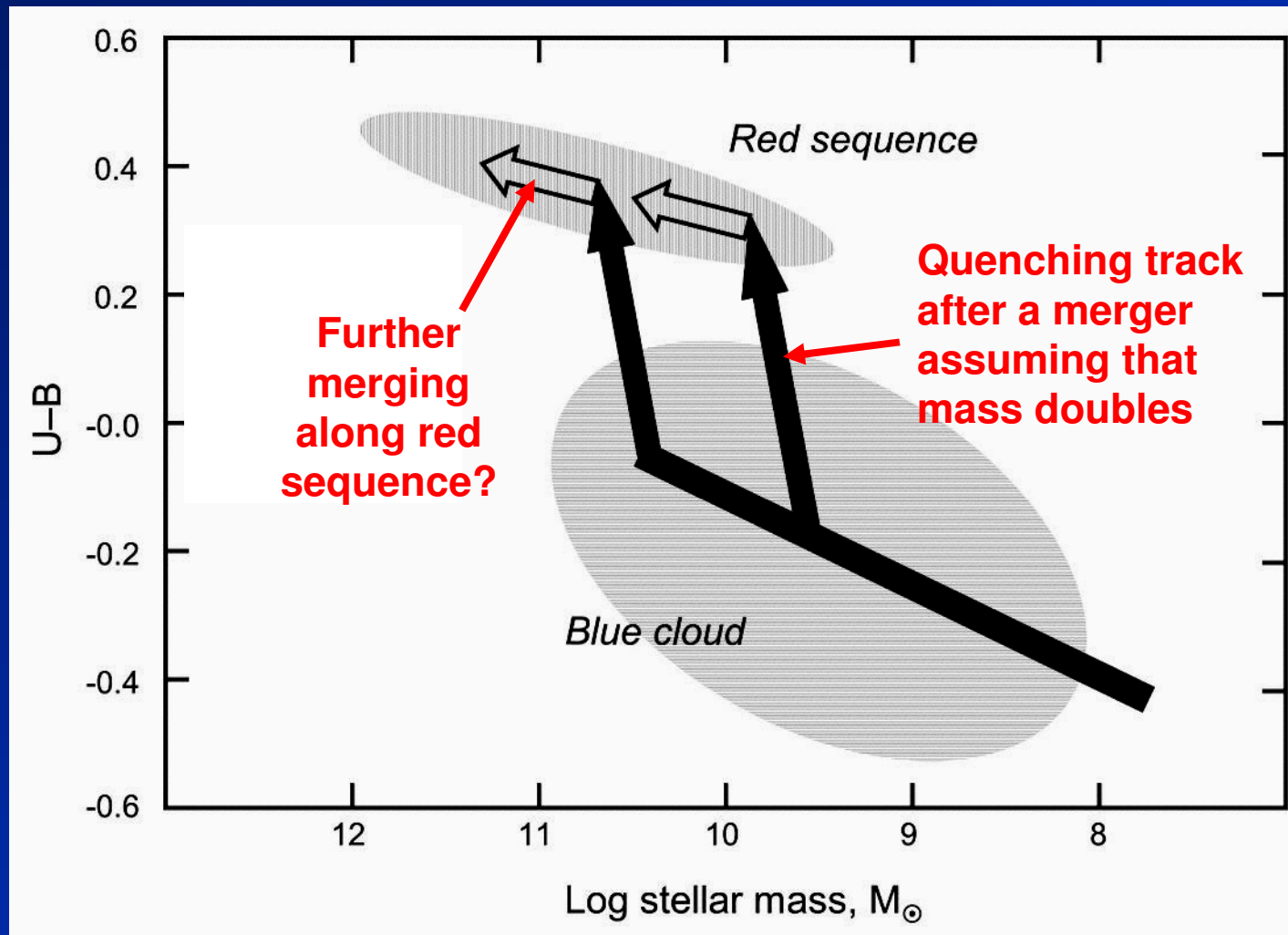
- **Dynamical conversion: flat rotating disks need to be “scrambled” into a roundish spheroid:**

***----> Easily done by mergers. No problem.***

- **Star formation needs to be stopped:**

***----> An idea that partially works: starbursts triggered by mergers, which provide feedback and drive out gas in a “galactic wind.”***

# Motion of galaxies in color-mass diagram if two *equal-mass blue galaxies* merge and quench





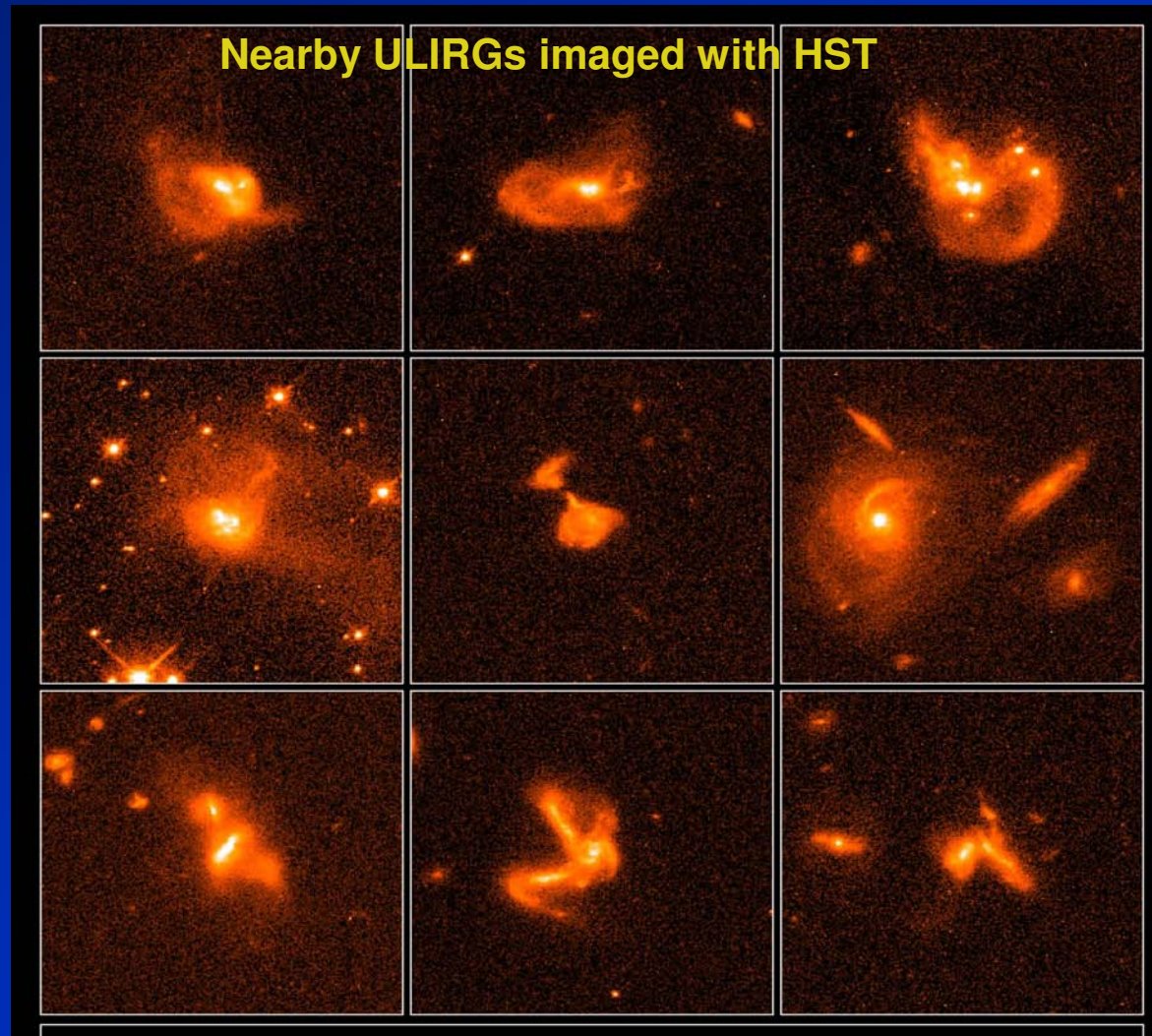
# Gas-rich mergers trigger *starbursts*, creating ultraluminous infrared galaxies (*ULIRGs*) that are briefly the most rapidly star-forming galaxies in the Universe

95% of all ULIRGS are seen to be double or interacting. Mean separation of nuclei only 2 Kpc. ***Late-stage mergers.***

Bright ULIRGs make stars at a rate up to ***100-1000  $M_{\odot}$ /yr.***

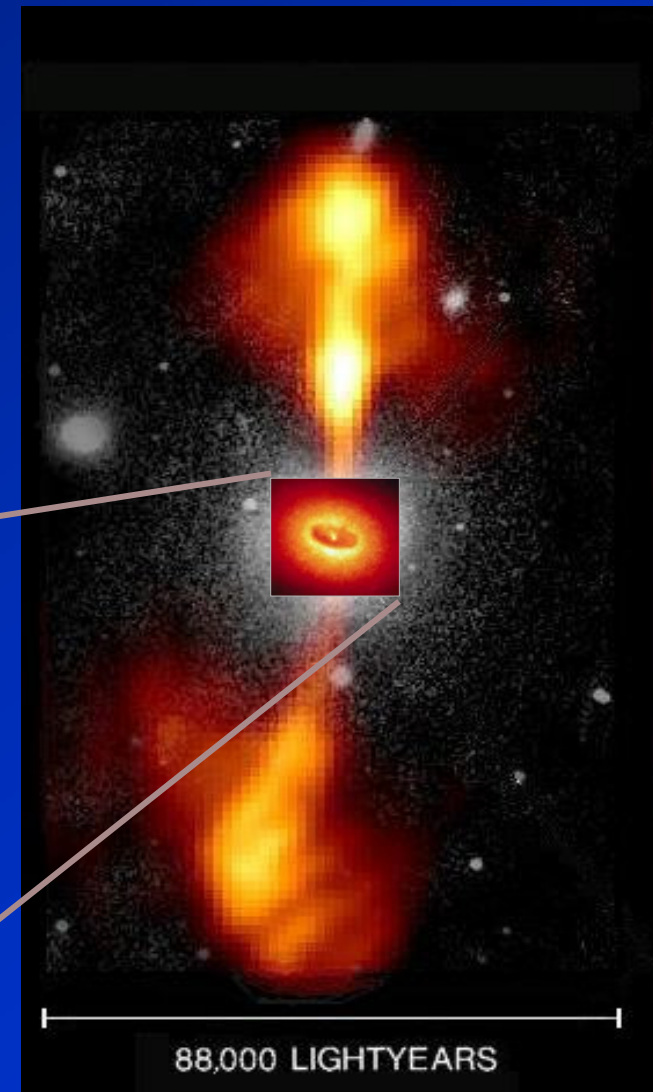
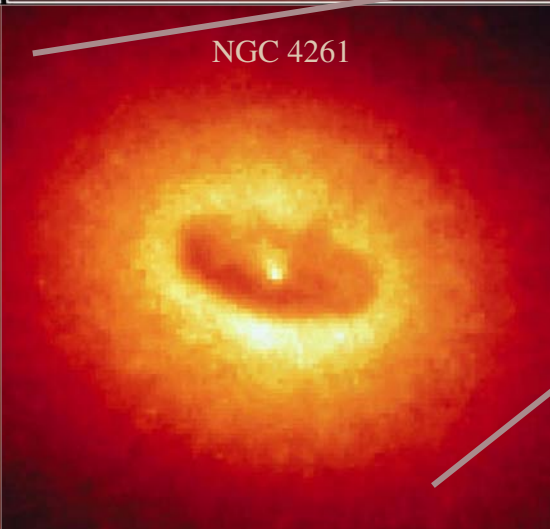
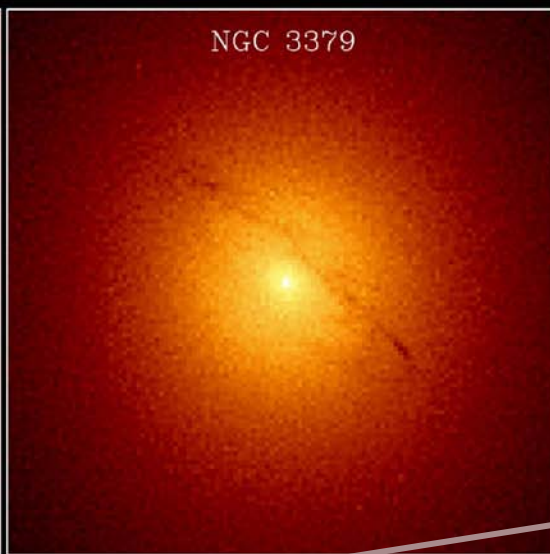
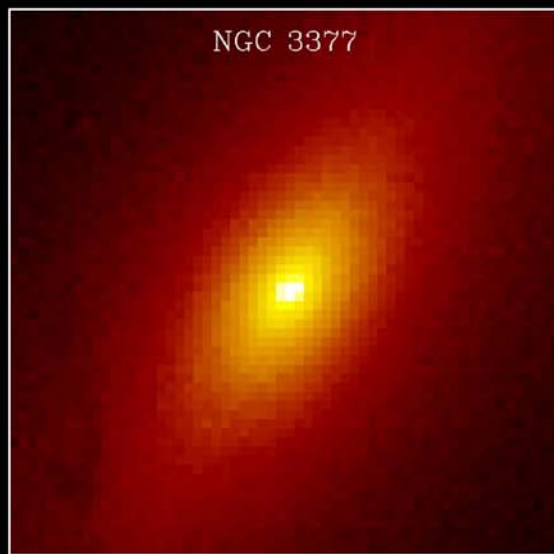
Normal disk galaxies make stars at a rate of  $\sim 1 M_{\odot}$ /yr.

Borne et al., 2000

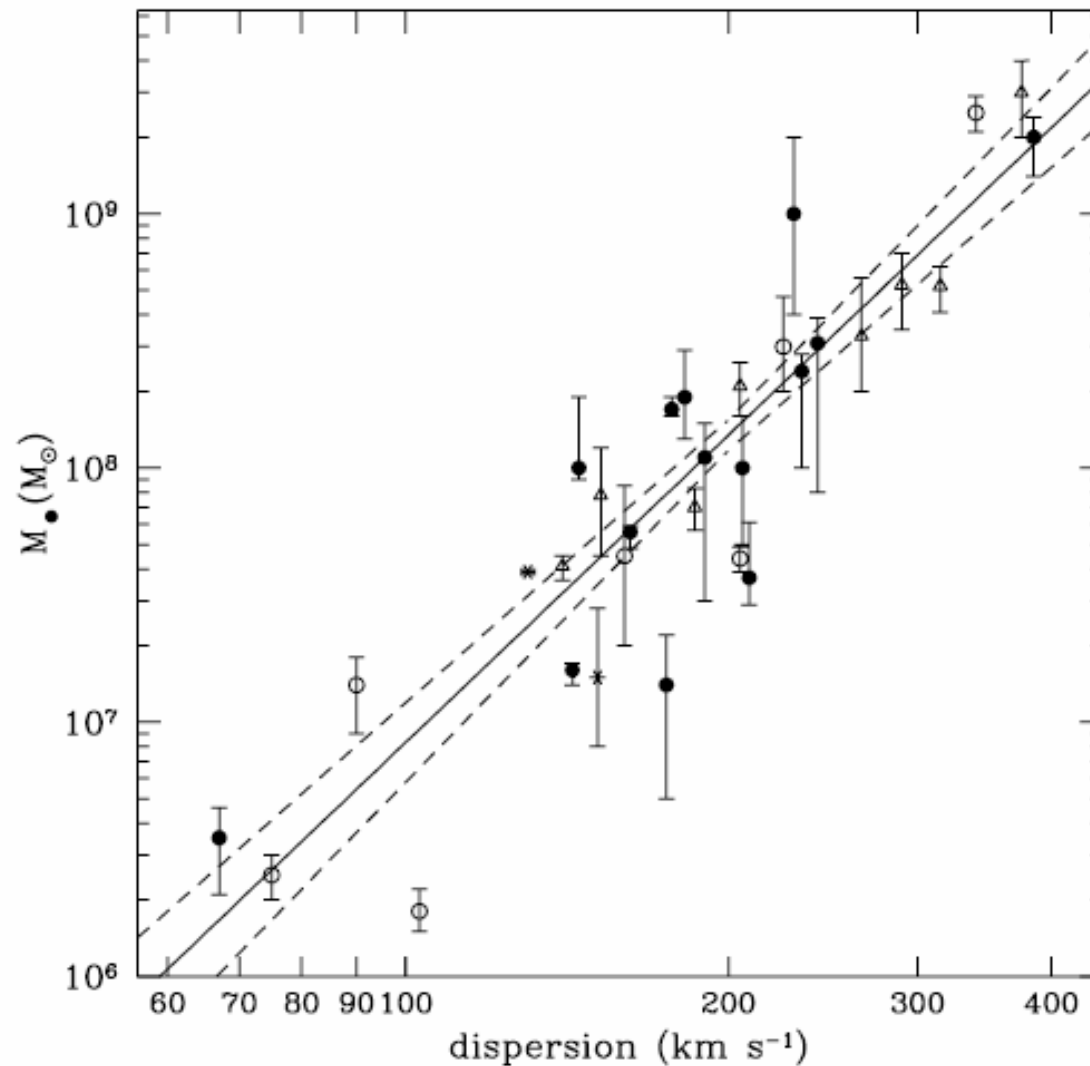




**Spheroids host massive central black holes, which power *quasars* and other kinds of *active galactic nuclei (AGNs)***



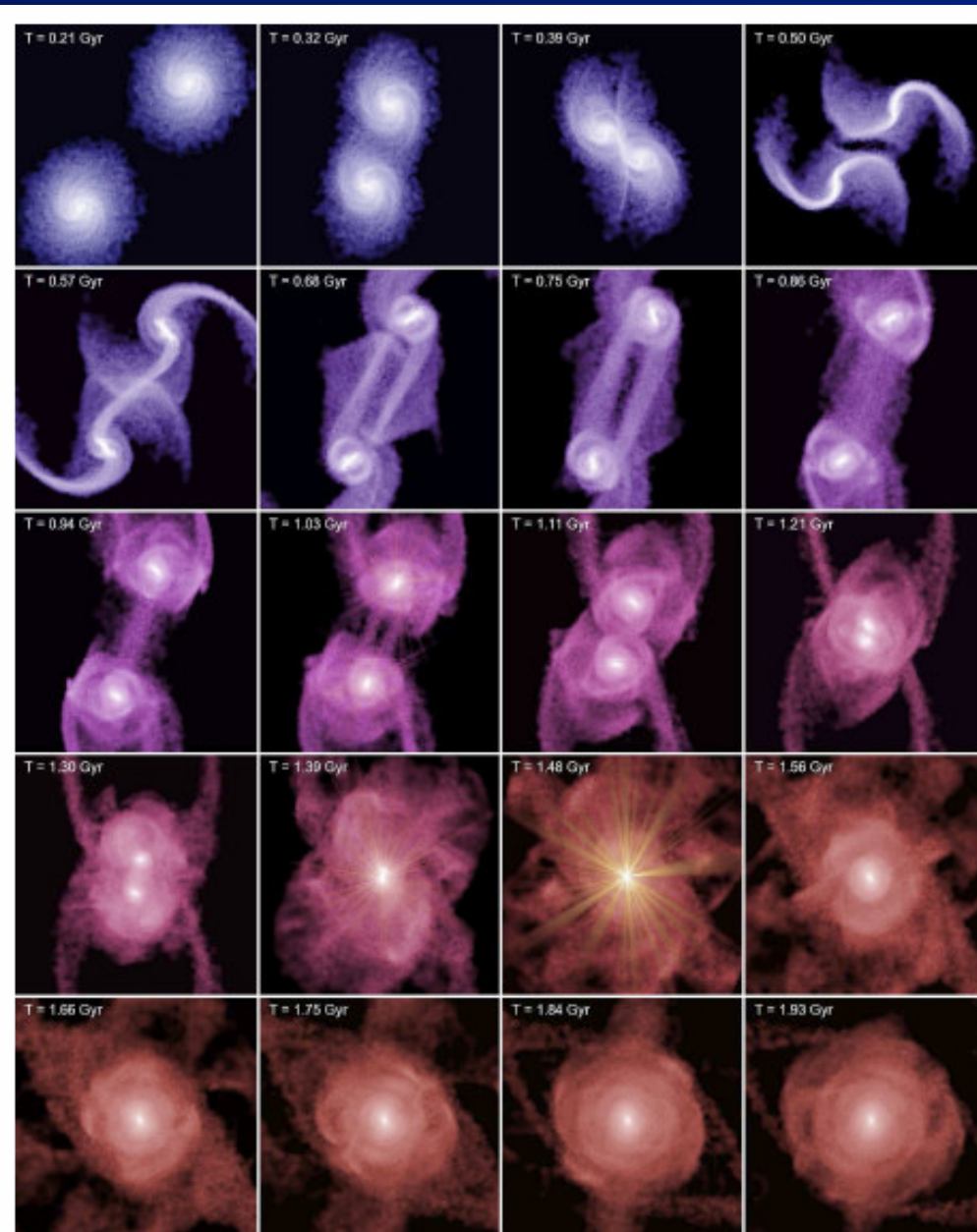
# The black hole - $\sigma^4$ relation



Virtually all spheroidal galaxies that have been looked at closely with the Hubbel Space Telescope have ***a massive black hole at their centers.***

The mass of the BH scales with the stellar velocity dispersion ( $\sigma^4$ ) or with the stellar mass (not clear which).

Tremaine et al. (2002)



Hopkins, Hernquist et al.

2005:

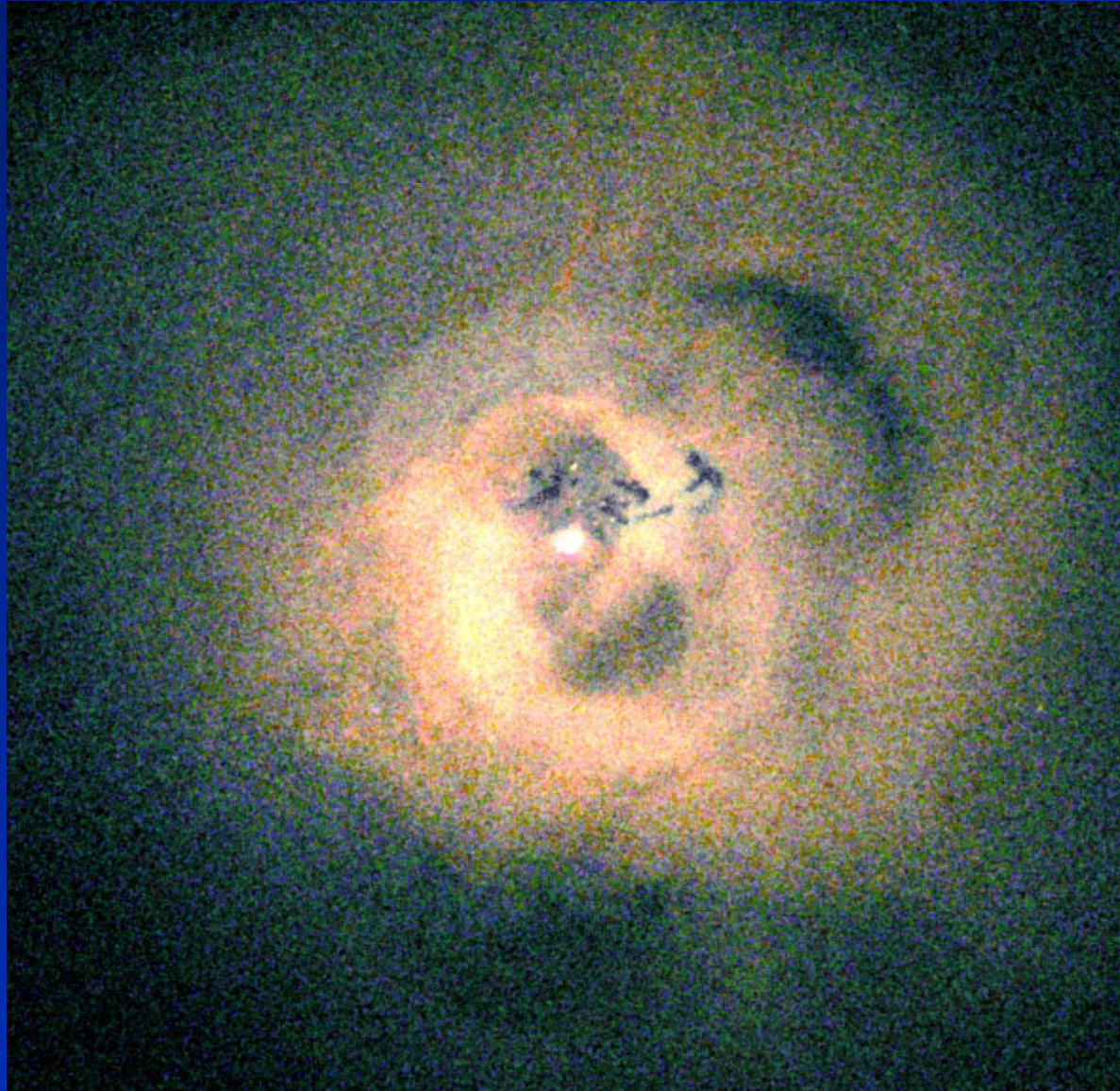
***Gas-rich mergers have multiple consequences:***

- \* Stellar disks are scrambled to make spheroids
- \* Orbital energy shocks gas, drives hot wind
- \* Fluctuating grav potential drives gas to center, fuels starburst, further driving wind
- \* Gas accretes onto central BH, fuels AGN, more feedback
- \* Models match the BH-mass relation with reasonable parameters



# Chandra X-ray map of Perseus Cluster

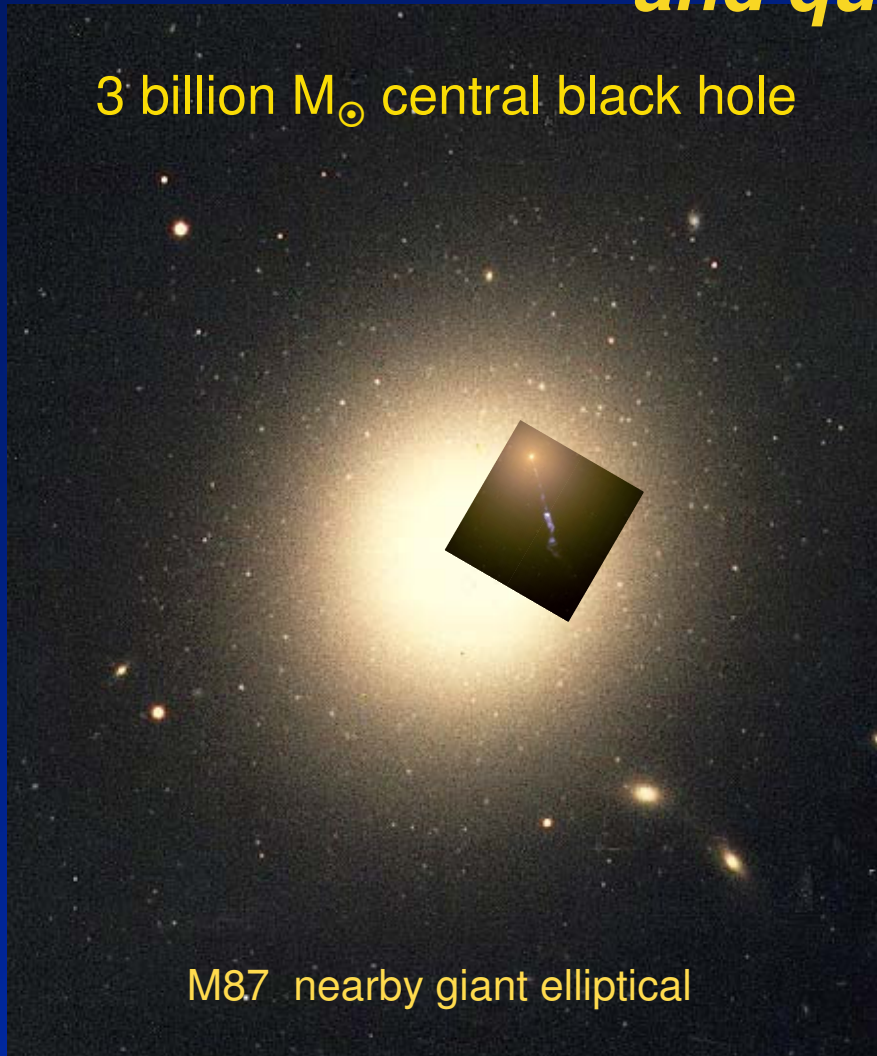
High resolution X-ray imaging shows that the central cluster gas is in fact highly disturbed.



Fabian et al. 2003

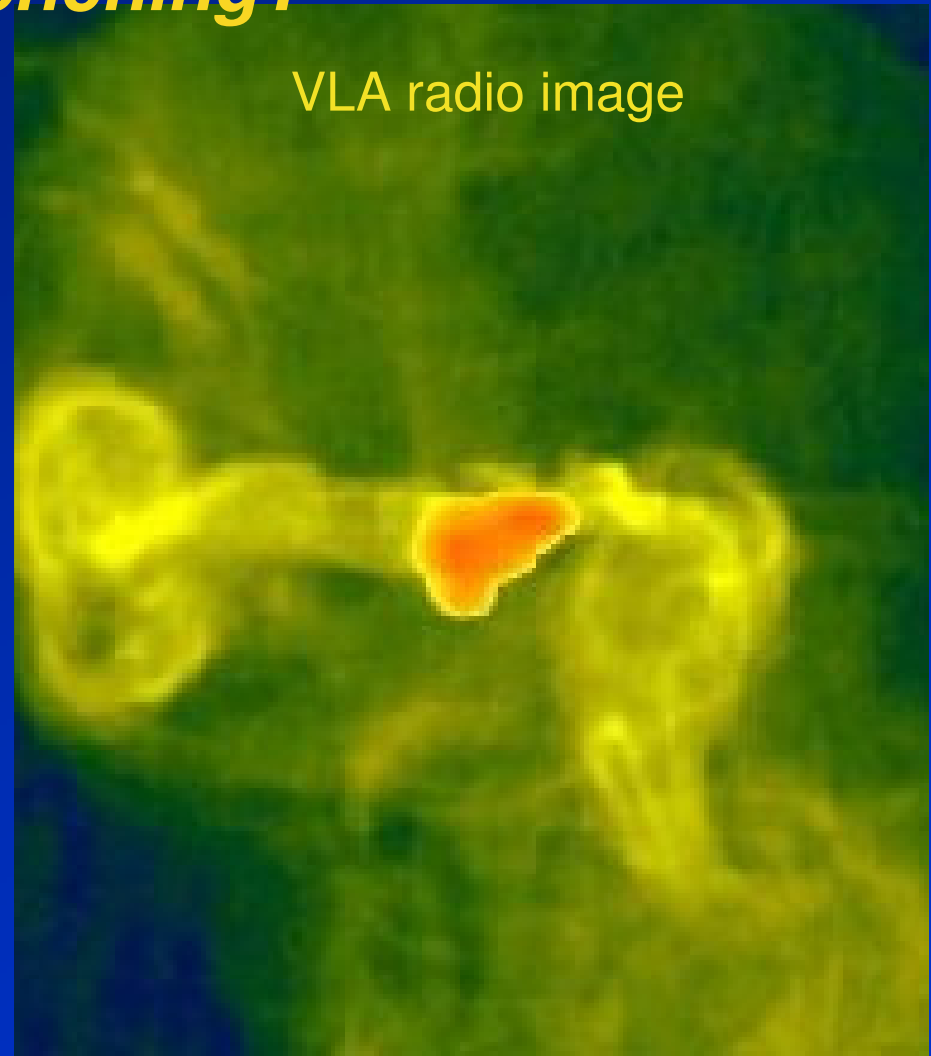
AGNs clearly have an “effect” on  
surrounding gas, but is this really *feedback*  
*and quenching*?

3 billion  $M_{\odot}$  central black hole



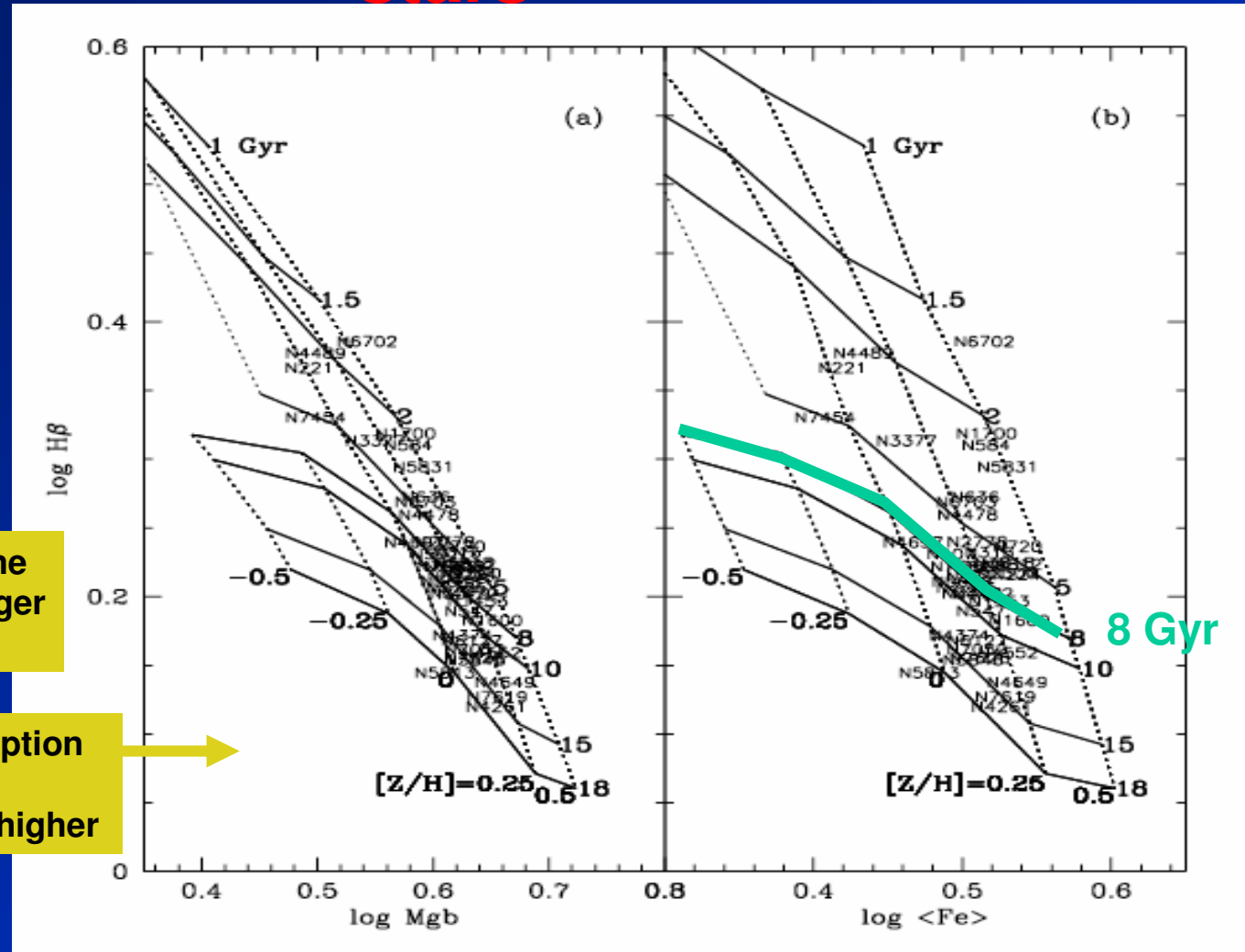
M87 nearby giant elliptical

VLA radio image



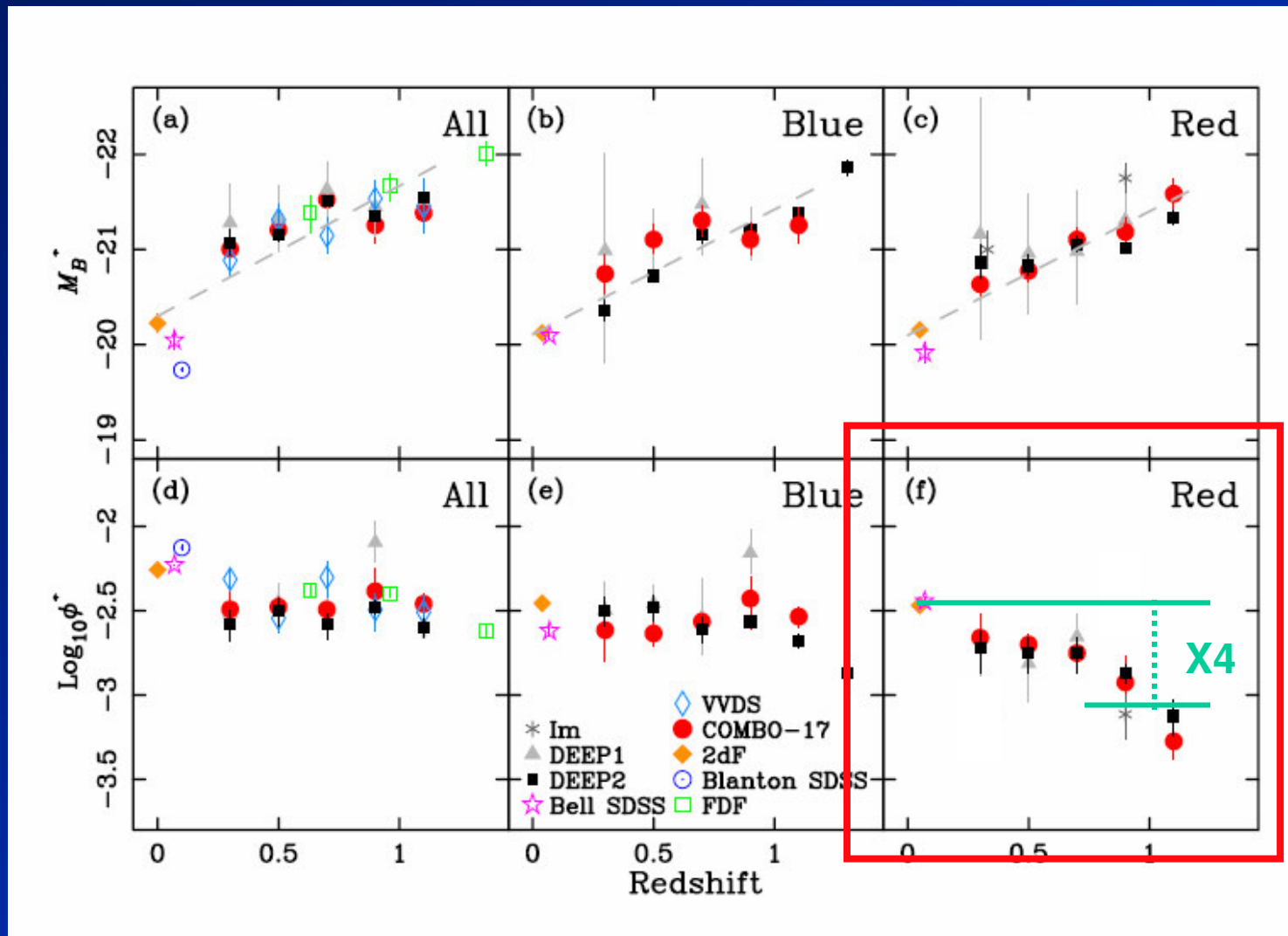


1993-2001: Balmer lines show *young stars*;  
mean age much less than age of Galactic halo  
stars



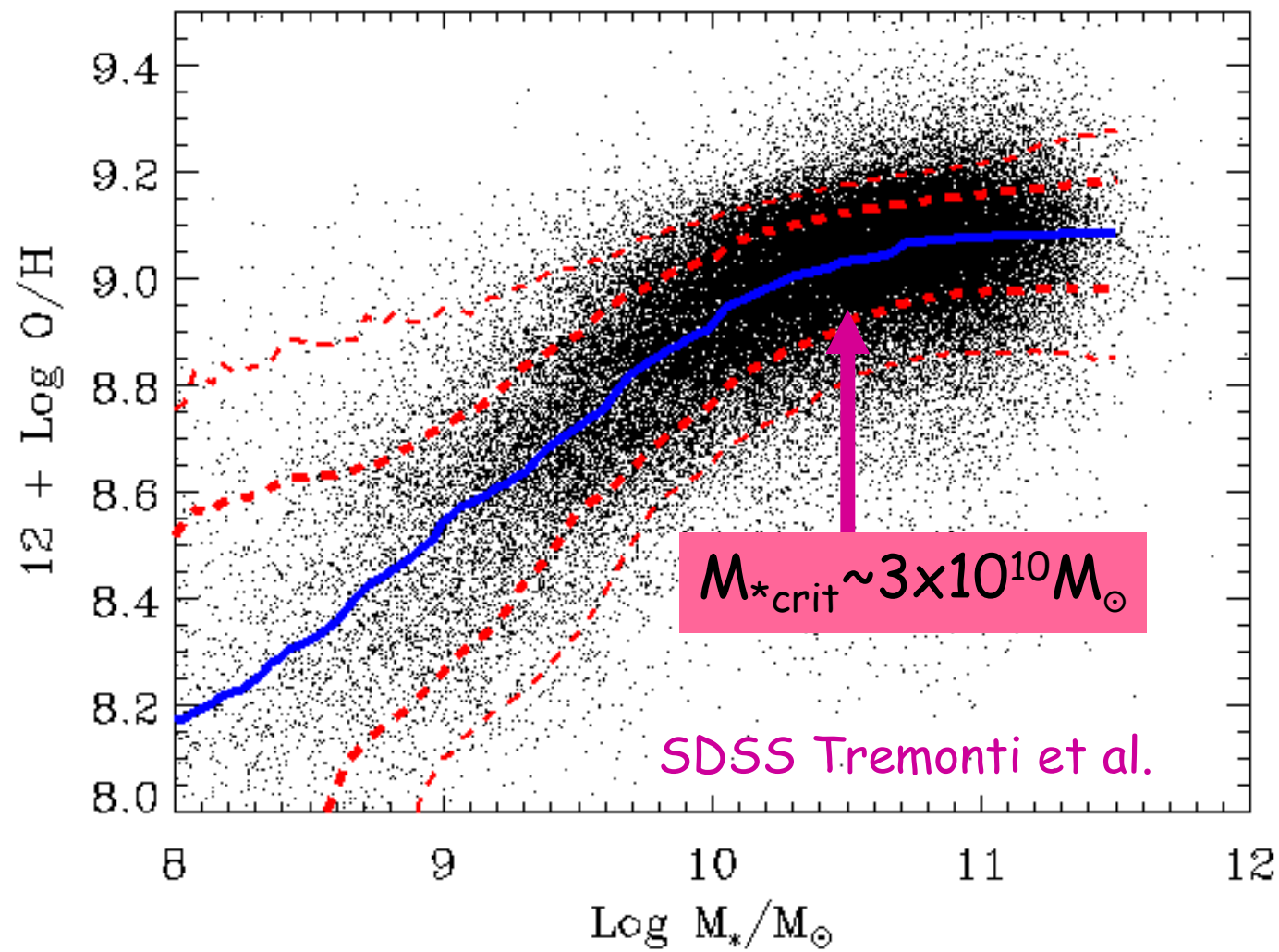
## Trager et al. 2001: Ages adjusted for non-solar abundance ratios

# DEEP2 and COMBO-17: Most red galaxies became red after $z = 1$



Willmer et al. 2005, Faber et al. 2005

# Transition in Metallicity



# Production Factors

